Master's Thesis 2013

Candidate: Colombage Kshanthi Kalyani Perera

Title: Optimization of a biomass gasification reactor

Telemark University College
Faculty of Technology
Kjølnes
3914 Porsgrunn
Norway

Telemark University College
Faculty of Technology
M.Sc. Programme

MASTER'S THESIS, COURSE CODE FMH606

Student:	**Colombage Kshanthi Kalyani Perera**
Thesis title:	**Optimization of a biomass gasification reactor**
Signature:	. . . . .
Number of pages:	83
Keywords:	**Biomass steam gasification, Barracuda, CPFD, Product gas**

Supervisor:	Prof.Britt M.Halvorsen	signature:	. . . . .
2nd Supervisor:	Rajan K.Thapa	signature:	. . . . .
Censor:	Prof. Christoph Pfeifer	signature:	. . . . .
External partner:	Vienna University of Technology	signature:	. . . . .
Availability:	Open		

Archive approval (supervisor signature)**:** signature: . . . . . **Date:** . . . . . .

Abstract:

Steam gasification is a well-known technology which is used to produce a high quality product gas, especially for power generation applications. The gas composition, gas quality and the purity are important for the end application. The biomass steam gasification was studied using the Computational Particle Fluid Dynamics (CPFD) simulation tool, 'Barracuda VR^{TM}'. The software is well suited for simulating the dense particle laden fluids due to its numerical solving methods for both the particles and the fluid.

Both the experiments and simulations were carried out for a cylindrical isothermal fluidized bed without chemistry, to compare the deviations of simulation results from the experimental results. The simulation results agreed well with experimental results and confirmed the same minimum fluidization velocity. Hence the model was used for further simulations.

Three dimensional simulations were carried out for a cylindrical geometry to study the energy and momentum transport within a simplified dual fluidized bed steam gasification reactor. The important chemistry was included. Simulations were performed under seven cases to investigate the effect of bed material size, consistency of biomass supply, steam temperature, steam input velocity, addition of CO_2 and the bio mass particle size on the rate of combustible gas production. According to the simulation results, the product gas was generated consistently over the time, except in one case. The product gas volume mainly consisted of ~ 40 % CO, ~ 15% H_2, ~ 25% CH_4 and ~20% CO_2.The highest cumulative production of combustible gasses (CO, CH_4 and H_2) was rated by Case-G, which was estimated as 400 Sm^3/day based on the simulation results.

According to the results it was found that the reduction of bed material size and choosing the optimum particle size for biomass enable to enhance the gas production. The rate of gas production was adversely affected by the decrease of steam temperature. Increase of the steam input velocity and substitute of steam in the biomass feed with CO_2 did not contribute for enhancing the product gas volume.

Table of contents

Preface

‘Optimization of a biomass gasification reactor’ contains the report of my master thesis. It is the fruit of hard work and enormous courage I had, to see the success of this task. Many people were behind me to support and encourage me towards this final outcome. First of all I’m thankful for almighty God, I love and worship, whom I believe as the beginning and final destination of my life.

The project had to be performed using the commercial software of ‘Barracuda VR^{TM}’. Being completely new software, I required a thorough training. In addition, the project required a good understanding of steam gasification process, the involved knowledge regarding to the chemistry and facilities for the experiments as well.

I’m very much thankful for my supervisor, Prof. Britt Halvorsen for her kind supports from the beginning to this moment. She arranged everything for the software training on time. I got the opportunity to present oral presentations out of my simulation work in the workshops at Telemark University College and in University of Agdar, which were held in March, 2013.In addition I could prepare a research paper for the conference, ‘‘Multi phase flows 2013’’ which will be held in July 2013, at Coruna, Spain. I’m thankful for my supervisor for her encouragement towards the success of all this tasks. She was always happy to allocate time for me from her busy schedule and never forgot to encourage me by her visits to my working table. It’s memorable to have such a friendly supervisor like her.

I received a big support from my co-supervisor, Mr.Rajan.K.Thapa, for the software installation and the experimental tasks. I’m thankful for all these supports and for all the helps during the training period in Aachen, Germany.

The software training was given by ‘aixprocess gmbh’, in Aachen, Germany. My gratitude goes for this institute and friendly instructors who gave me a proper guidance for the software.

There is a special person in my life, who always helps me by his knowledge and deeds. It’s my pleasure to remind my husband for all the moments he lovingly encouraged me. I’m not here without the love of my parents, grandmother and three sisters. Lot of thank for them too at this moment that I successfully end up my master thesis.

And last, but not least I’m thankful for my teachers and heart felt friends I had in Mary Immaculate Convent, De Mazenod College, University of Moratuwa in Sri Lanka and Telemark University College, Norway, who were a great strength for me throughout my career. Finally I would like to offer my bit of work for all the readers and I’m happy to clarify anything or consider any suggestions to give away a better outcome for all who are interested to read and study my work.

Porsgrunn, 30th May, 2013

Kshanthi Perera

Nomenclature

Abbreviations

CAD	Computer Aided Design
CHP	Combined Heat and Power
CPFD	Computational Particle Fluid Dynamics
DFB	Dual Fluidized Bed
DPM	Discrete Particle Method
HHV	Higher heating value
MP-PIC	Multi-Phase-Particle-In-Cell
CDBFB	Circulating Dual Bubbling Fluidized Bed

Units

µm	Micro meters
MJ	Mega joule
Nm^3	Normal cubic meter
Sm^3	Standard cubic meter
K	Kelvin
^0C	Celsius

Letters and expressions

ΔP	Pressure drop
Φ	Sphericity
α	Packed bed voidage
µ	Fluid viscosity
ρ	Fluid density
U	Fluid velocity
d_p	Diameter of the particle
ΔP_{mf}	Pressure drop at minimum fluidization
ΔV_{mf}	minimum fluidization velocity
db	Dry basis

List of figures

List of tables

1 Introduction

There is a growing demand for renewable energy options in the world due to negative environmental impacts of fossil fuels and in terms of energy security too. Biomass is one of the choices of many nations when they set their renewable energy targets, due to its less environmental impacts. There are many types of biomass resources including wood and wood wastes, agricultural crops and their waste byproducts, municipal solid waste, animal wastes, waste from food processing, aquatic plants and algae[1].But it is important that the harnessing of chemical energy stored in biomass should be environmentally and economically sustainable.

The biomass utilization technologies can be classified in to four, which are, direct combustion processes, thermochemical processes, biochemical processes and agrochemical processes [1]. Pyrolysis and gasification of biomass can be introduced as thermochemical conversion processes which can utilize the biomass for obtaining a considerable energy yield.

Gasification is a complex process and it is crucial to properly describe and combine the biomass characterization, solid fuel devolatilization, secondary reactions in the gas phase and char gasification features [2].

There are different modes and designs of gasification processes and it is important to consider the economical sustainability and required quality of product gas when selecting an appropriate type of gasifier for a particular application. Biomass steam gasification is seemed to be a promising technology that enables to obtain a high quality product gas with considerable heating value for advanced applications such as CHP cycles, which generate electricity with higher efficiencies.

Gasification process is involved with number of endothermic reactions and demands for energy. Being an allothermal process, steam gasification requires energy to be supplied externally [3].Hence Dual Fluidized Beds (DFB) have been developed as a solution to overcome this challenge by providing the required heat to the gasification reactor through the circulating hot bed materials[4].

For a successful design and operation of a gasification reactor, it is important to have a thorough knowledge regarding to the influence of fuel and operating parameters on the process [5]. The fuel composition, size of feed biomass, operating temperature, steam flow rate and temperature, bed material, use of catalysts, and change of many other variables might affect the gasification process significantly. Even though the experimental methods are fine for investigating the effect of these parameters, it is time consuming and can be a waste of energy and resources. Use of a computational tool for simulating this complex process would help in many ways to optimize the biomass gasification process. This study will focus on simulation of the biomass steam gasification process using the Computational Particle Fluid Dynamics (CPFD) software 'BARRACUDA VR^{TM} Series 15' aiming the optimization.

2 Problem description

The aim of this project is to optimize the biomass steam gasification process by performing a computational study. There are some success stories regarding to the DFB steam gasification, and the reactor concept used in the biomass CHP plant in Guessing/Austria, was referred in this study [4]. The DFB technology enables a successful operation of biomass steam gasification process as it separates the combustion zone from the gasification zone. In this process, the biomass gasification occurs in the gasifier and the non-converted char is transfered to the combustor together with circulated bed materials, where the combustion reactions take place between remaining char and air. This produces necessary heat energy to supply in to the gasifier in the means of recirculated hot bed materials[6].

As defined in the gasification reactor used in Guessing/Austria, five main material streams were identified in and out of the reactor. These are inlet biomass stream, steam input, bed material and unconverted char out to the combustor, hot bed material from the combustor and the product gas outlet. This is illustrated in Figure 6-1 [4].

For the simplicity, the combustor was removed from the simulation set up by considering only the gasifier, but having all the identified material streams. The gasification reactor was replaced by a cylindrical reactor which has a diameter of 8.4cm.

Barracuda VR^{TM} Series 15 is used as the software tool and it facilitates to perform the simulations, including necessary chemical reactions with their kinetics. Effect of changing important operating parameters such as biomass feed particle size, size of the bed materials, steam temperature and the steam flow rate are checked through the simulations for the optimization of the biomass steam gasification reactor.

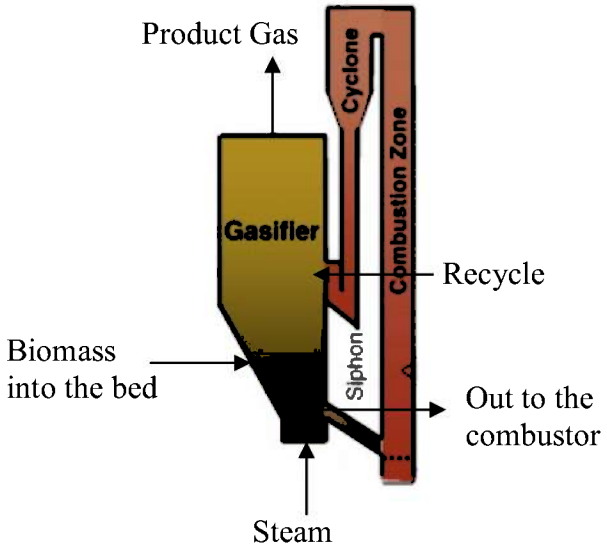

Figure 2-1:Inlet and outlet material streams of a DFB gasifier

3 Theory

This chapter contains the specific theoretical information that is relevant as the background knowledge for the optimization and simulation purposes of biomass steam gasification process.

3.1 Biomass Resources

The biomass resources that can be used for gasification can be classified in to three major categories such as wastes, forest products, and energy crops. Table 3.1 shows some examples for each category of these biomass resources [1]. The major constituents of the biomasses are hemicellulose, cellulose and lignin [2]. Different categories of biomass yield different product compositions in pyrolysis and gasification due to the differences in the proportion of their constituent elements and according to the process conditions. For example, higher char yields can be observed in the devolatilization of agricultural residues such as rice straw, in comparison to woody biomass. One reason is the higher lignin content in agricultural residues and that means it contains more carbon. This trend increases with the increase of process temperature [7]. Some more information related to the constituents of different fuels and biomass types are included in Appendix 3.

According to the proximate analysis, the biomass contains volatile matter, fixed carbon, some amount of moisture and ash. The ash content is also varied from one type of biomass to the other. Fewer amount of ash content in the biomass, reduces the operational problems. Olive stones are one example of biomass which has very low ash content (0.6 wt. %, db.) and currently used in the steam gasification process [8].

Table 3-1: Types of biomass resources

Wastes	Forest products	Energy crops
Agricultural production and processing wastes	Wood	Short rotation woody crops
Crop residues	Logging residues	Herbaceous woody crops
Mill wood waste	Trees, shrubs, and wood residues	Starch crops (corn, wheat and Barley)
Urban wood wastes	Saw dust, bark from forest clearings	Sugar crops,(cane and beet)
Urban organic wastes		Oil seed crops(Soybean, sunflower)

3.2 Fluidizing Beds

Fluidized beds involve particulate solid materials and fluid streams. The principal here is to pass a fluid upwards through a solid bed. A pressure drop is created in the solid bed due to the drag force applied by the fluid on the solid material. When the weight of the bed material equals to the fluid drag force, the particles are suspended in fluid medium without resting on each other. Fluidized beds are widely used in many industries for performing various chemical and physical processes, aiming enhanced product yields and efficient operation.

There are different designs of fluidized beds depending on the application. Some of the designs aim for heat recovery while others aim easy transportation or gas cleaning. Some examples for such designs are shown in Figure 3-1[9].

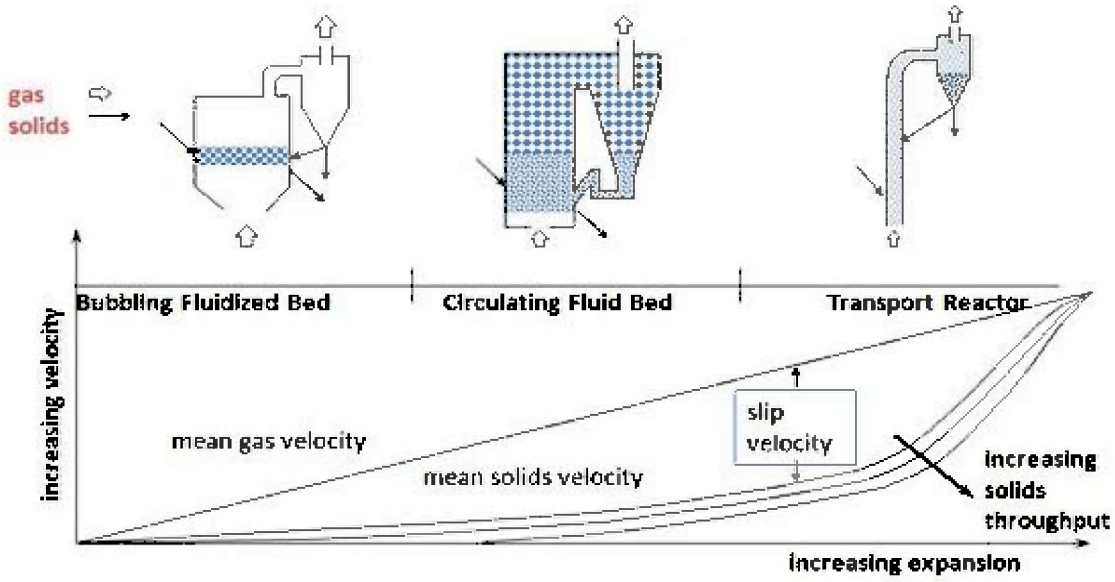

Figure 3-1: Different designs of fluidized beds

3.2.1 Fluidization flow regimes

The main fluidization flow regimes that can be experienced within a fluidized bed can be named as bubbling fluidization, turbulent fluidization, fast fluidization and pneumatic conveying [10]. Figure 3-2 illustrates how a solid particulate bed can behave when the fluid velocity is gradually increased [11].

(a) Fixed bed regime

This regime refers to where the fluid flow rate is too low to counter balance the weight of the bed material. Therefore the bed remains stationary.

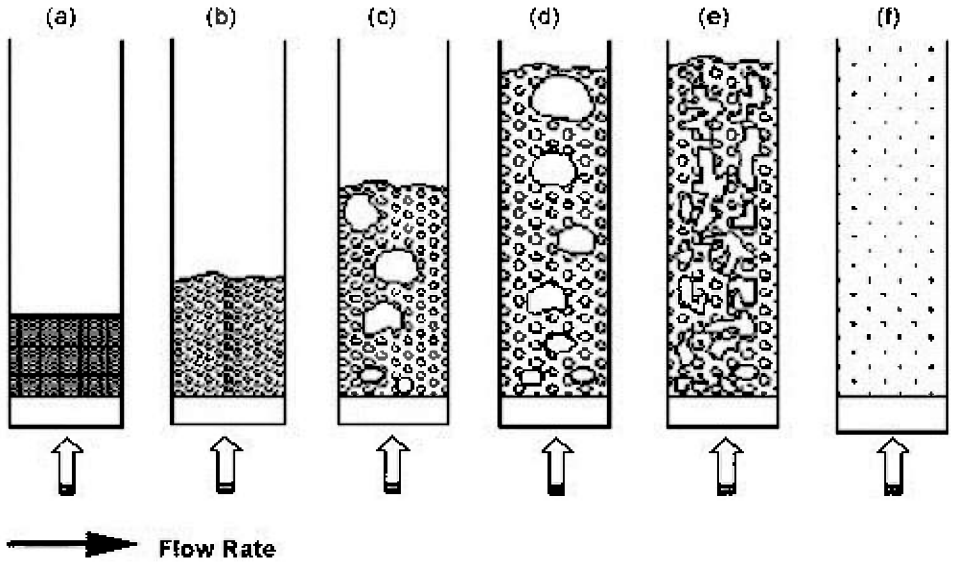

Figure 3-2:Fluidization flow regimes

(b) Minimum Fluidization

At this point the weight of the bed mass is counter balanced by the hydrodynamic forces exerted on the bed due to the fluid flow rate. This point is unstable and it has the tendency of easily converting in to a fixed bed or progress in to bubbling fluidization regime due to a small change in the flow rate [11].The fluid velocity at minimum fluidization is called as 'Minimum fluidization velocity'. The bed starts to expand beyond the minimum fluidization velocity.

(c) Bubbling bed regime

A slight increase to the minimum fluidization flow rate results with bubbles in the bed. This stage is then known to be bubbling bed regime.

(d) Sludging bed

When the fluid velocity is further increased it leads to large bubbles and this phenomenon can be significant in narrow reactors.

(e) Turbulent bed regime

When the pressure variation of the bed is started to level-off via the fluid velocity increment, it can be regarded as the starting point of turbulent bed regime. But the transition point of the bubbling and turbulent flow regime is hard to define [12].

(f) Pneumatic bed regime

The bed material is started to flow pneumatically with the fluid flow at this stage.

3.2.2 Pressure drop across a fluidized bed

The pressure drop across a fluidizing bed rises with the superficial velocity of the fluid applied on the solid bed, until it reaches the minimum fluidization velocity. When the bed weight is equal to the fluid drag force it reaches the minimum fluidization and further increase of superficial velocity leads to level-off the pressure drop across the bed. This phenomenon is shown in Figure 3-3 [13]. When the velocity is kept increasing, the solid bed would undergo the pneumatic transport stage and then the pressure drop will start to decrease back according to the figure.

The Ergun's equation shown in Equation (3-1), can be used to calculate the pressure drop across a fixed bed until it reaches minimum fluidization [14].

$$\frac{\Delta P}{H} = \frac{150(1-\alpha)^2}{\alpha^3}\frac{\mu U}{\phi d_p^2} + \frac{1.75(1-\alpha)}{\alpha^3}\frac{\rho U^2}{\phi d_p} \qquad (3\text{-}1)$$

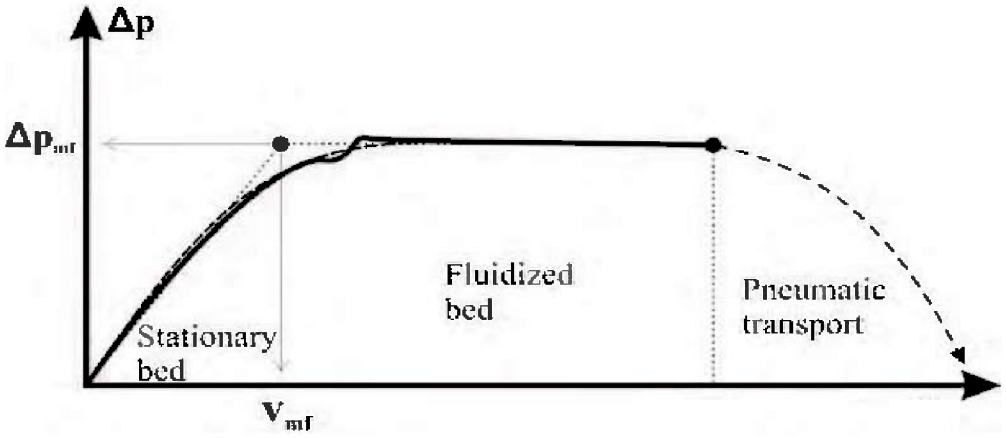

Figure 3-3:Pressure drop vs velocity

3.3 Gasification Technology

Gasification is a thermochemical process, used to breakdown the carbonaceous feed stocks into a useful product gas. The gas composition can vary depending on the type of biomass used, the gasification agent, the temperature, and other physical parameters. Gasification is the latest discovered option for harnessing the energy out of biomass. Nowadays it is used in electricity generation field to generate electricity, using combined cycle gas turbine systems, achieving higher efficiencies up to 50 % [1].

The feed stocks undergo pyrolysis prior to the gasification, due to the presence of required temperature and in the absence of air. The feedstock is mainly broken down to liquid, charcoal and non-condensable gases during this thermochemical process [1]. Pyrolysis product composition can vary depending on the temperature, heating rate and gas residence

time [1]. If the fast pyrolysis conditions such as high heat transfer rate to the biomass particles and short vapor residence time are there, a liquid fuel is produced that has a high yield of 70-80%, based on the started biomass weight [15]. For generating more combustible gasses, it requires a higher temperature, lower heating rate and long gas residence time [1].Typically the pyrolysis process occurs in the temperature range of 650K – 800K [1] .The increase of pyrolysis temperature leads to decrease of liquid and char while increasing the gas yield [16].The resulted char is then subjected to the gasification process which involves a series of heterogeneous and homogeneous reactions. Gasification has different definitions based on the gasification agent it uses, such as steam gasification, air gasification and Oxygen gasification. Gasification reactions are endothermic and demands for energy [5]. When the gasification agent is air or Oxygen, it virtually creates a partial oxidation zone within the reactor to generate the required energy via the exothermic combustion reactions. But the amount of Oxygen/air must be controlled so that it doesn't disrupt the conditions for gasification. But the condition changes in steam gasification as there is no room for exothermic combustion reactions. Hence it requires an additional energy supply in to the reactor.

Figure 3-4 shows the experimental results in yield of carbonaceous gasses and H_2 during the pyrolysis and gasification stages, tested in a CDBFB, for white oak saw dust, at different temperatures [6].

Tar formation is a highly discussed matter regarding to the biomass gasification process. This is undesirable due to the problems it causes by condensing in the process equipment, in the engines and turbines, that use the product gas in end applications [17].The minimum allowable tar and dust content in the gasses is $10mg/m^{-3}$ and the average tar concentration in the exit gas from a fluidized bed gasifier is around $10g/m^{-3}$[17]. Different approaches are being taken to reduce the tar content in the product gas. Use of catalytic bed materials in the gasification reactor is seemed to be a promising solution and Nickel based catalysts and olivine are among these materials [18].

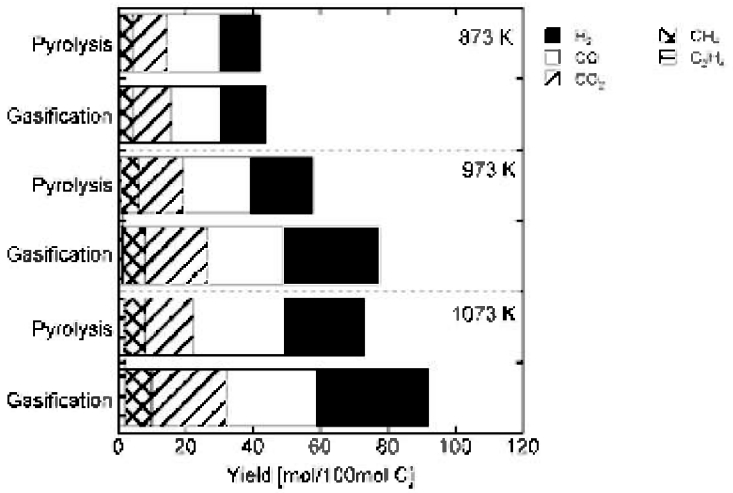

Figure 3-4: Yield of gasses in pyrolysis and gasification stages for white oak

3.3.1 Types of Gasifiers

The design of gasification reactors vary depending on the bed material movement, direction of biomass introduction and product gas movement, gasification agent, medium utilization and etc. Considering different gasifier designs found in literature, a summary for the classification of gasification reactors was done as shown in Figure 3-5.

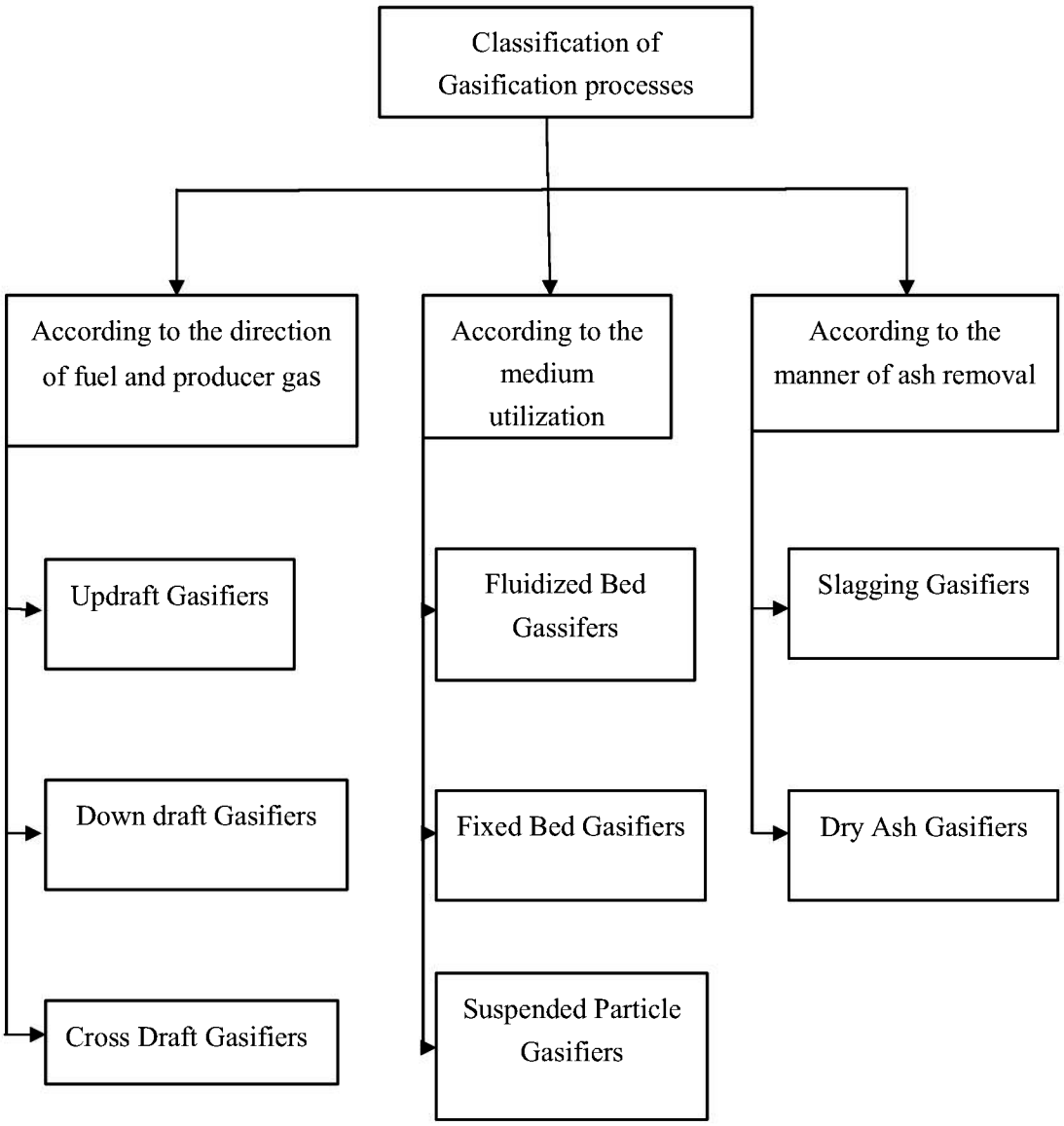

Figure 3-5:Classification of gasification reactors

3.3.2 Fluidized bed gasifiers

The gasification process occurs in fluidized bed gasifiers consists of initial drying, fast pyrolysis of solid fuel and gasification of resultant chars [19]. Due to the proper mixing, fluidized beds provide enhanced gas solid contact which ultimately leads to high reaction rates and conversion efficiencies [5].

Steam, air and Oxygen are some examples for gasification agents used in fluidized bed gasifiers and this can be varied upon the application. Steam gasification in fluidized beds has a growing concern due to the major drawbacks of air and Oxygen gasification, and also seems to be economically feasible and qualitatively favourable option.

The biomass is difficult to fluidize alone due to their uneven shapes, variation of sizes and densities. Therefore it is a usual practice to use a specific bed material such as silica sand, alumina or calcite to facilitate the biomass fluidization. On the other hand this bed material acts as a heat transfer medium in to the reactor too [20].

In fluidized bed gasifiers, the pyrolysis step is a short process that generates basically solid char and volatile gases. But during the gasification stage it involves a series of heterogeneous reactions that occurs between gasification agent and reactants as well as resultant gases and reactants [19]. It is possible to have homogeneous reactions among the generated gas species too. Hence gasification is a much slower process in comparison to the initial pyrolysis and it is dominant throughout the whole gasification process [19].

3.3.3 Biomass Steam Gasification

Biomass steam gasification has the ability to produce a quality product gas which comprises H_2, CO, CO_2, CH_4 and H_2O with negligible amount of N_2 and heavy hydrocarbons. This product gas has a medium calorific value ranges from 12-14 MJ/Nm^3 and this is far better than the low calorific product gas resulted from air gasification [21]. The summary of biomass gasification process is illustrated by Figure 3-6.

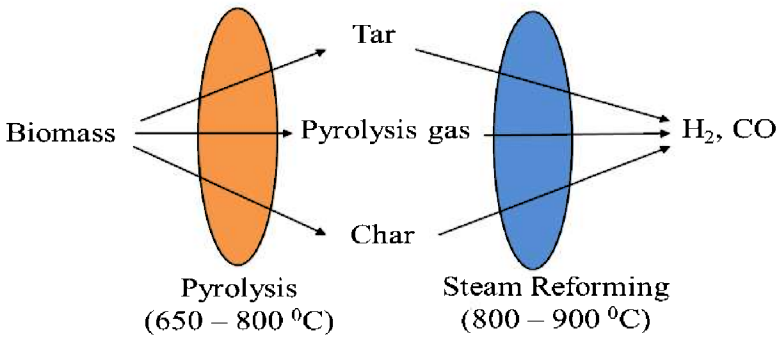

Figure 3-6:Biomass steam gasification process

The product gas produced by bio mass air gasification generally contains 8-14 vol.% of H_2, while the fluidized-bed steam gasification process is capable of producing a gas with a 30-60 vol.% of H_2, but this technology requires the steam temperature to be higher than 700^0C [22].When the steam is used as the gasification agent, it requires external heat energy, because there is no partial oxidation takes place to self-supply the heat for the process as in air gasification [4]. But for providing the required energy, it is important to let the combustion to takes place within the gasifier by supplying some air in to it. Then this will again cause extra problems such as, product gas dilution with N_2 in the air and partial oxidation of valuable volatile gasses in to CO_2 [6]. DFB is a better technique for supplying the necessary energy demand for the steam gasification process [5]. DFB steam gasifiers are generally connected with a combustor to supply the heat energy required for endothermic gasification reactions via the circulated hot bed materials. The temperature in a fluidized bed gasification zone is typically around 850^0C (1123K)[23].The steam gasification process in a DFB reactor is illustrated schematically by Figure 3-7 [24].

High char content is preferred in steam gasification of bio mass, desiring more Carbon to react with steam and aiming a less tar content in products. A high char production can be expected from a process when there is a low temperature, low heating rate and a long gas residence time. But when the aim is to have more combustible gasses, then a higher temperature is preferred with lower heating rate and a longer gas residence time for the pyrolysis step [1].

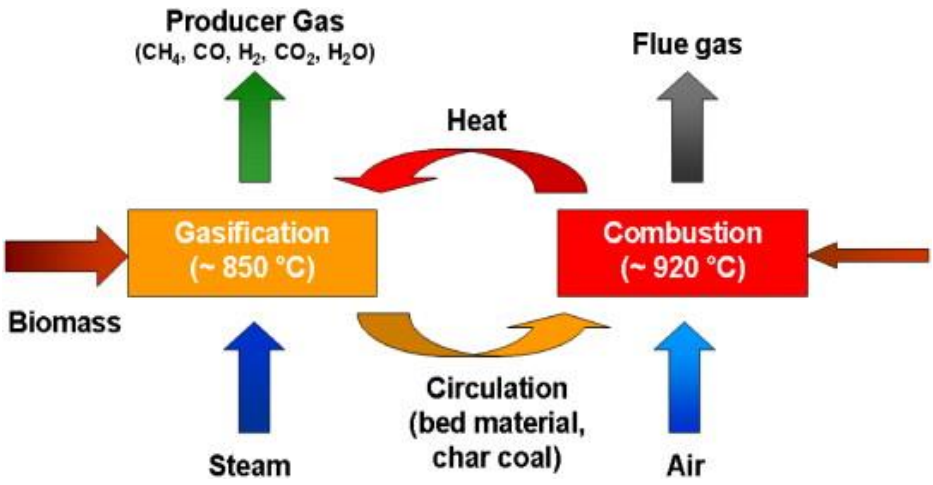

Figure 3-7: Gasification process in a DFB

3.4 Computational Particle Fluid Dynamics (CPFD) and Gasification

Different methods have been used to model the particulate multiphase flows. According to previous studies, continuum approach for both liquid and solid phases or continuum approach for the fluid and Lagrangian computational model for the particle phase has been used [25-31]. The two fluid continuum approach has many draw backs when it comes to the modeling of flows with different particle types and sizes [32, 33]. On the other hand this approach uses an averaging procedure which leads to many unclosed terms [31].

DPM is another model used for modeling the solid fluid flow behavior. It uses a finite number of discrete semi rigid particles interacting through contact forces and transferring momentum to and from the fluid by a drag closure model [25].This model is used in ANSYS FLUENT software to simulate the particulate flows. Even though it enables flows with wide range of particle types, sizes, shapes and velocities it limits its usage when the particle volume fraction is greater than 5%. This is due to the high collision frequency and the computational complexity that occurs in the presence of dense particle flows [34]. Therefore DPM solutions have been limited to the order of 2×10^5 number of particles and two dimensional solutions without a fluid phase [29].

The CPFD method developed by Snider [35] is suitable for modeling the reacting, thermal, particle laden fluid flows regardless of the solid volume fraction in the fluid (G0). It incorporates the numerical methodology called ‘multi-phase-partcle-in-cell’ (MP-PIC) [27, 35].This is a hybrid numerical method that uses Eulerian computational grid for solving the fluid phase and Lagrangian computational particles for modeling the solid phase [33]. The CPFD approach enables to solve the fluid and particle equations in three dimensions. Averaged Navier-Stokes equations which are strongly coupled with particle phase are used to describe the fluid dynamics, while particle momentum equations are ordinary differential equations with coupling to the fluid [35]. In the CPFD scheme, particles that have similar properties are defined as a numerical particle and this numerical particle is similar to a numerical control volume where a spatial region has a single property for the fluid[36]. ‘Barracuda VR ™’, the commercial software used in this study includes the CPFD approach for solving particle laden fluid flows.

Biomass steam gasification involves different streams of particle laden fluid flows. Especially biomass inlet streams and recycling streams contains higher particle volume fractions. Based on the applications there is a range of biomass types, sizes, shapes and velocities. Hence it was understood that ‘Barracuda’ is one of the best available tools for simulating biomass steam gasification process.

4 Model validation

An experiment was performed to check for the deviation of simulation results from that of the experimental. The test rig of a fluidized bed at Telemark University College was used for the experiment. Glass beads were used as the bed material and air was the fluidizing agent. There were pressure sensors placed in the bed and six pressure sensors were considered from 3cm, 13cm, 23cm, 33cm, 43cm and 53cm above the air distributor respectively. The height of the bed material was 52.5cm. Figure 4-1 shows a sketch of the test rig.

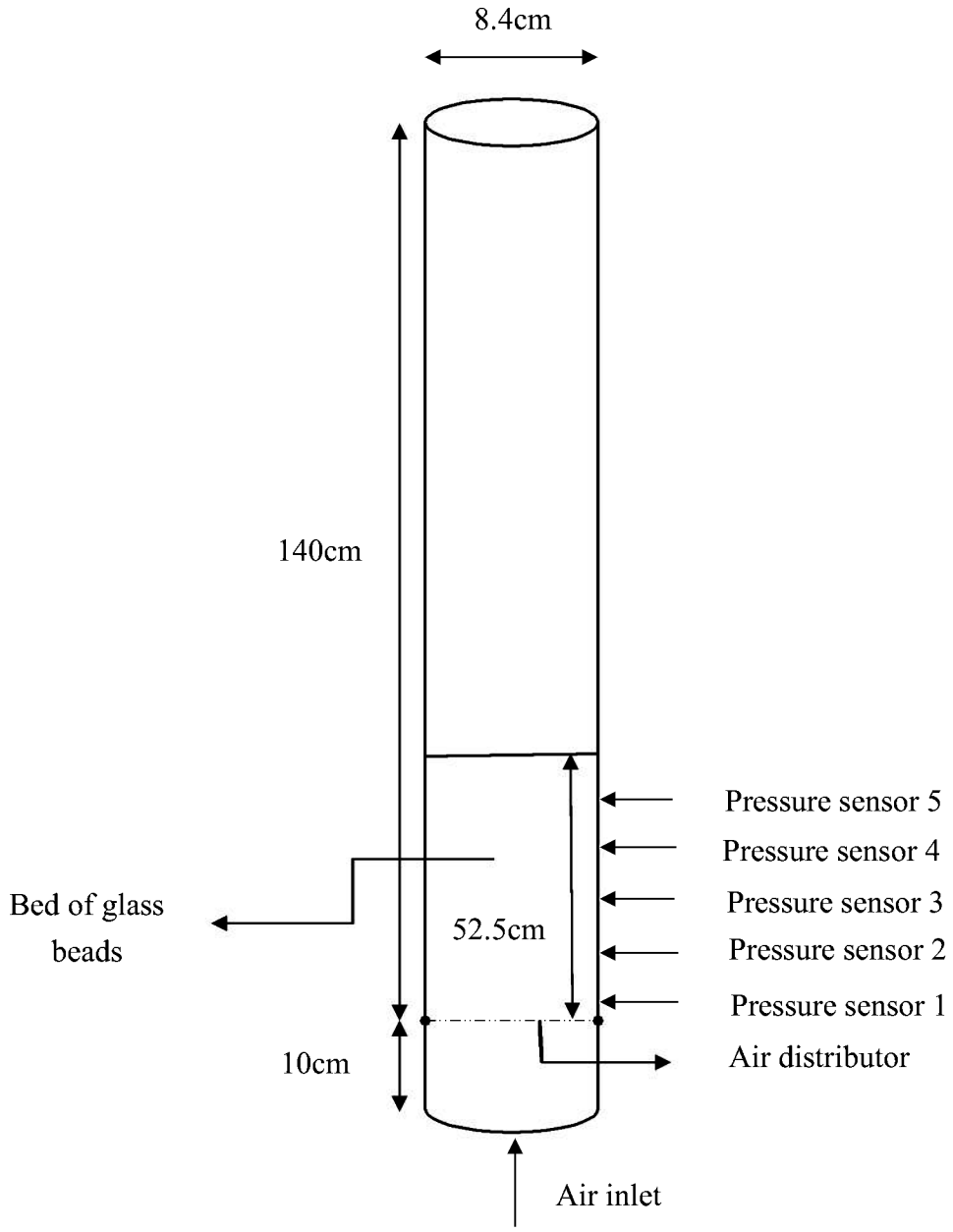

Figure 4-1: Sketch of the test rig for the fluidization

The air flow was adjusted to give the required air velocity in to the bed and the pressure sensors were connected to a Labview program for data acquisition. The pressure readings were recorded by the pressure sensors, corresponding to each air flow rate. A sieve analysis was performed, and the particle distribution of the bed material was found to be 300-400μm. The simulations were run under the same conditions as in the experiment (same geometry, same size range of bed materials, same inlet velocities, isothermal and without chemical reactions) using Barracuda. The experimental and the simulation results are plotted Figure 4-2 and the results agreed well. Both the experimental and the simulation results highlight a minimum fluidization velocity of 0.14m/s. This result proves that the simulation results are acceptable and the model can be used in the future work.

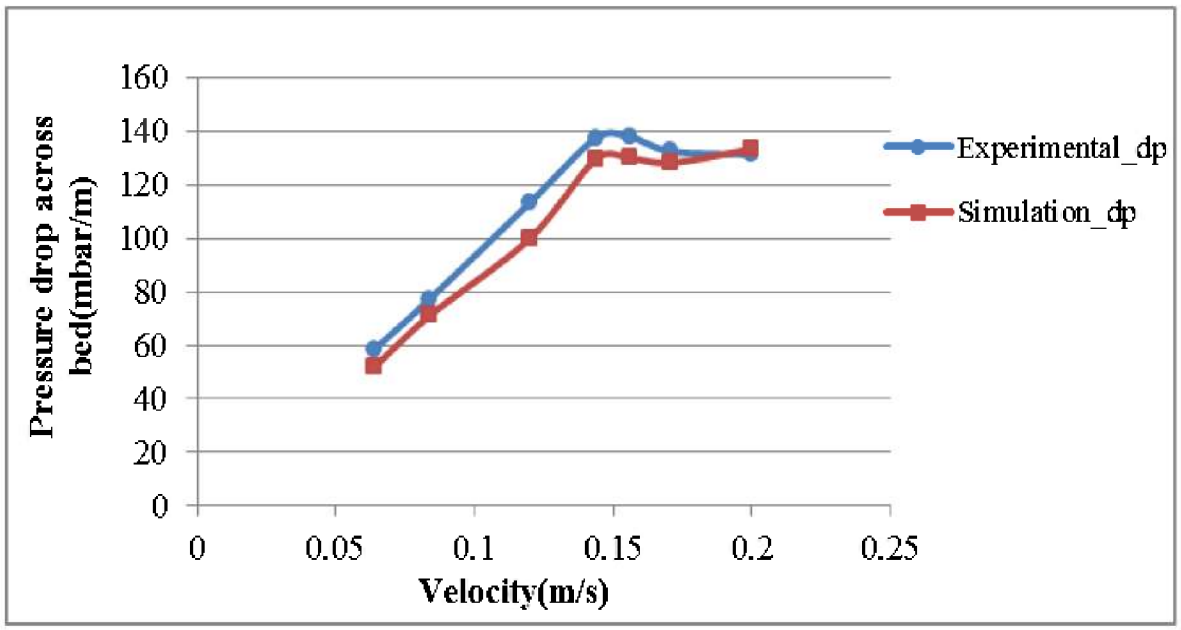

Figure 4-2: Pressure drop vs velocity

5 Simulation of cellulosic biomass gasification

This chapter explains how the 'Barracuda' software was used to optimize the steam gasification process. Basically the study will be done in seven sub cases, by varying the size of bed material, size of feed particles, the steam flow rate and steam temperature by aiming the quality of product gas. The biomass is considered to be made up of 65%volatiles and 35% fixed carbon for the simplicity [37].

5.1 Geometry and Mesh

A cylindrical geometry of 8.4cm diameter and 140cm height was considered for the gasification reactor. Five streams were considered as steam input, biomass input, hot bed material recycle, char and bed material out and product gas out from the top surface. The geometry and the input and output streams are shown in Figure 5-1.

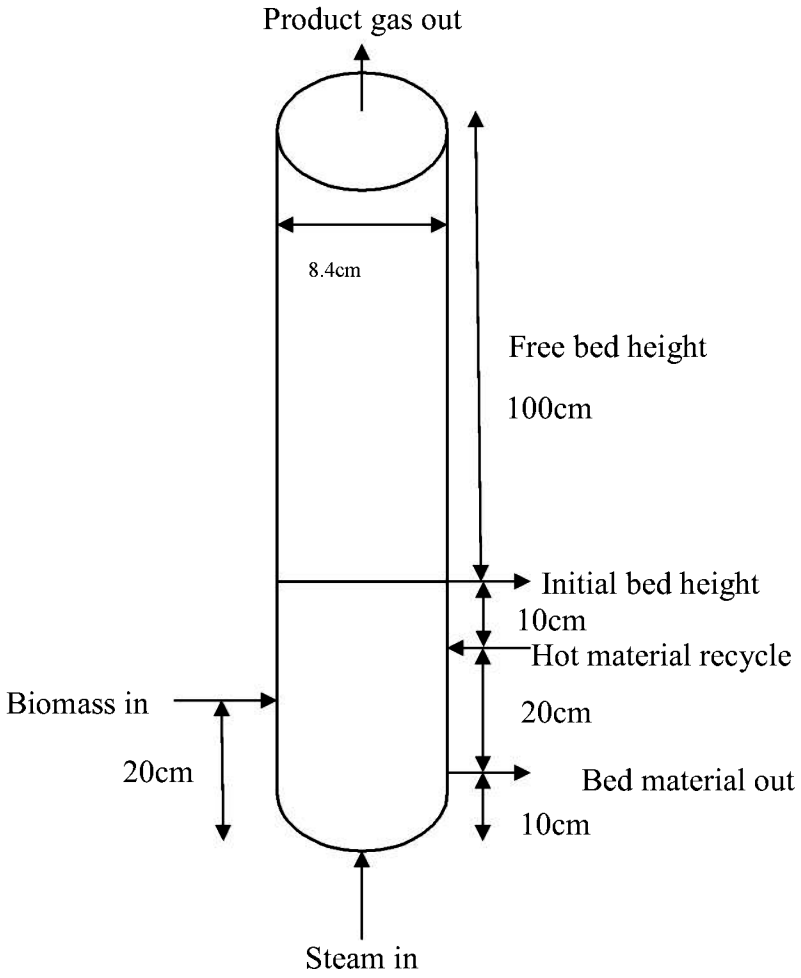

Figure 5-1:Simulation set up for biomass steam gasification

The geometry was drawn using Solid works software, imported to Barracuda as '.STL' file and meshed, so that the mesh can be adequately covered by the cylindrical volume. The irregularities of meshing were overcome by adding and moving grid lines across x, y, z directions as facilitated in Barracuda. The advanced options enabled to merge and remove the small cells which have volume fraction less than 0.04. The summary of mesh is recorded in *Table 5-1*. The CAD geometry and the meshed cylinder are shown in *Figure 5-2* (a) and (b).

Table 5-1: The summary of the mesh

X range(m)	0-0.084
Y range(m)	0.000-0.0889
Z range	0.002-1.399
Number of x grid cells(nx)	7
Number of y grid cells(ny)	6
Number of z grid cells(nz)	116
Total number of real cells	4408

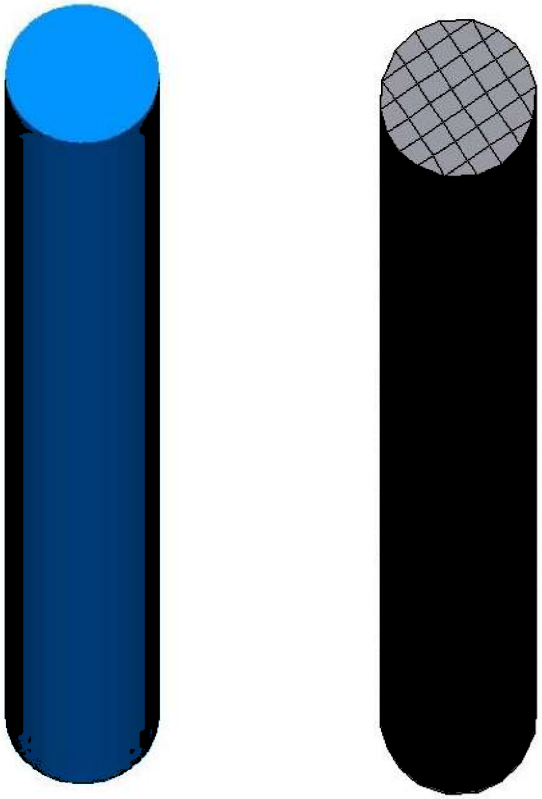

Figure 5-2:(a)The CAD geometry (b)The meshed geometry

5.2 Assumptions

The simulations are based on the following assumptions.

- Concerning the absence of air in the reactor, combustion reactions are neglected
- Biomass is broken in to 65% volatile gases and 35%char in the pyrolysis stage [37]
- The density of the biomass is close to that of softwood chips and assumed to be 180kg/m^3 in dry and ash free basis [38].
- Biomass is well dried and the water content is negligible.
- There is negligible Sulfur and Nitrogen content in the biomass fuel
- Biomass char is considered as mainly the pure carbon [19, 39].
- The size of the char particles is assumed to remain constant within the gasifier bed.
- The char coming from the combustion reactor becomes 1/10^{th} of its original size after undergoing the combustion reactions.
- According to Kern et al, [3] for a circulated fluidized bed steam gasification rector, the carbon conversion is typically higher than 99% for the whole system when the char present in the product gas stream is neglected.
- Gasification occurs at the temperature of 850^0C (1123K) [23].
- Product gas mainly contains CO, CO_2, H_2, CH4 and H_2O gases.

5.3 Input data

There are five streams which come in and go out of the biomass gasification reactor as explained in chapter 2, under the problem description. Table 5-2 shows the general data of the specific streams in and out of the gasification reactor during the simulations.

According to Kern etal [3], the gasification was assumed to occur at the height in the middle of the bubbling bed and therefor, the biomass feed was fed at the middle of the static bed assuming there will not be a considerable change of the height when the bed is fluidized.

Biomass pyrolysis occurs at the initial stage prior to the gasification stage and the released gas composition of volatile gases was recalculated from the data taken from literature [40].These pyrolysis data had been found for Birch wood with nearly 30% char generation and tar released conditions. Hence the recalculated data are approximations and mentioned in the Table 5-3.

Table 5-2:Input data for the material streams

Biomass inlet stream	
Solid	Cellulosic biomass
Fluid	Steam/CO_2
Particle size	(Vary on the case)
Solid flow rate(kg/h)	(Vary on the case)
Fluid flow rate(kg/h)	(Vary on the case)
Temperature(K)	(Vary on the case)
Steam in to the reactor	
Temperature (K)	Vary on the case
Pressure (bar)	1
Flow rate (m/s)	Vary on the case
Inlet area fraction	1
Bed material out to the combustor	
Solid	20%Char, 80% SiO_2
Fluid	Steam
Flow rate(kg/h)	Vary on the case
Temperature	1123K(850^0C)
Bed material recycle from the combustor	
Solid	1%Char, 99%SiO_2
Fluid	H_2O
Solid flow rate(kg/h)	Vary on the case
Fluid flow rate(kg/h)	Vary on the case
Temperature	1473K(1200^0C)
Bed material	
Composition	20%C, 80%SiO_2
Char Particle size(mm)	1
SiO_2 Particle size	Vary on the case

Table 5-3: Gas mass fractions resulted from pyrolysis

Gas component	Mass fraction
CO	0.48
CO_2	0.343
H_2	0.011
CH_4	0.166

5.4 Chemistry

The possible Chemical reactions which are considered to occur in a steam gasification reactor are Steam gasification (R1), CO_2 gasification (R_2), Methanation (R_3) and Water gas shift reaction. These reactions are listed from Equation (5-1) to (5-4).

R1 is dominant in a steam gasification reactor and R2 that is dominant when the gasification medium is air or Oxygen. The rate of reaction of R1 is higher than R2. R3 is mainly occurred with freshly devolatilized char. The reaction involves a volume increase, and hence high pressure and rapid heating encourage the reaction [41].

R4 is the most important reaction that is involved to generate more H_2. No volume increase is involved with this reaction and therefore it is insensitive to changes in pressure. The gas yield at equilibrium is reduced with increasing temperature and hence a lower temperature is seemed to be better. A higher temperature is important to maintain higher reaction rates too. Hence, in this situation, catalysts are required to achieve favorable yields through this reaction [41].

These chemical reactions and their kinetics were included in the simulations under the chemistry data input. The forward and backward reactions were taken into account and the reaction rates are tabulated in Table 5.4, with relevant to the reaction. The reaction heats for the involved reactions at 850^0C are shown in Table 5-5 [3]. Heat of reactions highlight, that the reaction R1 and R2 are highly endothermic while the reaction R3 and R4 are mildly exothermic. Anyhow, the net heat of reactions is endothermic and this tells the gasification process demands for energy.

(R1); Steam gasification

$$C(s) + H_2O \underset{r1b}{\overset{r1f}{\Leftrightarrow}} CO + H_2 \qquad (5\text{-}1)$$

(R2); CO_2 gasification

$$C(s) + CO_2 \underset{r2b}{\overset{r2f}{\Leftrightarrow}} 2CO \tag{5-2}$$

(R3); Methanation

$$0.5C(s) + H_2 \underset{r3b}{\overset{r3f}{\Leftrightarrow}} 0.5CH4 \tag{5-3}$$

(R4); Water gas shift

$$CO + H_2O \underset{r4b}{\overset{r4f}{\Leftrightarrow}} CO_2 + H_2 \tag{5-4}$$

Table 5-4: Rate of reactions for the gasification involved reactions

Reaction	Reaction rate
Steam gasification [42]	$r_{1f} = 1.372 m_s T \exp\left(\frac{-22645}{T}\right)[H_2O]$
	$r_{1b} = 1.044\times10^{-4} m_s T^2 \exp\left(\frac{-6319}{T} - 17.29\right)[H_2][CO]$
CO_2 gasification [42]	$r_{2f} = 1.272 m_s T \exp\left(\frac{-22645}{T}\right)[CO_2]$
	$r_{2b} = 1.044\times10^{-4} m_s T^2 \exp\left(\frac{-2363}{T} - 20.92\right)[CO]^2$
Methanation [42]	$r_{3f} = 1.368\times10^{-3} m_s T \exp\left(\frac{-8078}{T} - 7.087\right)[H_2]$
	$r_{3b} = 0.151 m_s T^{0.5} \exp\left(\frac{-13578}{T} - 0.372\right)[CH_4]^{0.5}$
Water gas shift [43, 44]	$r_{4f} = 7.68\times10^{10} m_s T \exp\left(\frac{-36640}{T}\right)[CO]^{0.5}[H_2O]$
	$r_{4b} = 6.4\times10^{9} m_s T \exp\left(\frac{-39260}{T}\right)[H_2]^{0.5}[CO_2]$

Table 5-5:Heat of reactions for the gasification involved reactions

Reaction	Heat of reaction $\Delta_{HR,850}$ [kJ/mol]
Steam gasification	+135.7
CO_2 gasification	+169.4
Methanation	-89.8
Water gas shift	-33.6

5.5 Boundary conditions and Initial conditions

Boundary conditions were defined at material inlet and outlet points. The defined boundary conditions are presented in the Table 5-6. The steam input, biomass input, recycle input and the bed material output points were defined as 'Flow boundary conditions'. The product gas outlet surface was defined as 'Pressure boundary conditions'.

Barracuda demands the initial conditions for both the fluid and particle phases. Hence they were defined with reference to the grid geometry. The cylindrical gasification reactor was initially filled with pure N_2 under the atmospheric pressure at a temperature of 1123K (850^0C). With regarding to the particles, it was initially filled with 20% char and 80% SiO_2 which has an initial bed temperature of 1123K. The close pack volume fraction was defined to be 0.6.

Table 5-6:Boundary conditions

Material stream	Location	Boundary condition
Steam input	Bottom face of the gasifier	Flow BC
Gas outlet	Upper face of the gasifier	Pressure BC
Feed biomass in	20cm upwards from the bottom surface	Flow BC
Char and bed material out	10cm upwards from the bottom surface facing from opposite side of feed biomass	Flow BC
Char and bed material recycle	30cm upwards from the bottom surface facing from opposite side of feed biomass	Flow BC

5.6 Sub cases

Different parameters were changed in the following cases to study about the effect of bed material size, feed biomass particle size, steam temperature and the gasification agent over the output gas quality. The difference of each case is explained in the following subcases.

5.6.1 Case-A; larger size bed material, low biomass feed flow

The specialty of Case-A is the size of the bed material (SiO_2) which was selected to be 2mm. The variables used in this case are tabulated in Table 5-7.

Table 5-7: Input data for Case-A

Biomass inlet stream	
Fluid	Steam
Particle size(mm)	1
Solid flow rate(kg/h)	10
Fluid flow rate(kg/h)	10
Steam in to the reactor	
Temperature (K)	900
Flow rate (m/s)	0.12
Bed material out to the combustor	
Fluid flow rate(kg/h)	3.6×10^{-9}
Bed material recycle from the combustor	
Solid flow rate(kg/h)	10
Fluid flow rate(kg/h)	10
Bed material	
SiO_2 Particle size(mm)	2

5.6.2 Case-B; Smaller bed material size, higher biomass feed flow with system mass controller

From Case-B onwards (All the other cases except Case-A), the size of bed materials were lowered down to 0.5mm which is $1/4^{th}$ of the size from Case-A. The special aim of this case is to observe the effect of discrete supply of biomass in to the reactor, by introducing a controller into the biomass feed stream. The case specific data is tabulated in Table 5-8.

Table 5-8:Input data for Case-B

Biomass inlet stream	
Fluid	Steam
Particle size(mm)	1
Solid flow rate(kg/h)	36
Fluid flow rate(kg/h)	3.6
Steam in to the reactor	
Temperature (K)	900
Flow rate (m/s)	0.001
Bed material out to the combustor	
Fluid flow rate(kg/h)	1.8×10^{-3}
Bed material recycle from the combustor	
Solid flow rate(kg/h)	36
Fluid flow rate(kg/h)	3.6
Bed material	
SiO_2 Particle size(mm)	0.5

5.6.3 Case-C to Case-G; Smaller bed material size, higher biomass feed flow with adjusted flow of bed material out

Case B was modified by increasing the rate of bed material and char flow, out of the reactor at the bottom to formulate Case-C. The aim was to avoid interruptions to the feed biomass due to the controller action and to assure the constant bed mass. In case D, the steam temperature was reduced down to 500K to investigate the effect of steam temperature for the gasification process. Case E was performed to study about the effect of increased input velocity on the steam gasification process. Hence the steam velocity was increased ten times compared to

Case C and the other variables were kept constant. Case-F was aimed to study about the effect of replacing H_2O with CO_2 in the biomass feed stream. Therefore the H_2O in the Case-C was replaced with CO_2 in Case-F and other variables were kept unchanged. The size of biomass was increased up to 5mm in Case-G. This is five times bigger than in the previous cases. The rest of the variables were kept as in Case-C. These data is summarized in Table 5-9. The variables which were changed in each case are highlighted for the clarity.

Table 5-9: Input data for Case-C to Case-G

Case number	C	D	E	F	G
Biomass inlet stream					
Fluid	Steam	Steam	Steam	CO_2	Steam
Particle size(mm)	1	1	1	1	5
Solid flow rate(kg/h)	36	36	36	36	36
Fluid flow rate(kg/h)	3.6	3.6	3.6	3.6	3.6
Steam in to the reactor					
Temperature (K)	900	500	900	900	900
Flow rate (m/s)	0.001	0.001	0.01	0.001	0.001
Bed material out to the combustor					
Fluid flow rate(kg/h)	1.44×10^{-2}	1.44×10^{-2}	1.44×10^{-2}	1.44×10^{-2}	1.44×10^{-2}
Bed material recycle from the combustor					
Solid flow rate(kg/h)	36	36	36	36	36
Fluid flow rate(kg/h)	3.6	3.6	3.6	3.6	3.6
Bed material					
SiO_2 Particle size(mm)	0.5	0.5	0.5	0.5	0.5

6 Results

This chapter includes the results of seven simulation cases. All the graphical results are taken at 15s of simulation time for the clarity of explanation and to avoid complications.

6.1 Case-A

In Case-A the simulation was run with 2mm size SiO_2 as the bed material. Figure 6-1 shows the molar composition of product gas. The fraction of CO is 42%, CH_4 is 25%, CO_2 is 19% and H_2 is 14%. Initially, a fluctuation of the gas composition was observed, but after very short time the composition is stable.

According to Figure 6-2, which shows the rate of gas production with time, CO is produced in the highest rate and H_2 in the lowest rate. CH_4 is seen to be produced in a higher rate than expected in comparison to H_2.

Figure 6-3 shows the cumulative gas production with time. Accordingly the total combustible gas production (CO, CH_4, H_2) during the 20s time period is 16 $\times 10^{-3} Sm^3$. This can be predicted as 70 Sm^3/day.

The individual gas mass fractions of H_2, CO and H_2O across the reactor cross sectional area at 15s are illustrated in Figure 6-4. The overall water mass fraction at the outlet of the reactor was calculated and it is as high as 84%. The rest 16% is the product gas. The biomass inlet region has high product gas concentration and the water concentration is dropped from bottom steam inlet to top where the product gas is taken out. But the water concentration is seemed to be lowest around the biomass inlet point.

As shown in Figure 6-5, the bed mass is kept nearly steady over the simulation time. The particle volume fraction, particle mass fraction of SiO_2 and C are shown in Figure 6-6 (a), (b) and (c) respectively at 15s of simulation. The bed seems to fluidize well and the particles remain within the reactor without being transported out with the gas flow. The calculated amount of particles released out with product gas stream is 33% of the input mass (biomass input and recycle input), which is considerable.

The pressure, temperature and the vector magnitude is shown by Figure 6-7(a), (b) and (c) respectively. The pressure is higher in the bottom bed region and gradually reduced across the bed. The pressure drop across the bed is 3000pa at 15s.The temperature seemed to be uniform within the reactor around 1125K except the red spot of hot bed material at the recycle point. The vector magnitude is to show the instantaneous fluid velocity at the given time. According to the Figure 6-7(c), which is an enlarged section of the bottom part of the reactor, the fluid velocity is higher at the hot bed material recycle point and at the biomass feed point as well as in some areas across the reactor upwards. The velocity is more or less zero around the point where the char and bed material is discharged out.

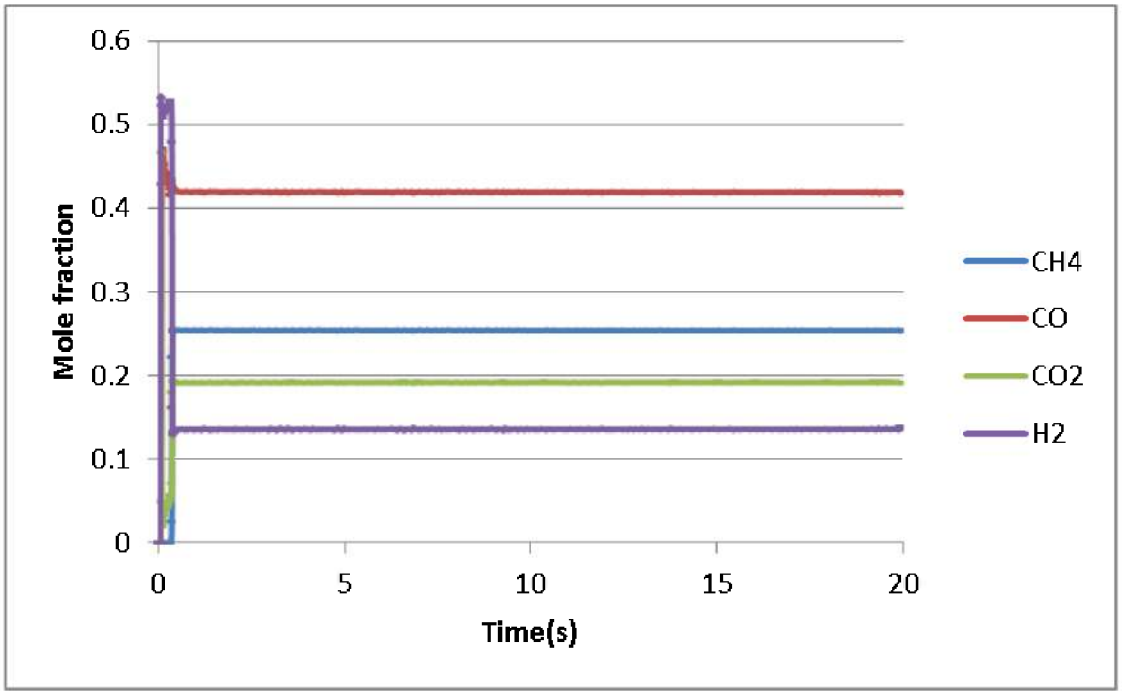

Figure 6-1: Molar composition of product gas vs time

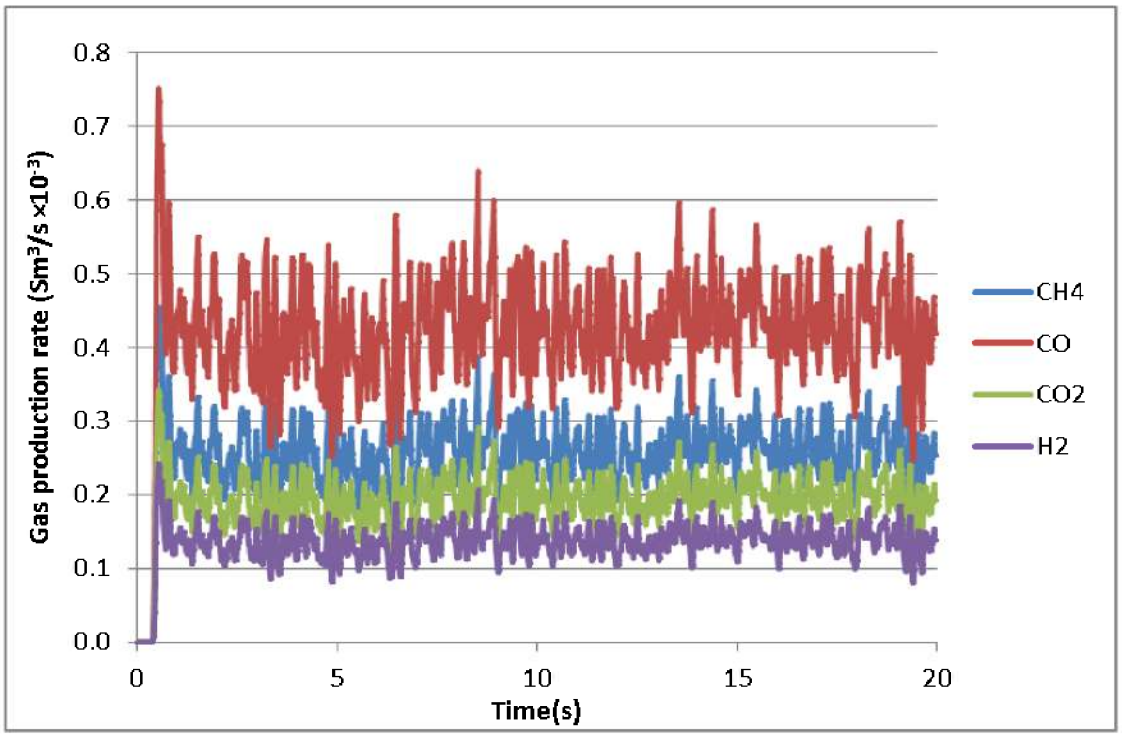

Figure 6-2: Rate of gas production vs time

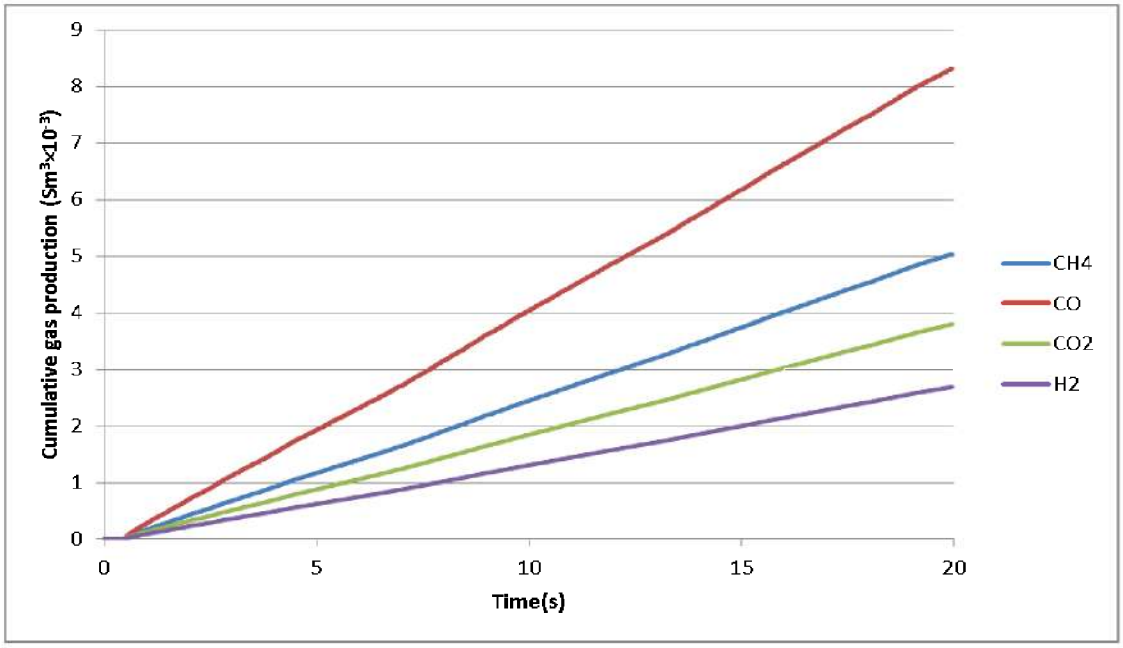

Figure 6-3: Cumulative gas production vs time

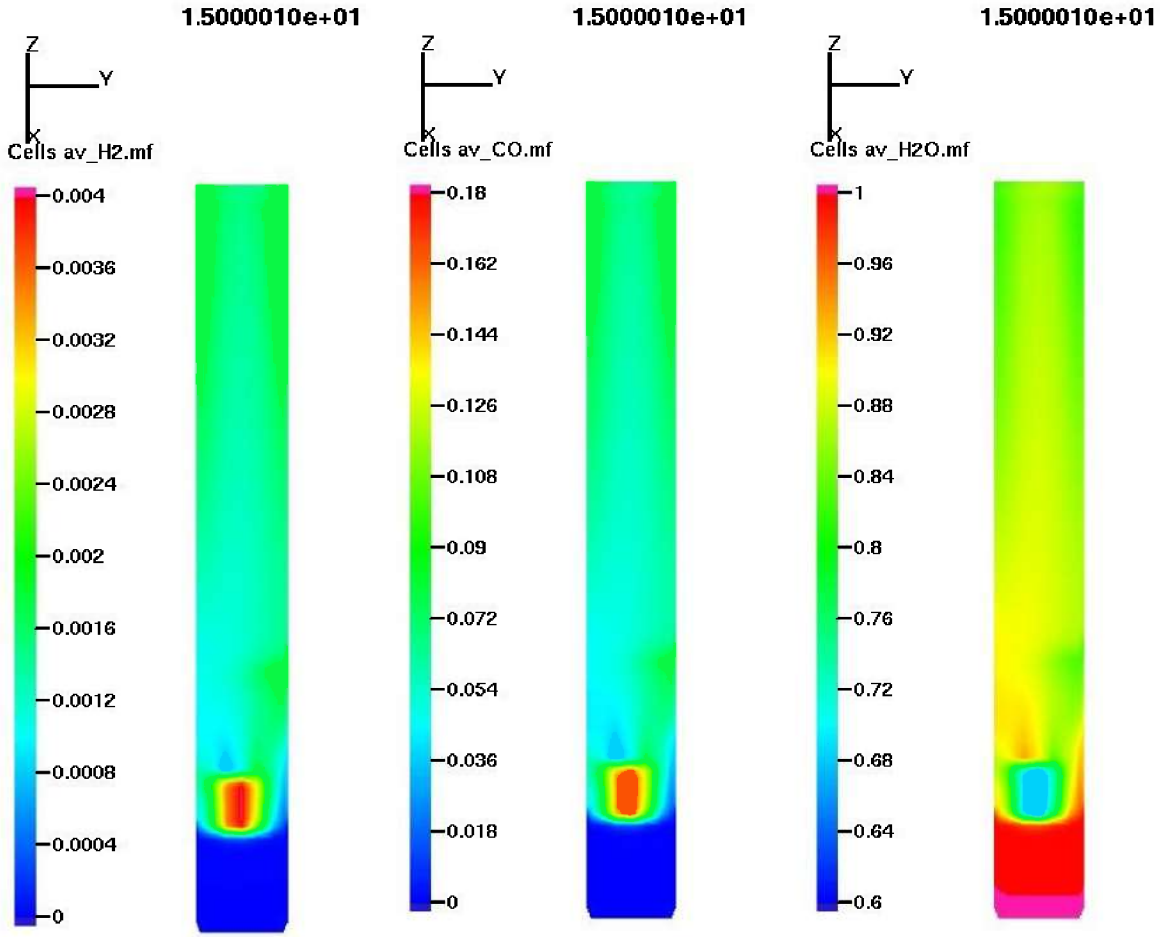

Figure 6-4: Mass fraction of (a)H2 (b)CO (C)H2O at 15s

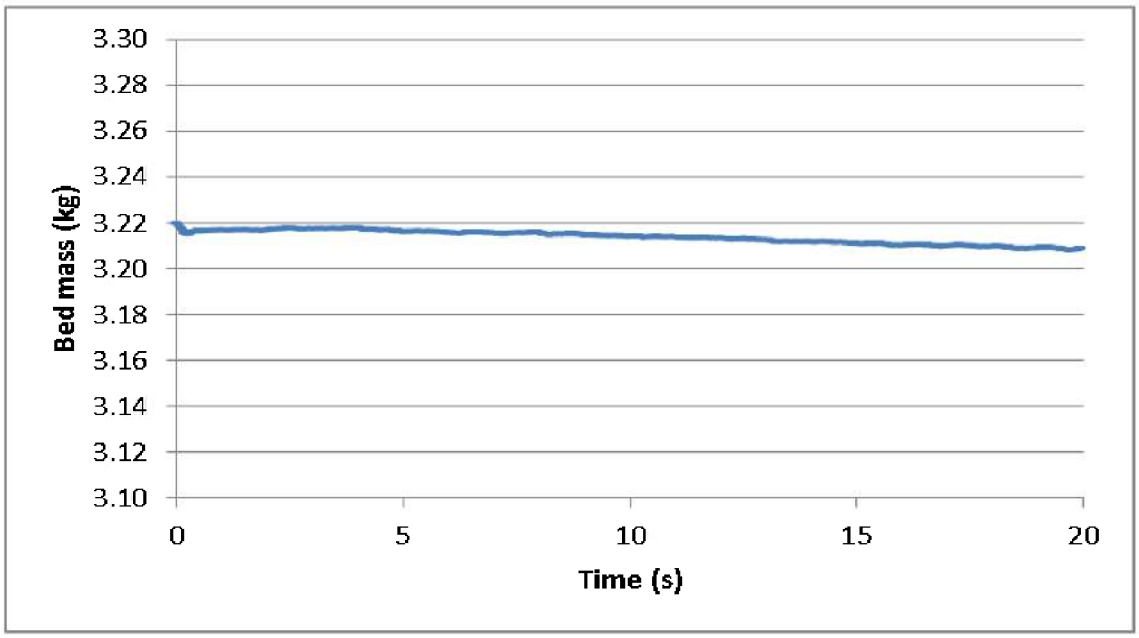

Figure 6-5: Reactor bed mass vs time

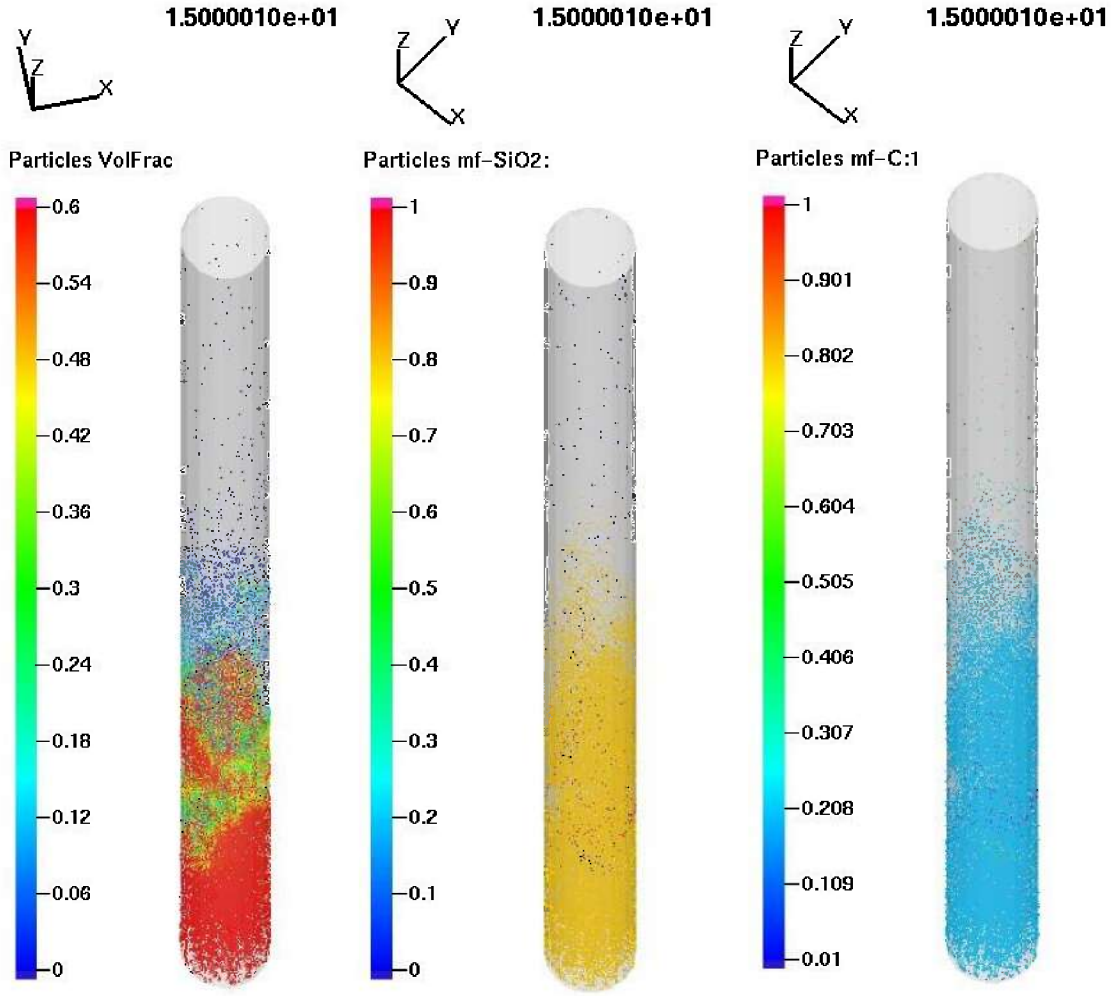

Figure 6-6:(a)Particle volume fraction (b) Mass fraction of SiO2 (c) Mass fraction of C

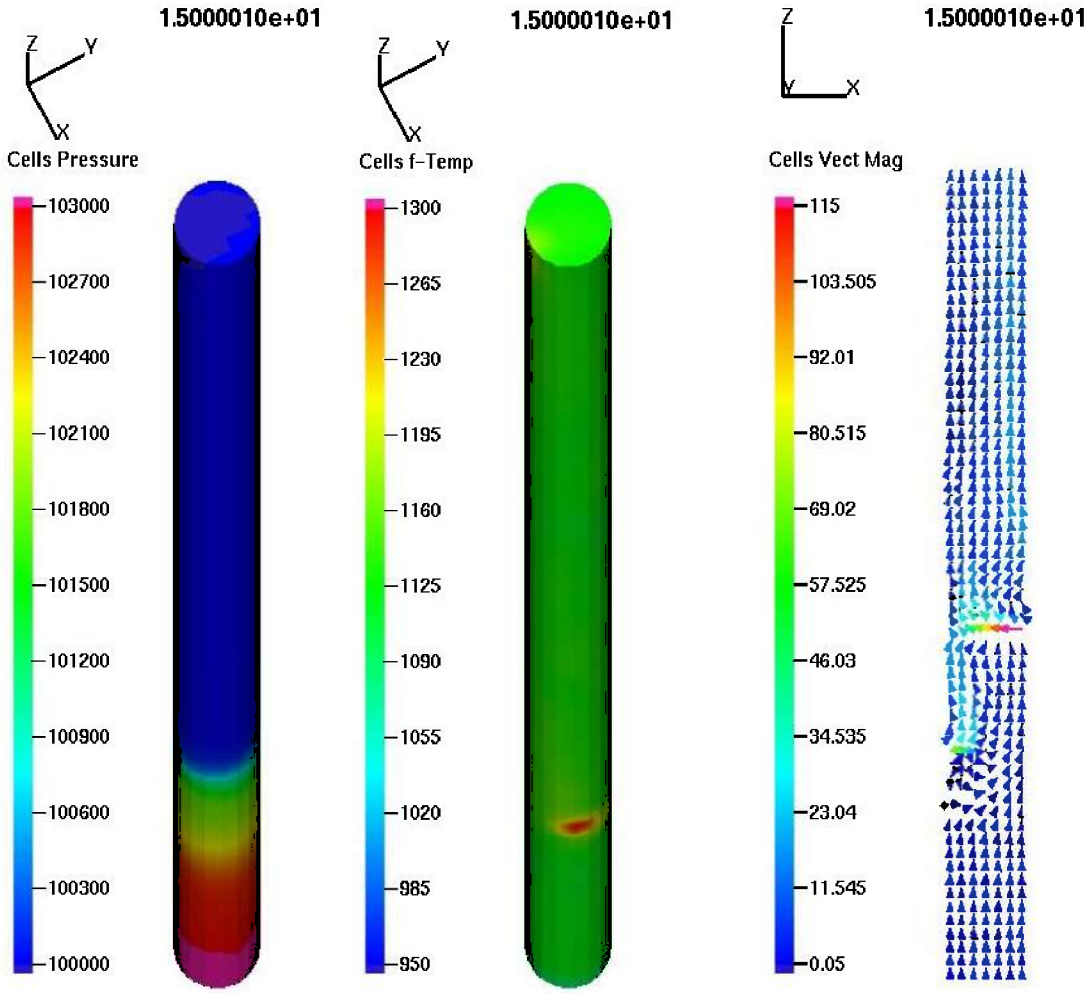

Figure 6-7:(a) Pressure (b) Temperature (c) Fluid velocity vectors across cross section

6.2 Case-B

The bed material size was reduced down to 500µm in this case. To maintain approximately constant system mass, the biomass feed and the recycle feed was increased. The required steam input velocity was lowered to 0.001m/s due to reduction of bed material size in order to avoid the pneumatic transport of bed material. In addition, a controller was given to the biomass feed to control the system mass. Accordingly the minimum allowed bed mass was set to 2.6kg and maximum was set to 2.61kg.

The product gas composition is shown in Figure 6-8 and there is no significant difference from Case-A. Figure 6-9 illustrates the rate of gas production over the time. The gas production is varied periodically such that the gas is produced for some time in constant rate and then dropped down periodically. Still the leading component is CO.

The cumulative gas production is presented by Figure 6-10 and the total production of combustible gases is around $30\times10^{-3}Sm^3$ for the simulated time and this can be extrapolated to 130 Sm^3/day. This is approximately twice the production of Case-A.

As Figure 6-11illustrates, the bed mass is fluctuated between 2.6kg to 2.61kg. Once the mass reaches the upper limit of the controller it falls down to lower limit and then starts to rise up again.

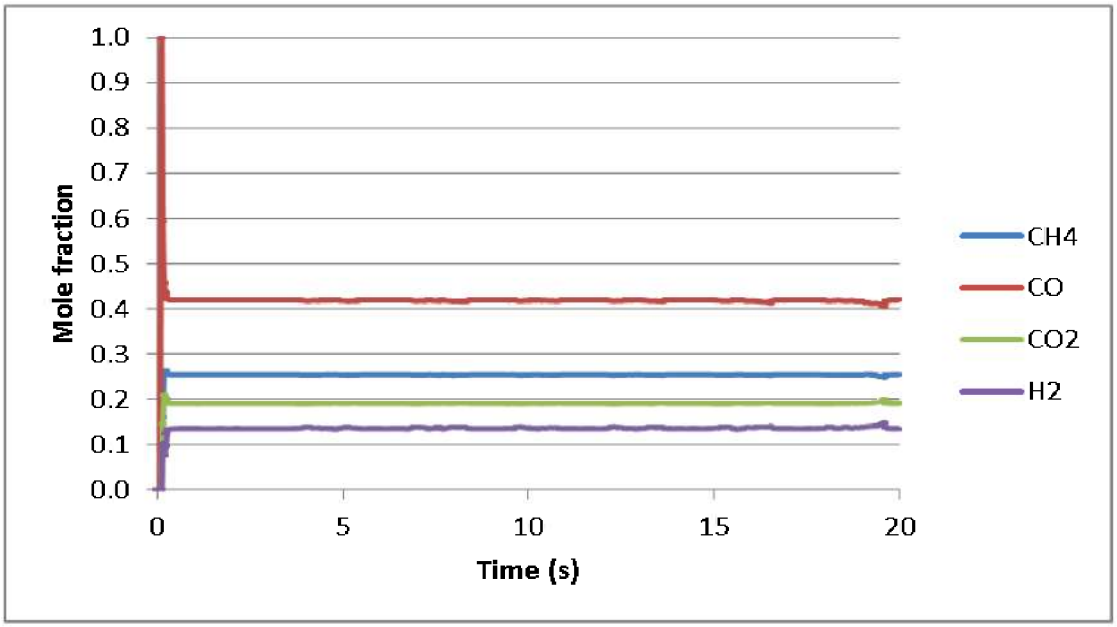

Figure 6-8: Molar composition of product gas vs time

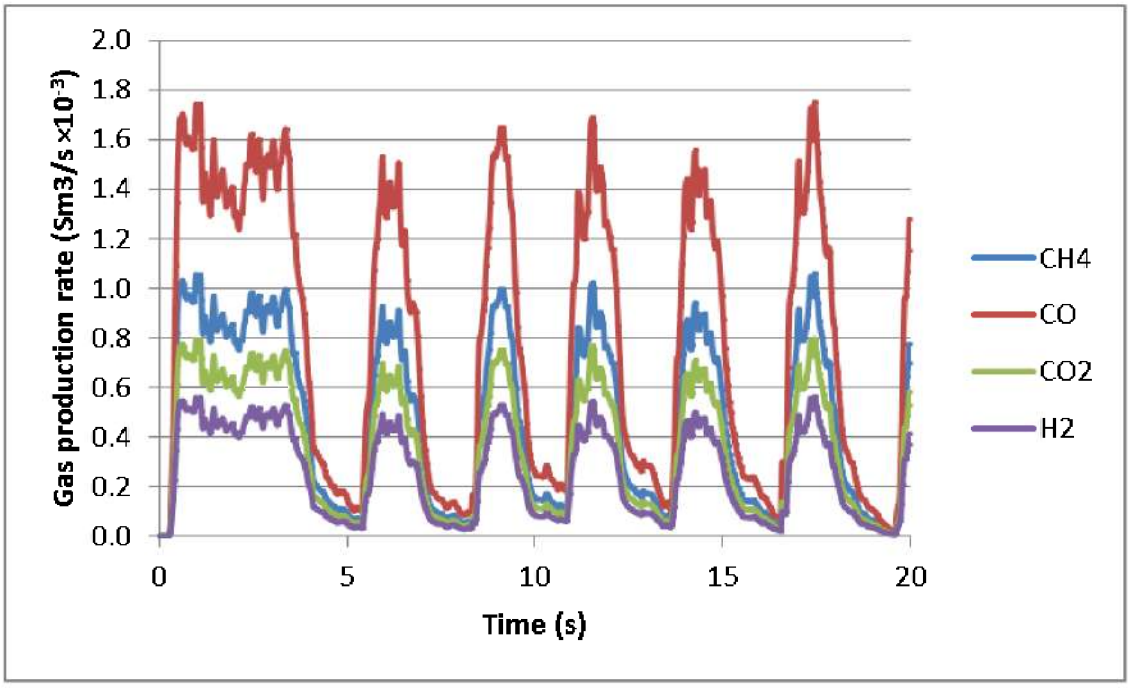

Figure 6-9: Rate of gas production vs time

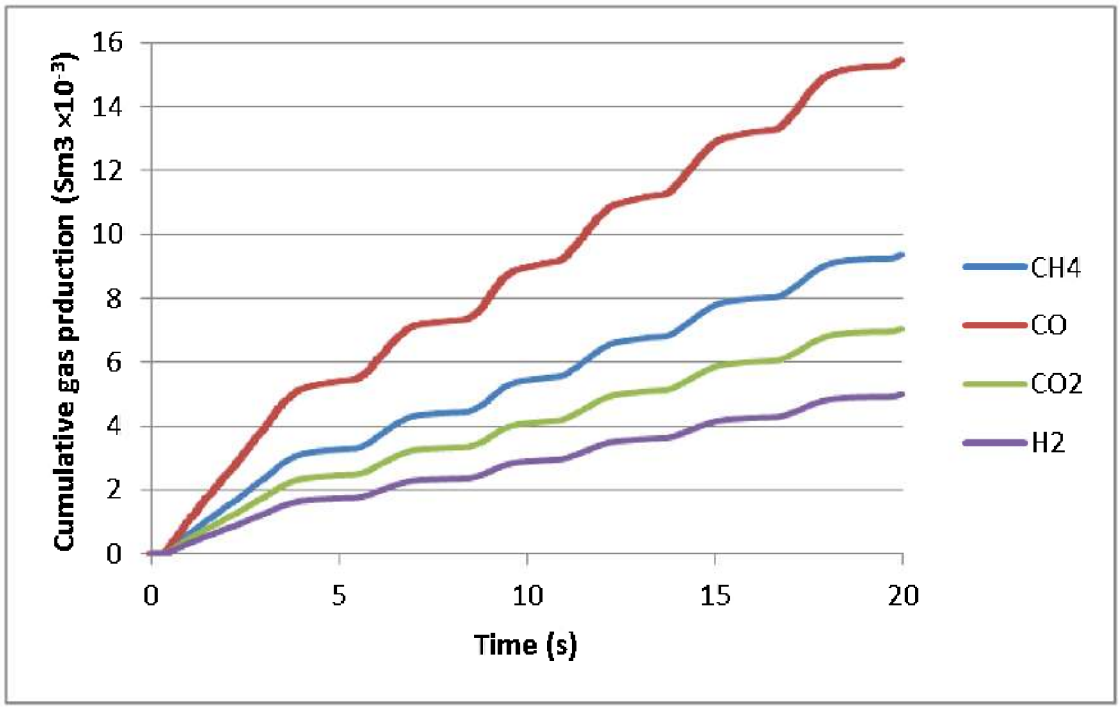

Figure 6-10: Cumulative gas production vs time

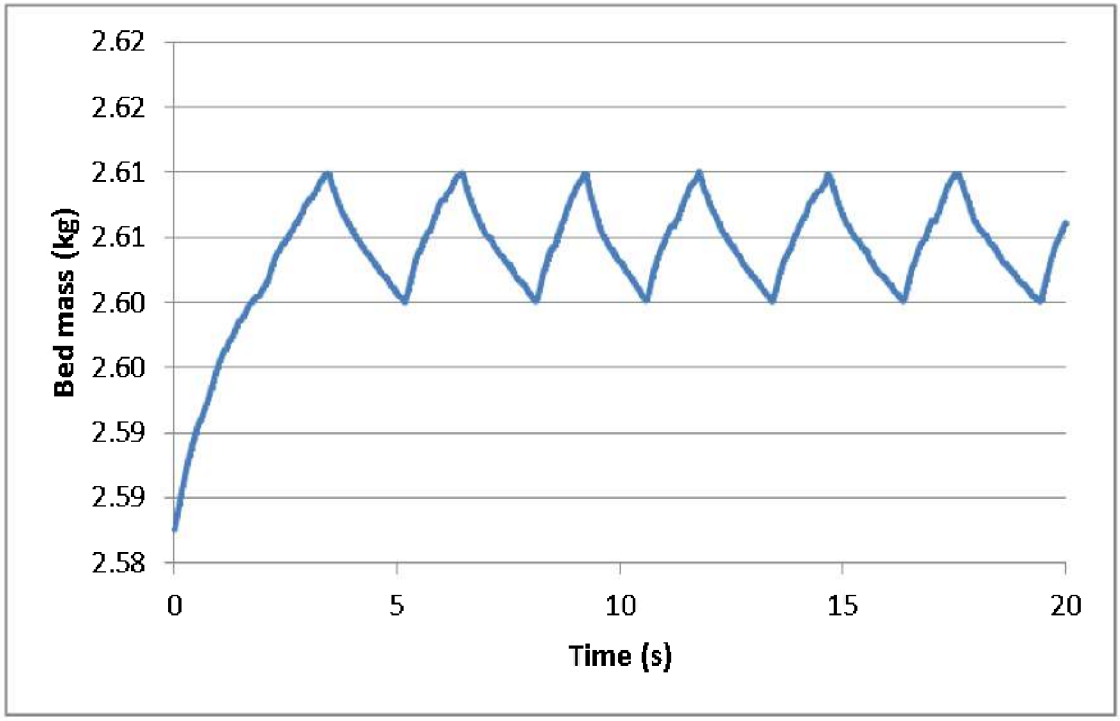

Figure 6-11: Reactor bed mass vs time

6.3 Case-C

Case B was modified by increasing the bed material and char flow, out of the reactor at the bottom. The aim was to avoid interruptions to the feed biomass due to the controller action and to assure the constant bed mass. Figure 6-12 shows a similar product gas composition as for the previous cases at the reactor outlet. According to Figure 6-13, the rate of gas production has been improved compared to Case-A and Case-B, as the production is kept steady over the time. As Figure 6-14 illustrates, the cumulative gas production is also improved, showing a total cumulative combustible gas production of 60×10^{-3} Sm^3 over 20s. This production can be predicted as 260 Sm^3/day.

The mass concentrations of H_2, CO and H_2O within the reactor and across the cross section are shown in Figure 6-15, Figure 6-16 and Figure 6-17 at 15s. The overall water mass fraction was calculated as 34% at the product gas outlet and this is conciderably lower than in Case-A. Figure 6-18 shows the bed mass over the simulation time and the trend assures a steady bed mass with insignificant fluctuations.

The particle volume fraction, mass fraction of SiO_2 and the mass fraction of C within the gasifier at 15s are illustrated in Figure 6-19(a), (b) and (c) respectively. According to these figures, there is a fraction of C particles that can be seen to release with the outlet gas stream. According to the calculations, the released particle amount at the outlet is 31% of the input mass.

Figure 6-20(a), (b) and (c) are a representation of instantaneous pressure, temperature, and fluid vectors at 15s of simulation. The pressure drop across the bed is approximately 2000 Pa which is quite less than in Case-A. As shown in Figure 6-20(b), the reactor has low temperature regions especially in the upper part. The velocity vectors have not changed much, but upper region seems to accelerate more than in Case-A.

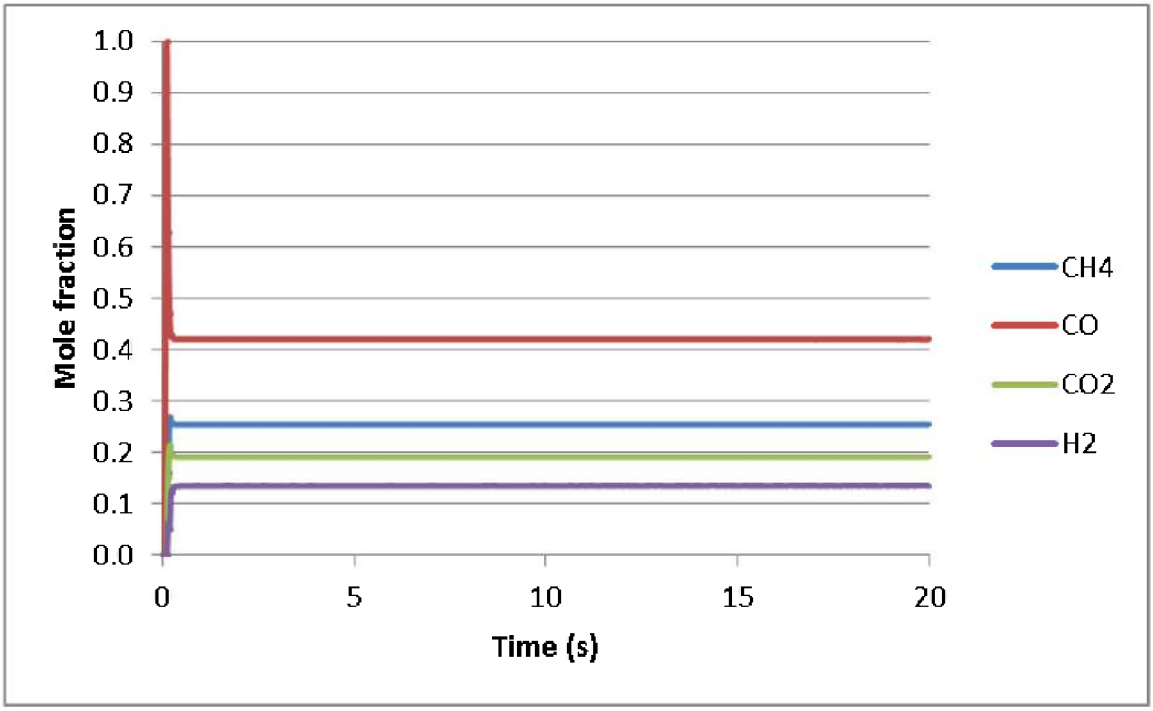

Figure 6-12: Molar composition of product gas vs time

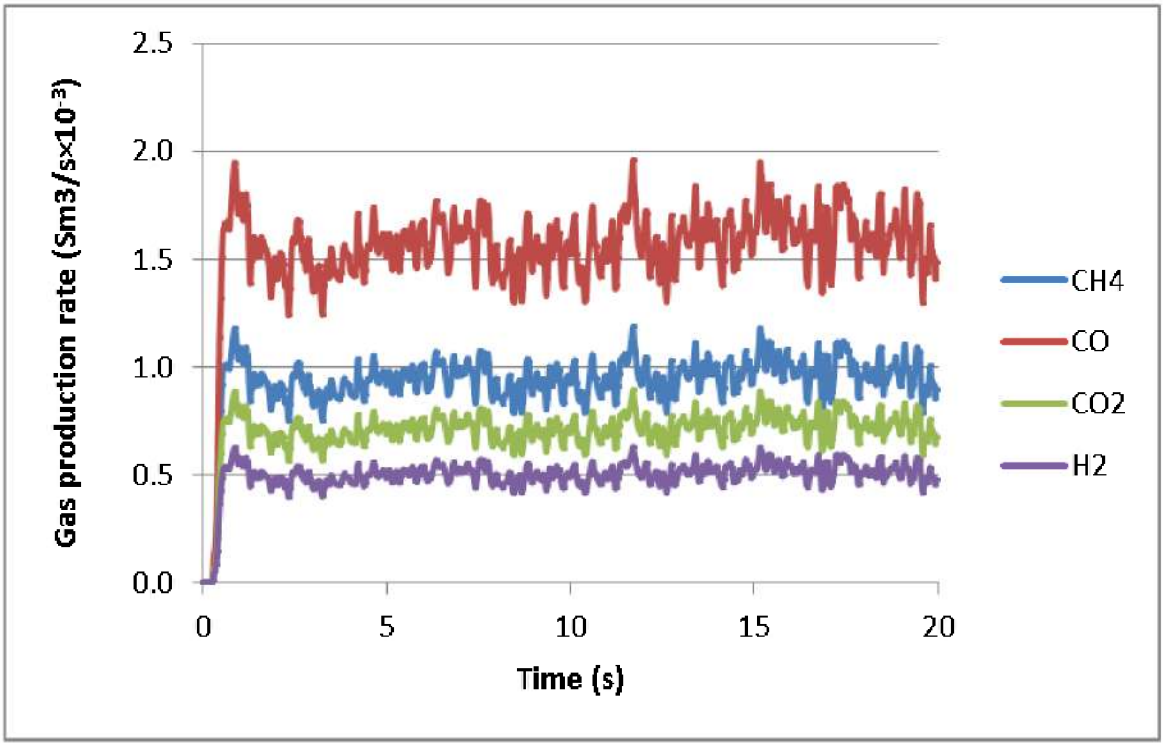

Figure 6-13: Rate of gas production vs time

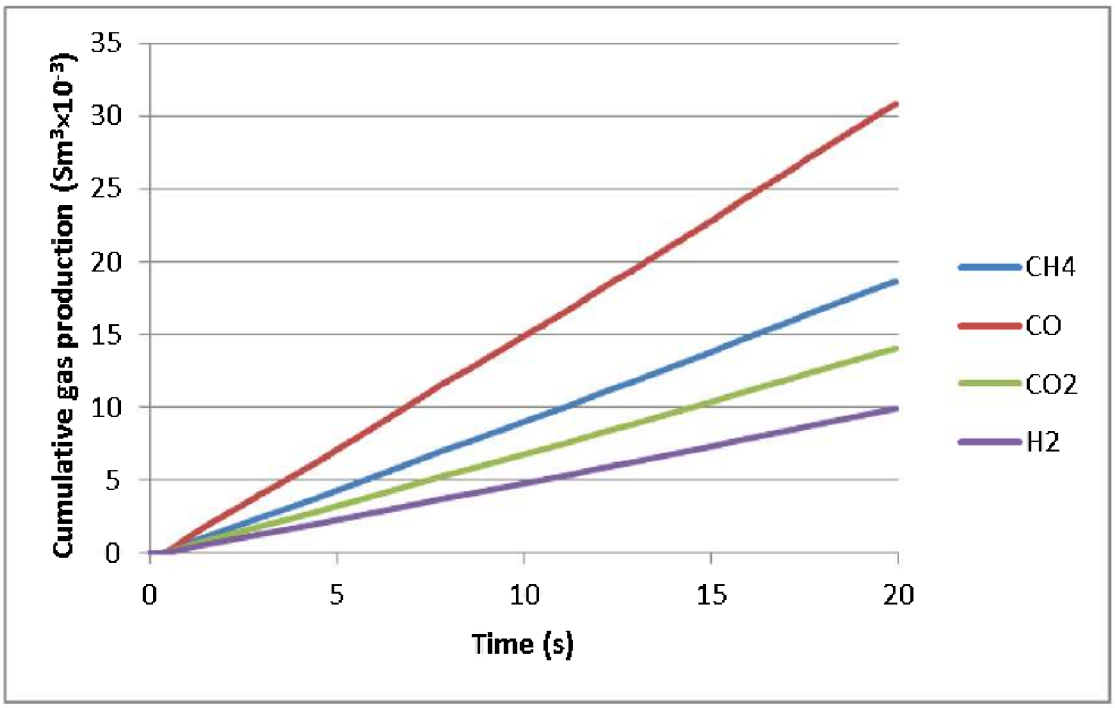

Figure 6-14: Cumulative gas production vs time

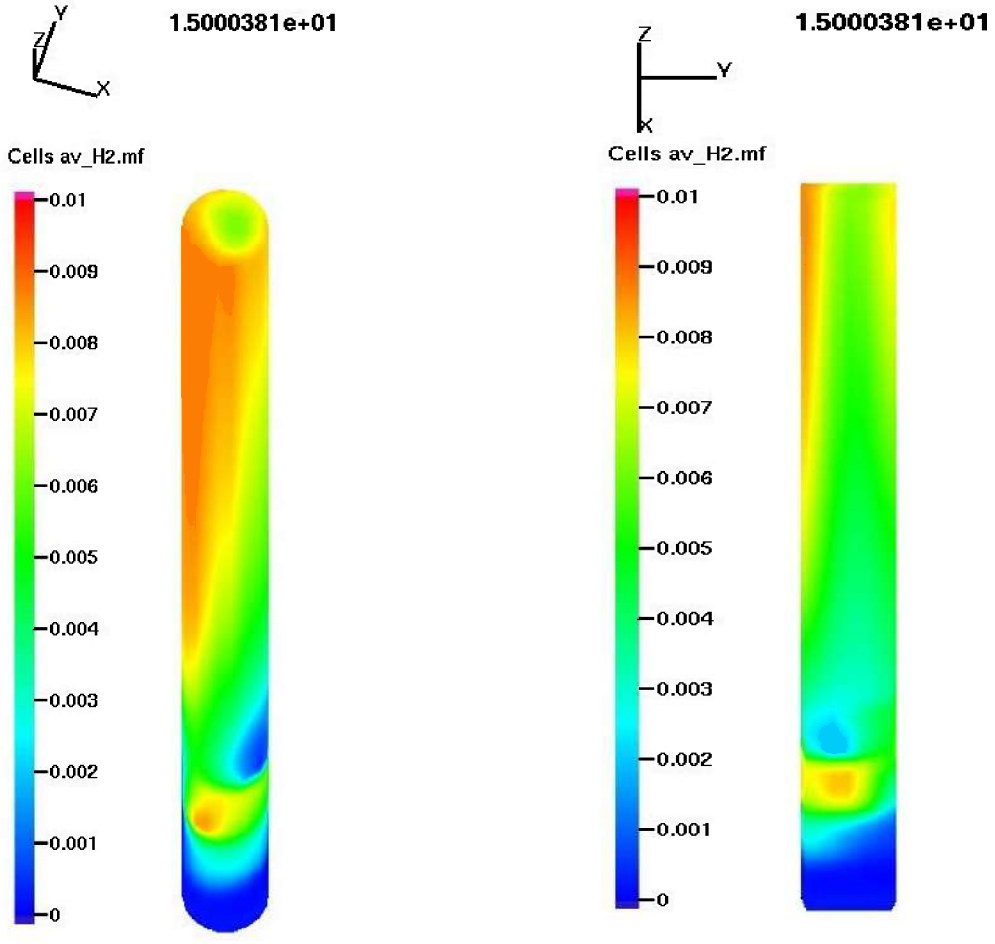

Figure 6-15: Average mass fraction of H2

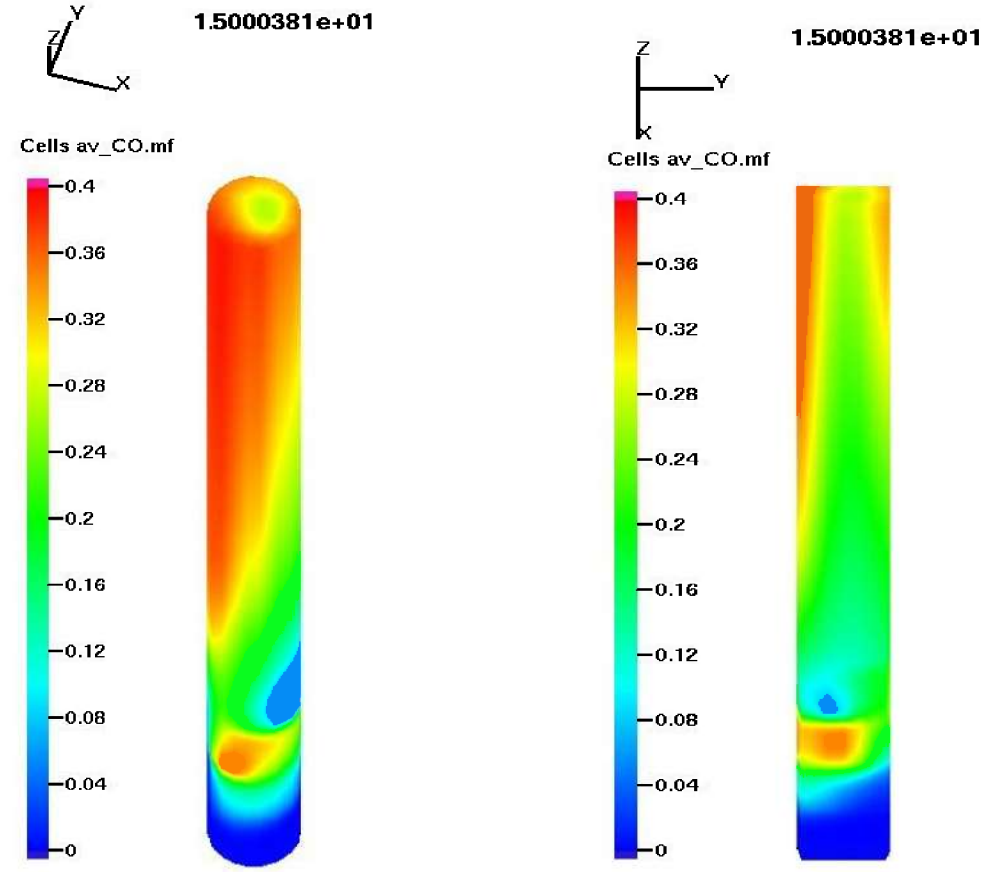

Figure 6-16:Average mass fraction of CO

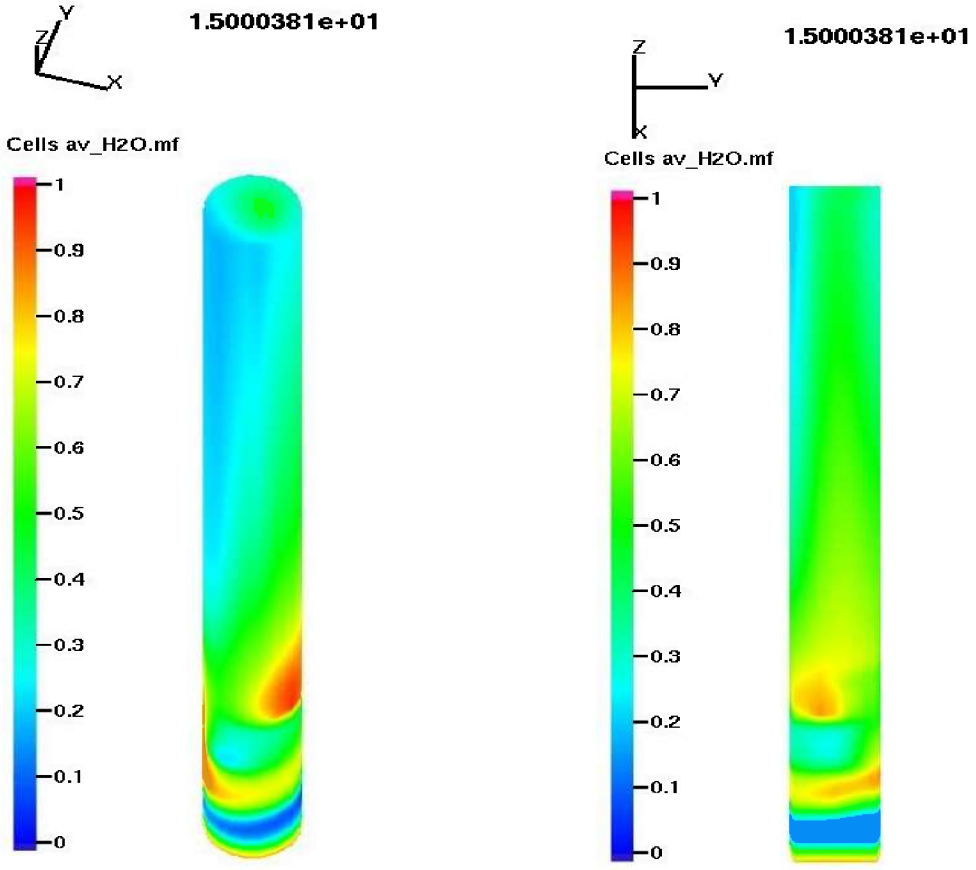

Figure 6-17: Avrage mass fraction of H2O

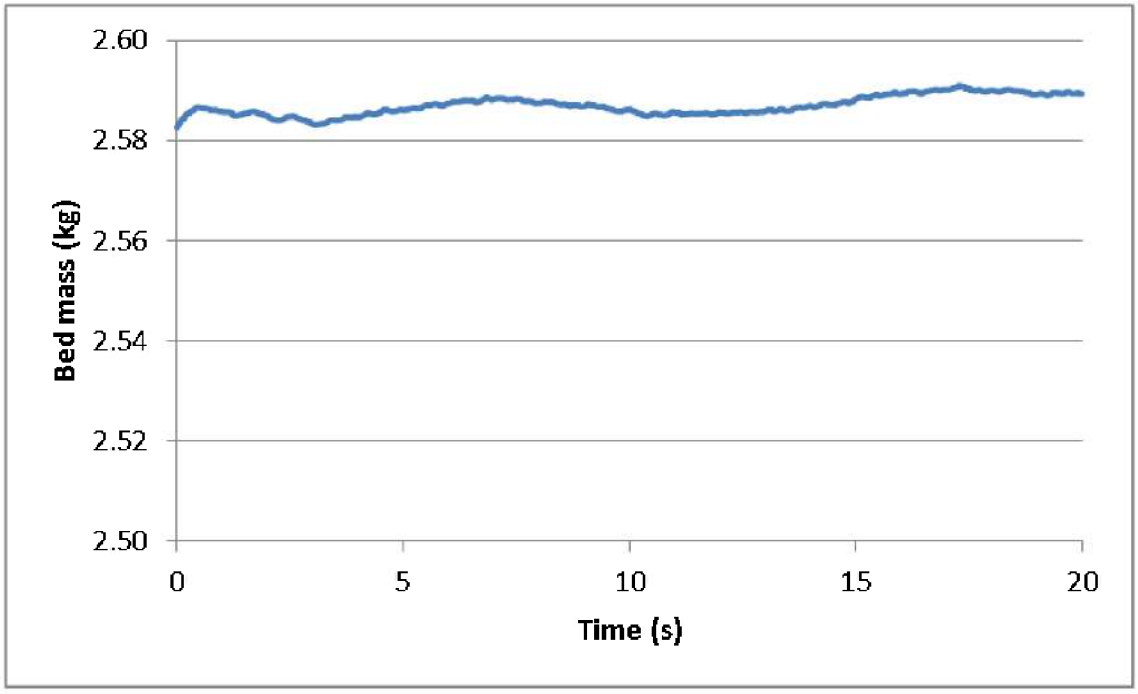

Figure 6-18: Reactor bed mass vs time

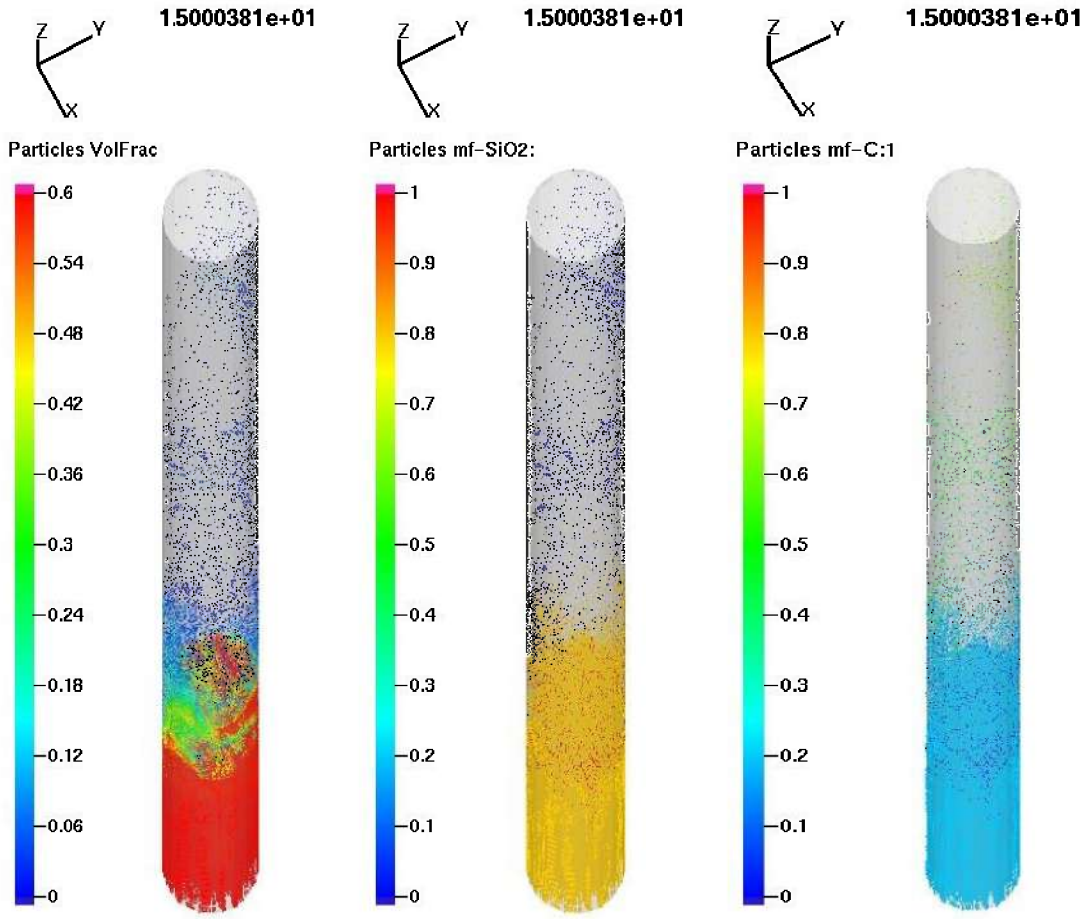

Figure 6-19:(a)Particle volume fraction (b)Mass fraction of SiO2 (c)Mass fraction of C

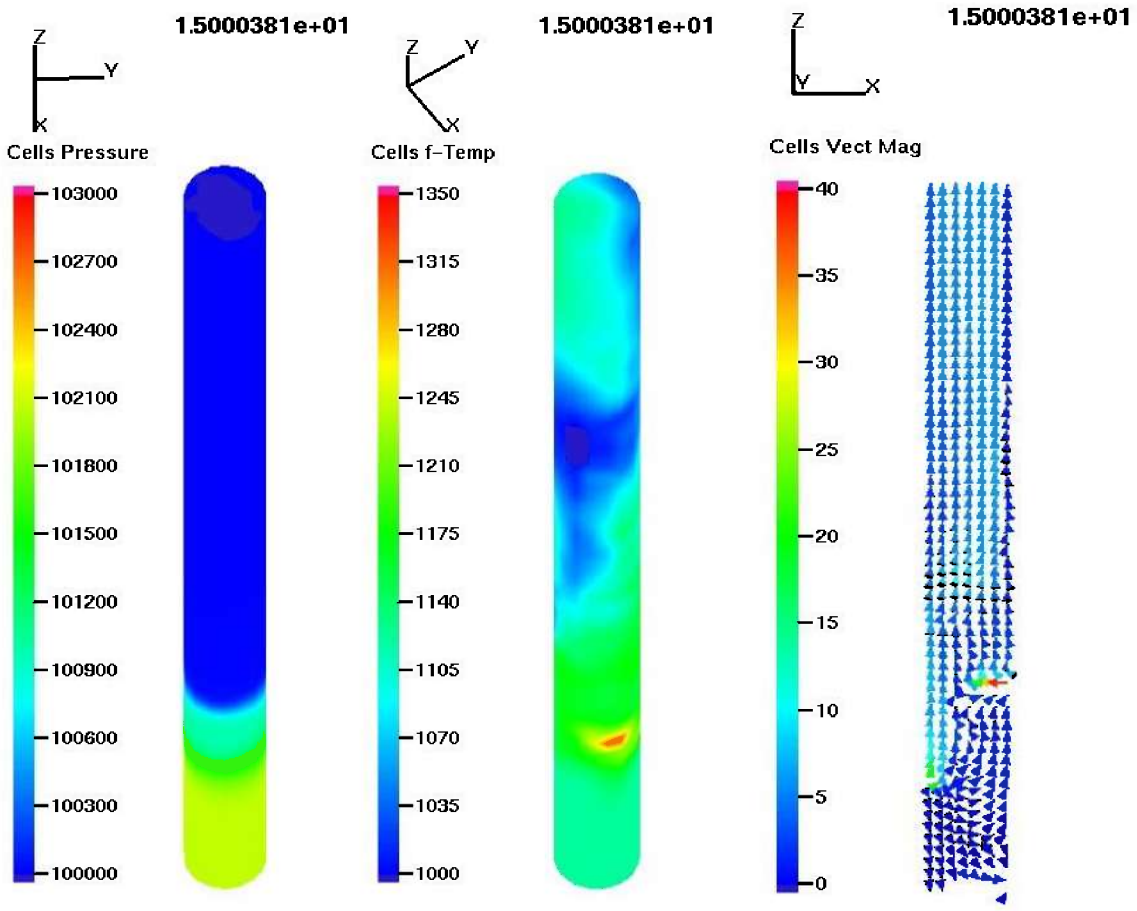

Figure 6-20:(a)Pressure (b)Temperature (c)Fluid vectors across cross section

6.4 Case-D

In case D, the steam temperature was reduced down to 500K to investigate the effect of steam temperature for the gasification process. Figure 6-21 shows the molar fraction of gas components with time and the composition shows no difference from the previous cases. But according to Figure 6-22 and Figure 6-23, the rate of gas production and the cumulative gas production has decreased significantly in comparison to Case-C. The cumulative volume of combustible gasses is $42\times10^{-3}Sm^3$ over the simulation time and this can be extrapolated to 181 Sm^3/day.

Figure 6-24 is a representation of gas mass fractions of H_2, CO and H_2O. The overall water mass fraction was calculated as 41% and this is little higher than in Case-C.

The reactor bed mass seems to be constant within the simulation time as presented in Figure 6-25. Figure 6-26 shows the particle volume fraction, mass fraction of SiO_2 and C within the reactor at 15s simulation time. According to these figures it is visible that some amount of particles that contain more Carbon, are released out with the product gas. The amount of particles released at the reactor outlet was calculated as 35% of the input mass.

The fluid pressure, temperature and instantaneous velocity, at 15s of simulation time, are shown in Figure 6-27(a), (b) and (C) respectively. The pressure drop across the bed can be approximated as 1100 Pa and this is considerably low in comparison to the Case-A and Case-C. The temperature is seemed to vary significantly within the reactor and cold spots and regions are visible above the bed. The trend of fluid velocity vectors look similar to the previous cases, but have higher values at the fluid entering points.

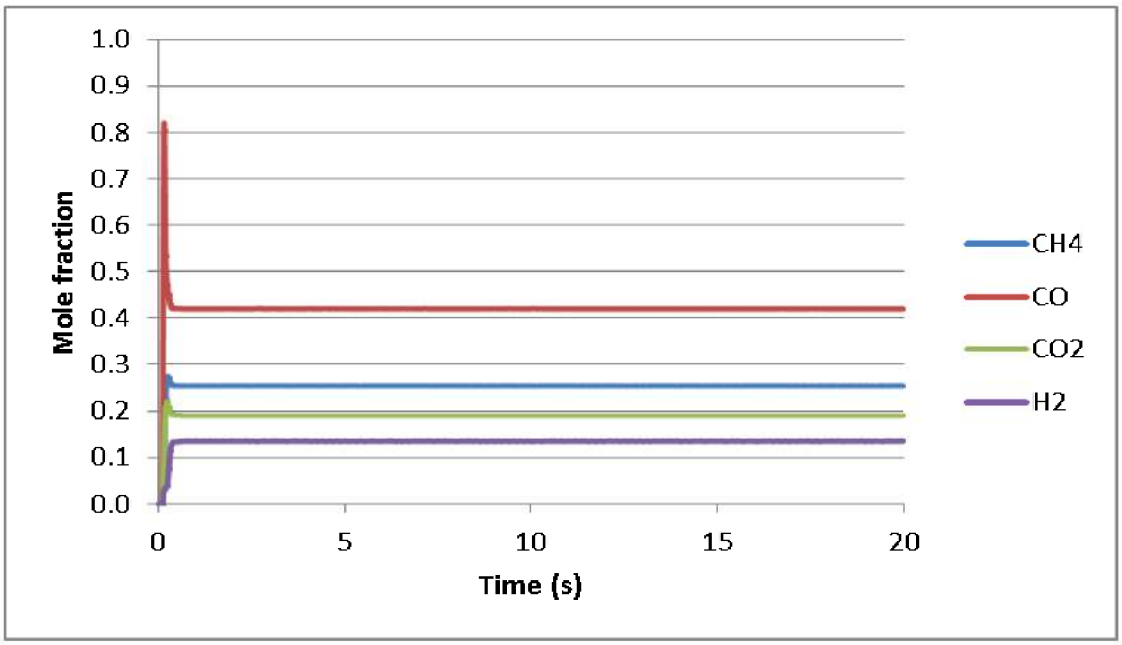

Figure 6-21: Molar composition of product gas vs time

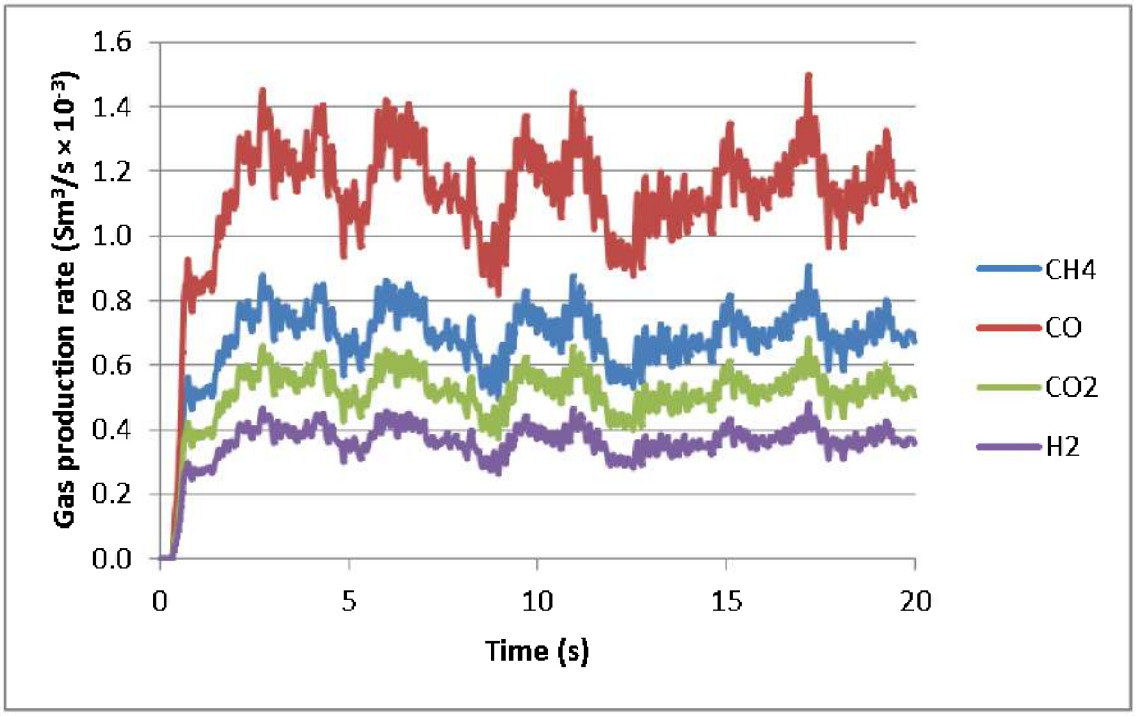

Figure 6-22: Rate of gas production vs time

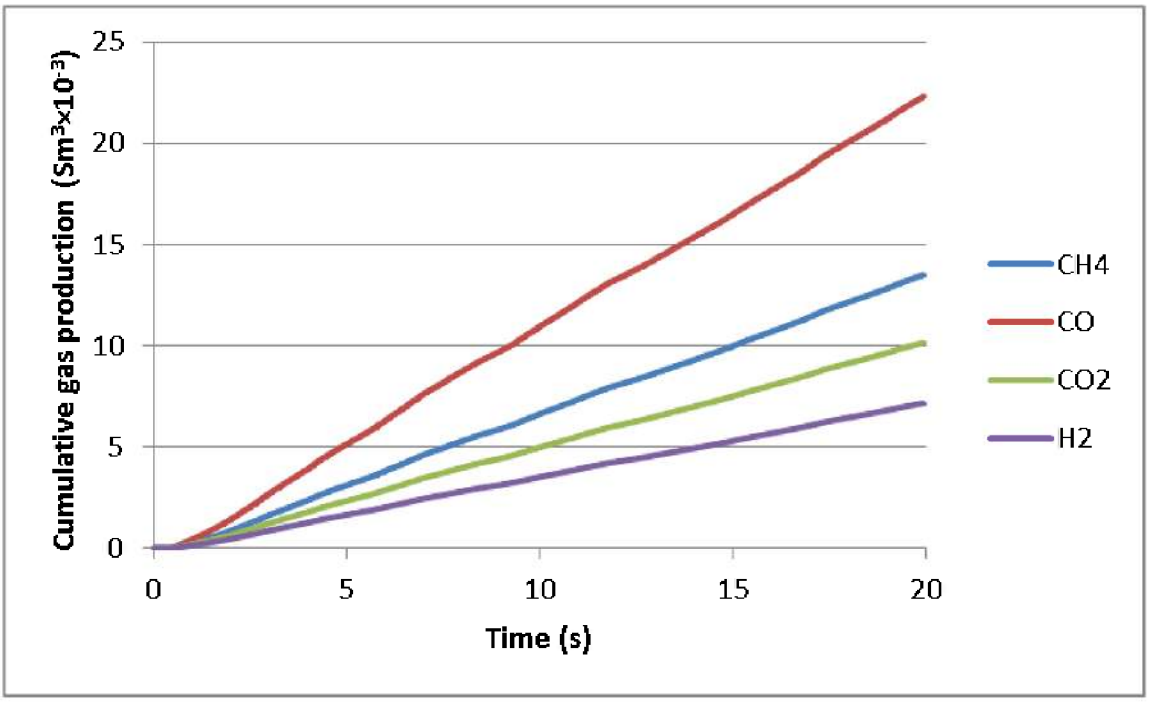

Figure 6-23: Cumulative gas production vs time

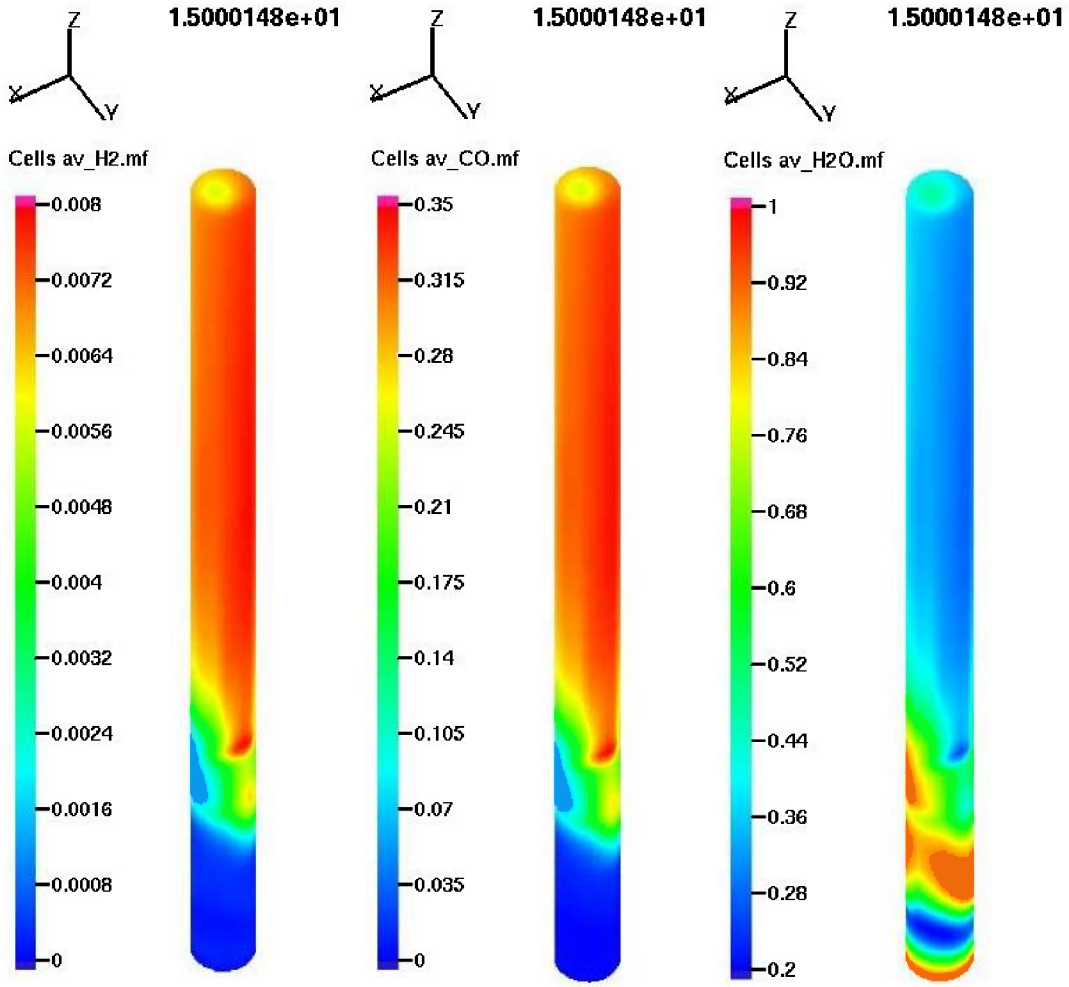

Figure 6-24 :Average mass fraction of (a) H2 (b)CO (c)H2O at 15s

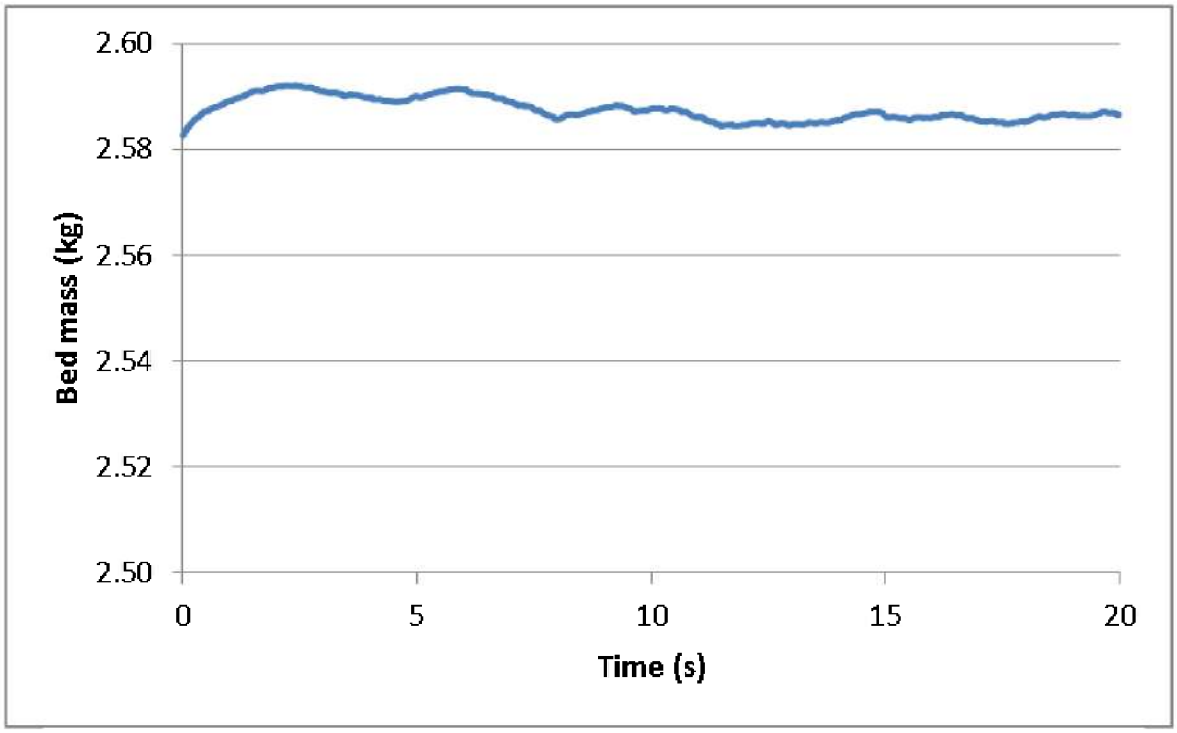

Figure 6-25: Reactor bed mass vs time

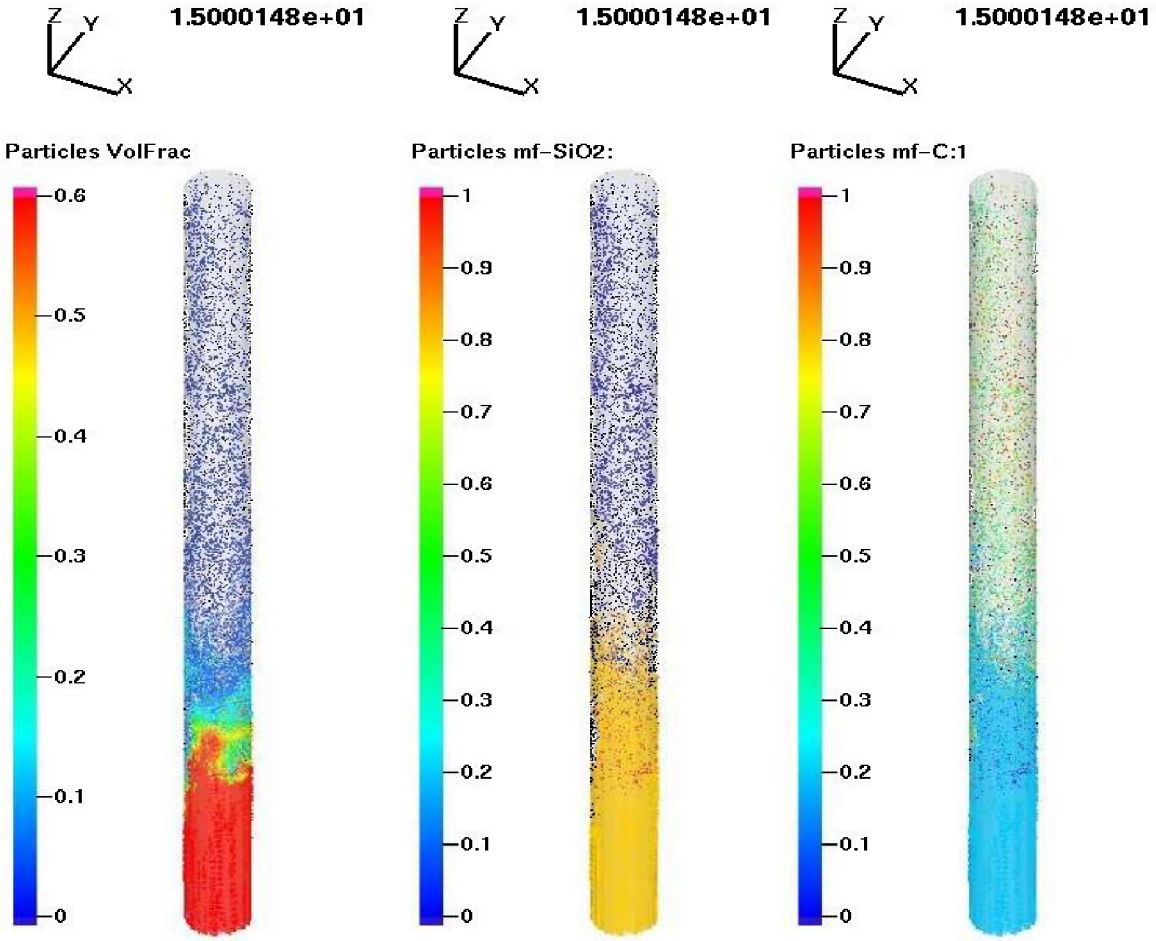

Figure 6-26:(a)Particle volume fraction (b)Mass fraction of SiO2 (c)Mass fraction of C

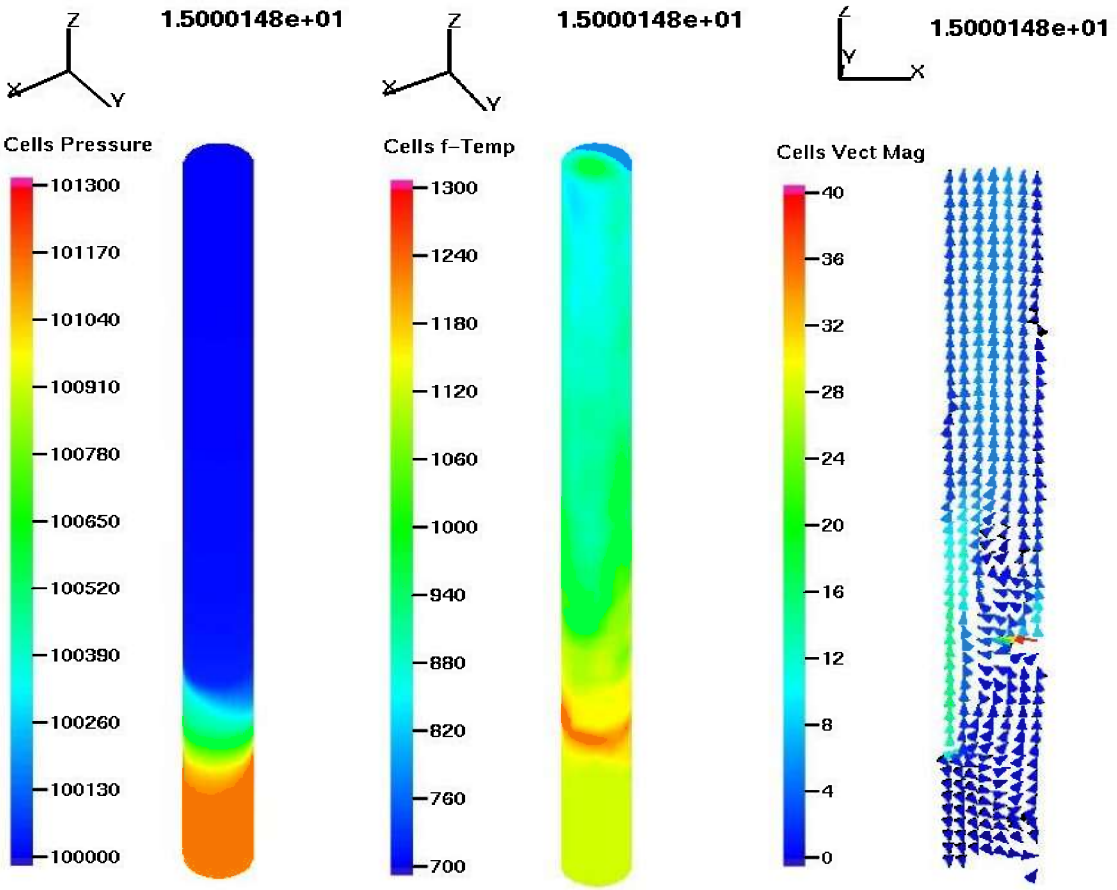

Figure 6-27:(a) Pressure (b)Temperature(c) Fluid velocity vectors across cross section

6.5 Case-E

Case E was performed to study the effect of increased input velocity of the steam gasification process. Hence the steam velocity was ten times than in Case C, and is now 0.01m/s. The other variables were kept constant.

Figure 6-28 shows the molar composition of the product gas at the outlet of the reactor and no considerable differences from the previous cases are observed. The rate of gas production for each component is shown in Figure 6-29 and the results are somewhat closer to gas production rates in Case-C and higher than in Case-A. As shown in Figure 6-30, the cumulative production of combustible gasses is 59×10^{-3} Sm^3 and this can be predicted as $255Sm^3$/day.

Figure 6-31 illustrates the gas mass fractions of H_2, CO and H2O at 15s of simulation time. According to the calculations, the overall water mass fraction in the product gas is 34% and this is exactly the same as in Case-C.

The bed mass variation of the reactor over the simulation time is shown in Figure 6-32. Even though the bed mass is seemed to be nearly constant, it shows a decreasing trend. As shown in Figure 6-33, some fraction of the particles, mainly C, in the reactor seems to be released out with the product gas. Calculations show that this amount is 31% of the input mass.

Figure 6-34(a), (b) and (c) shows pressure profile, temperature and vector magnitude across the cross section at 15s. The pressure drop across the bed is approximately 1800 Pa at the moment. The temperature is also varied in different regions of the reactor while cold regions can be seen especially in the upper part of the reactor. According to Figure 6-34(c), there are distinct velocity profiles within the reactor. The velocity is higher at biomass inlet point, at the recycle input and in some regions across the upper part of the rector.

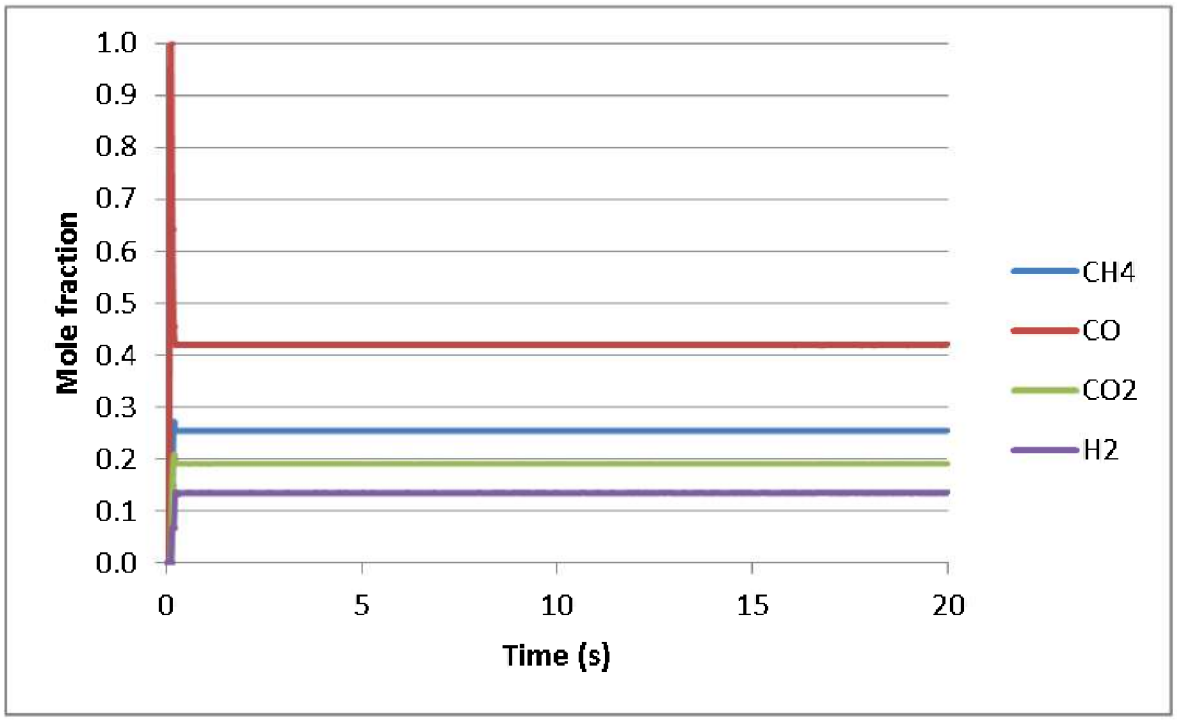

Figure 6-28: Molar composition of product gas vs time

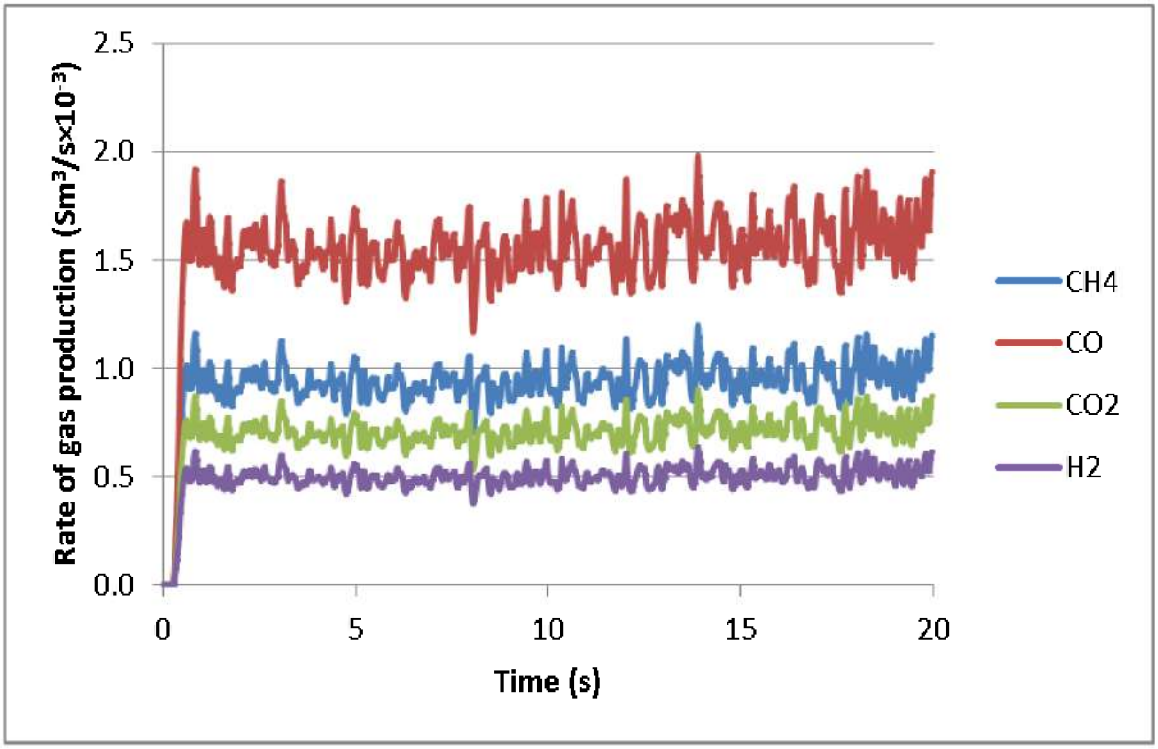

Figure 6-29: Rate of gas production vs time

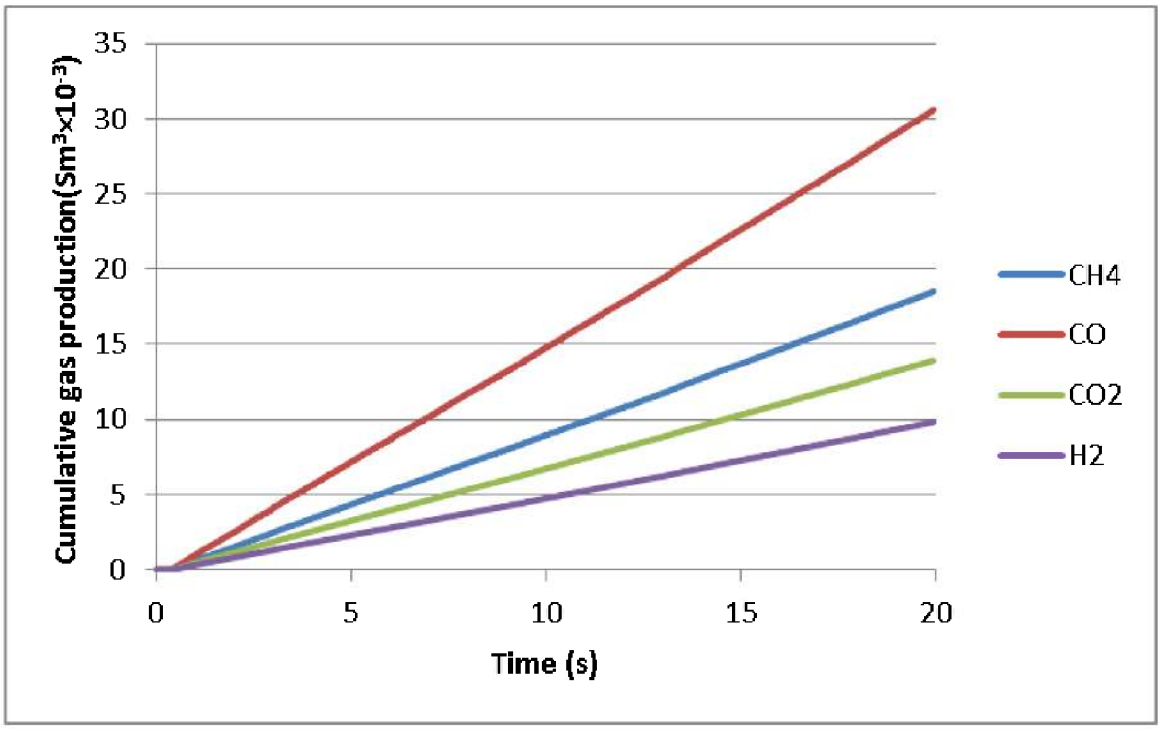

Figure 6-30: Cumulative gas production vs tiime

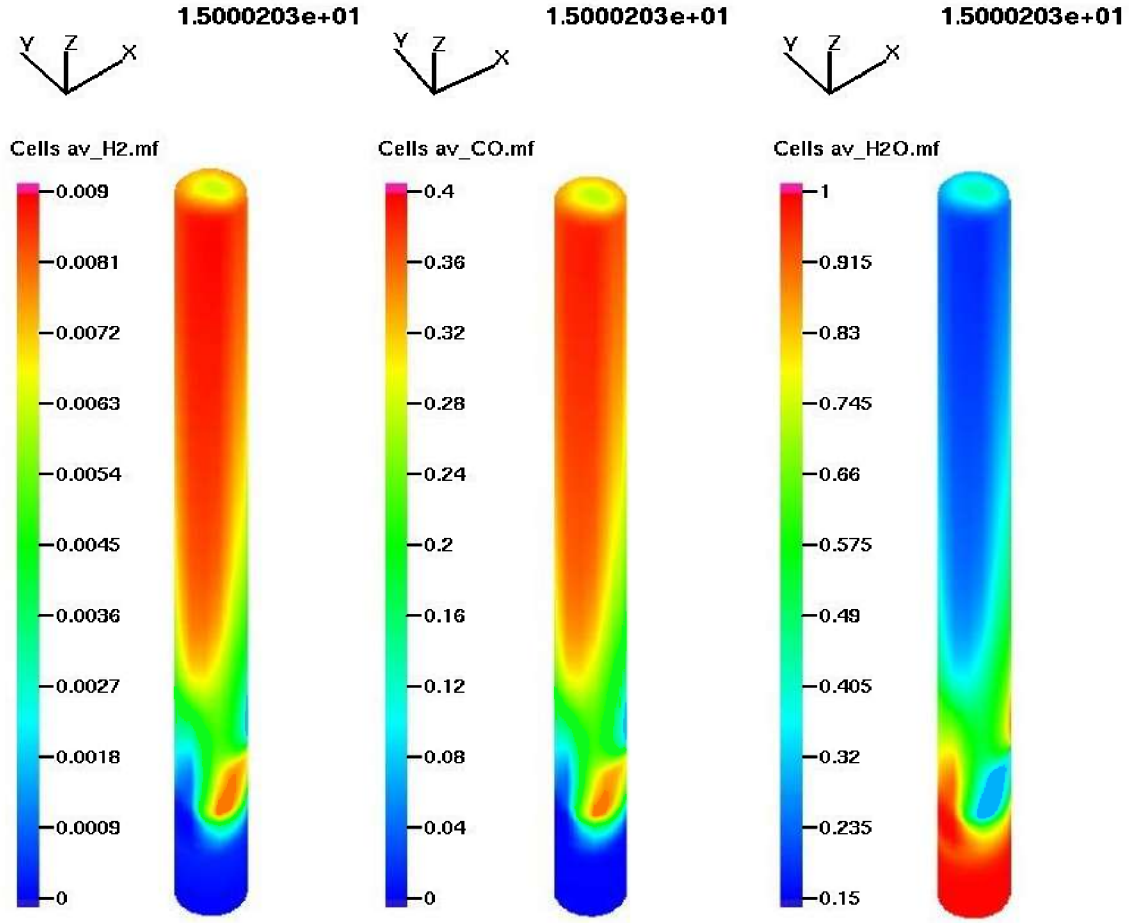

Figure 6-31: Average mass fraction of (c)H2 (b)CO (c)H2O at 15s

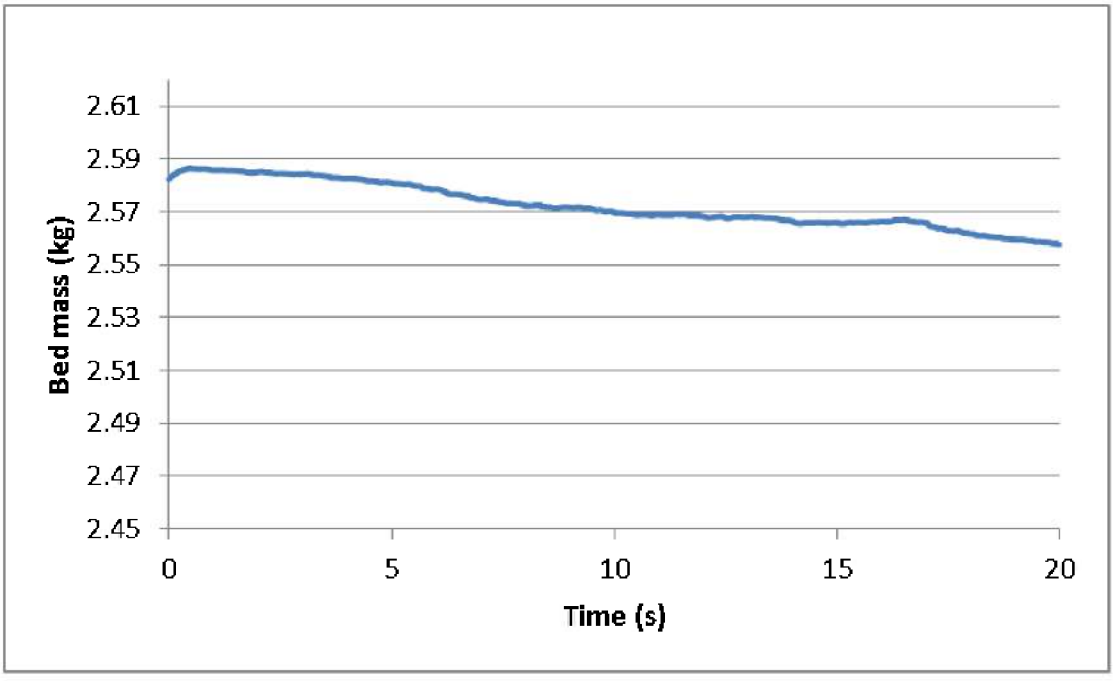

Figure 6-32: Reactor bed mass vs time

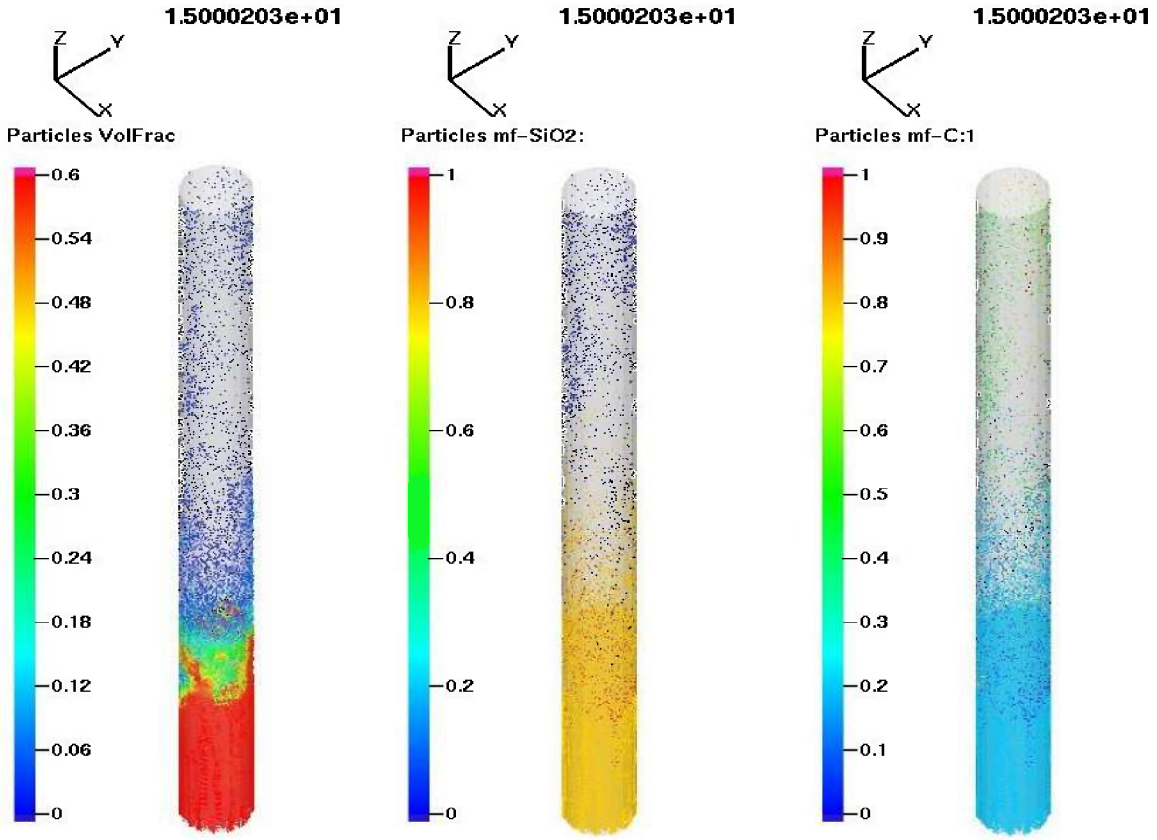

Figure 6-33:(a)Particle volume fraction (b)Mass fraction of SiO2 (c)Mass fraction of C

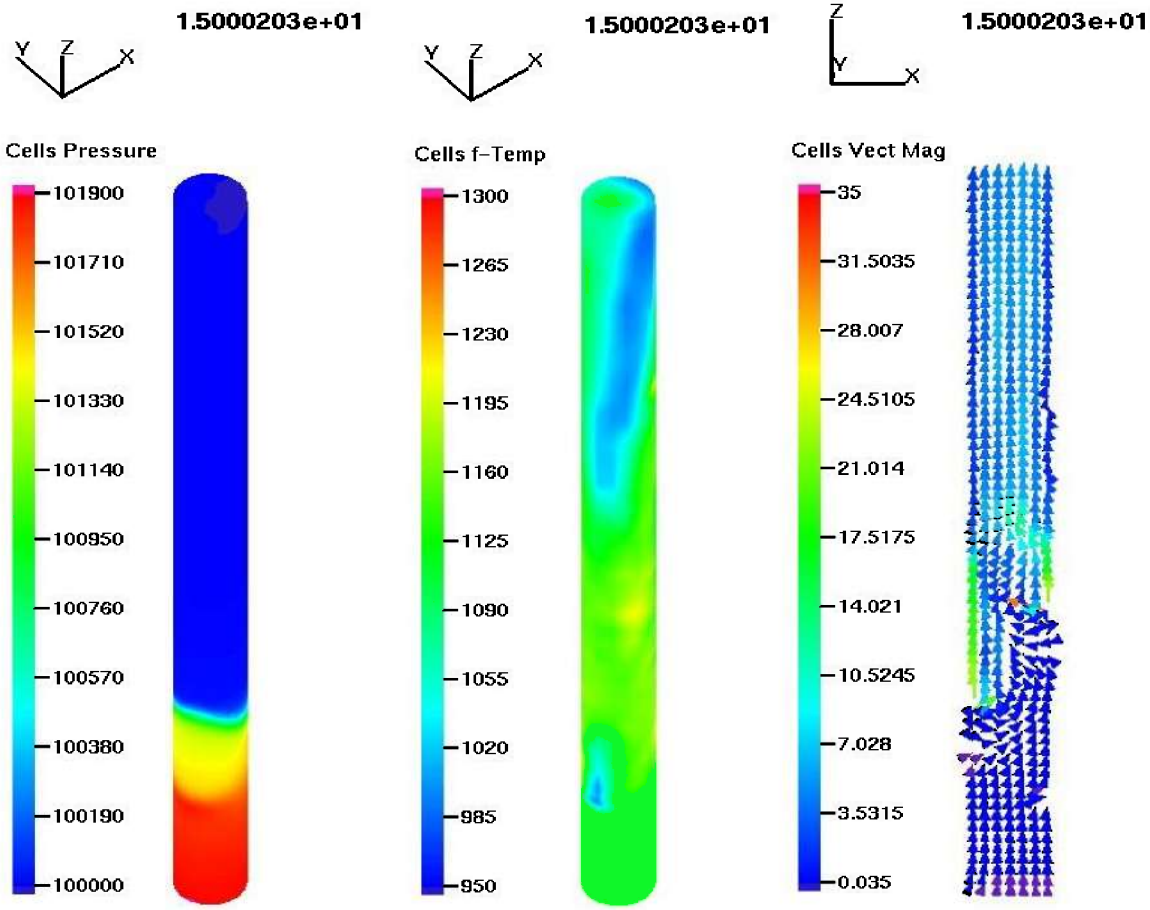

Figure 6-34:(a)Pressure (b)Temperature (c)Fluid velocity vectors across cross section

6.6 Case-F

Case F- was aimed to study the effect of replacing H_2O with CO_2 in the biomass feed stream. Therefore H_2O in Case-C was replaced with CO_2 to in Case-F and other variables were kept unchanged.

Figure 6-35 shows the gas composition of the product gas and this is quite different from the results of previous cases. The molar fractions of individual components show a fluctuating behavior instead of the steady production in previous cases using steam with the biomass inlet. On the other hand the molar composition of the present case is such that 38% of CO, 30% of CO_2, 23% of CH_4 and 12% of H_2. There is an increase of CO_2% in the product gas and the same situation is revealed by Figure 6-36 which shows the rate of gas production over the simulation time. Hence there is more CO_2, less H_2 and CH_4. According to the Figure 6-37, the cumulative production of combustible gasses is 61×10^{-3} Sm^3 which can be extrapolated to 264 Sm^3 .This result shows no big difference from Case-C and Case-E.

Figure 6-38 illustrates the mass fractions of H_2, CO, H_2O and CO_2. The significant change here is that the calculated overall mass fraction of H_2O in product gas has been reduced down to 16%. The rest 84% is product gas and this condition is the opposite of Case-A.

The bed mass variation over the simulation period is shown by Figure 6-39. Even though a nearly constant bed mass can be considered, it has a rising trend. Figure 6-40 shows the particle volume fraction and the mass fractions of SiO_2 and C at 15s. According to the figure, a fraction of bed mass is released with the product gas and this was calculated as 30%.

Figure 6-41(a), (b) and (c) shows the temperature, pressure and vector magnitude respectively. The pressure drop across the bed is 2300 Pa at the moment and the temperature of the reactor upper part seems colder than in the bed region. The appearance of the velocity vectors has no significant change from previous cases.

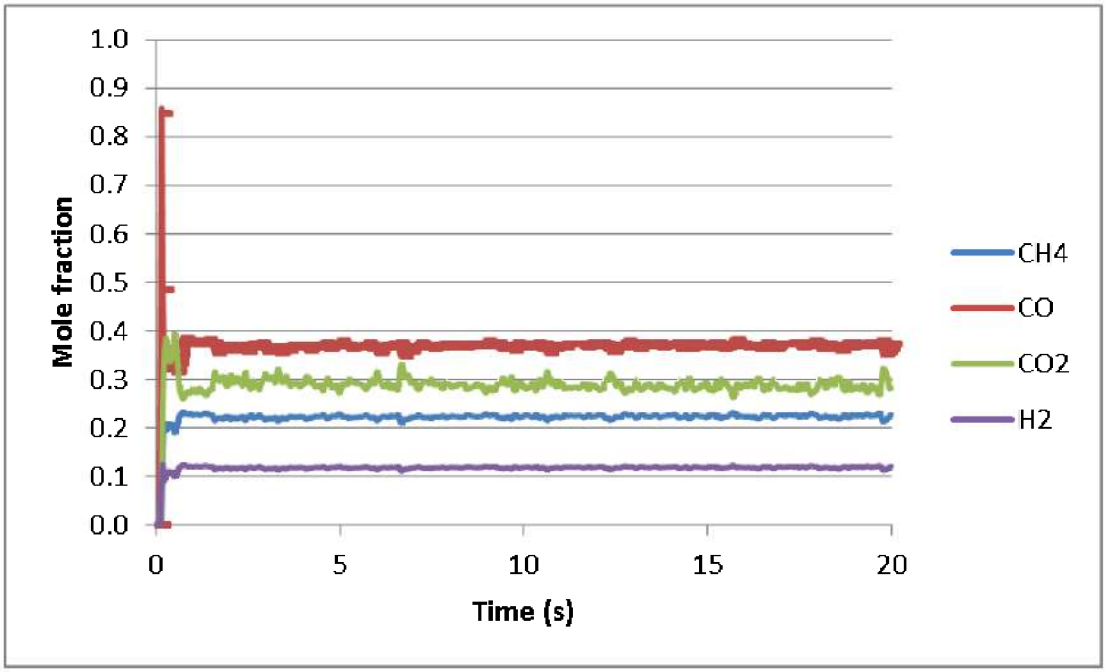

Figure 6-35: Molar composition of product gas vs time

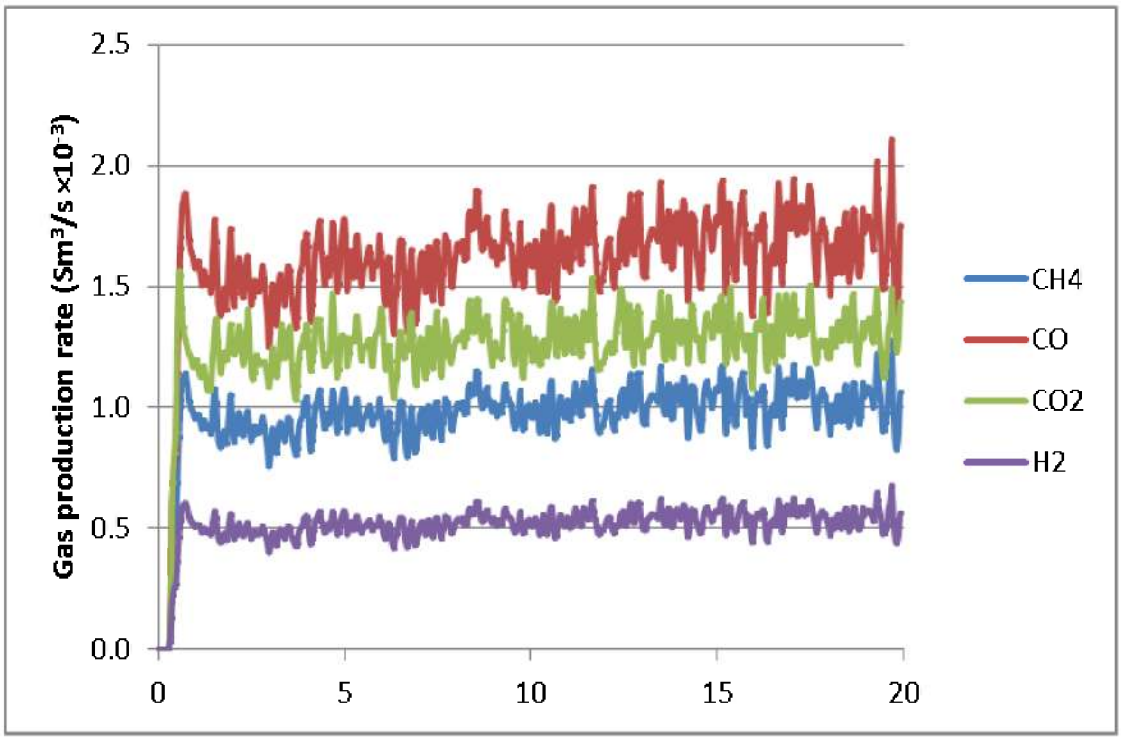

Figure 6-36: Rate of gas production vs time

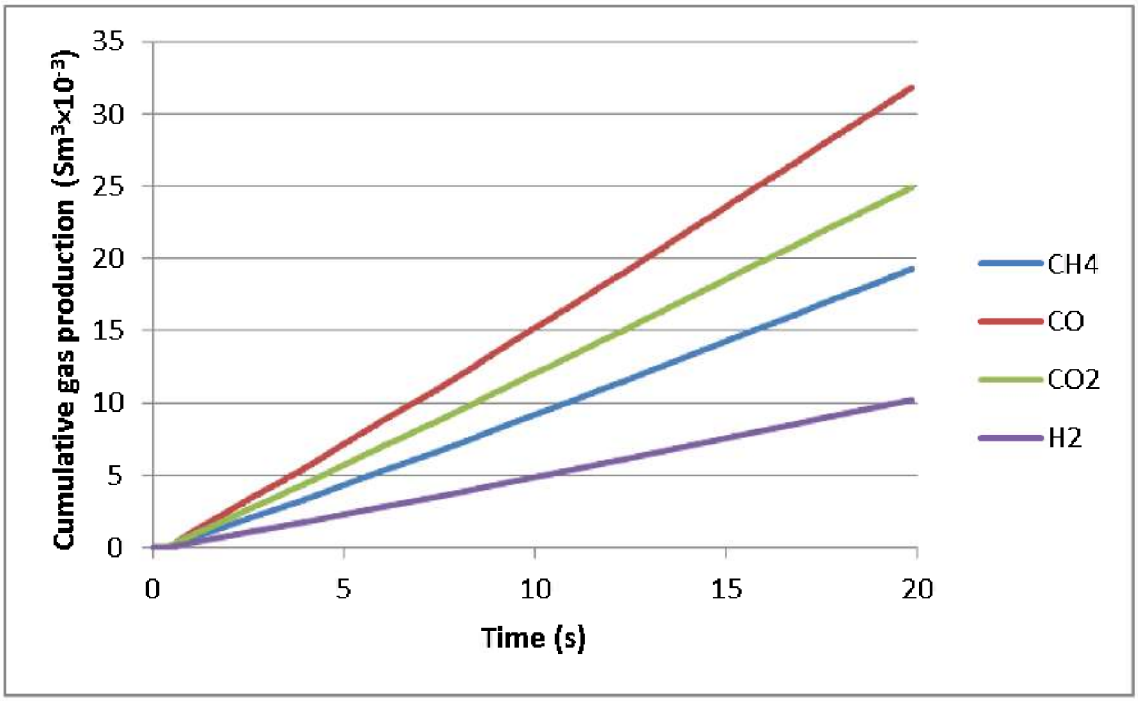

Figure 6-37: Cumulative gas production vs time

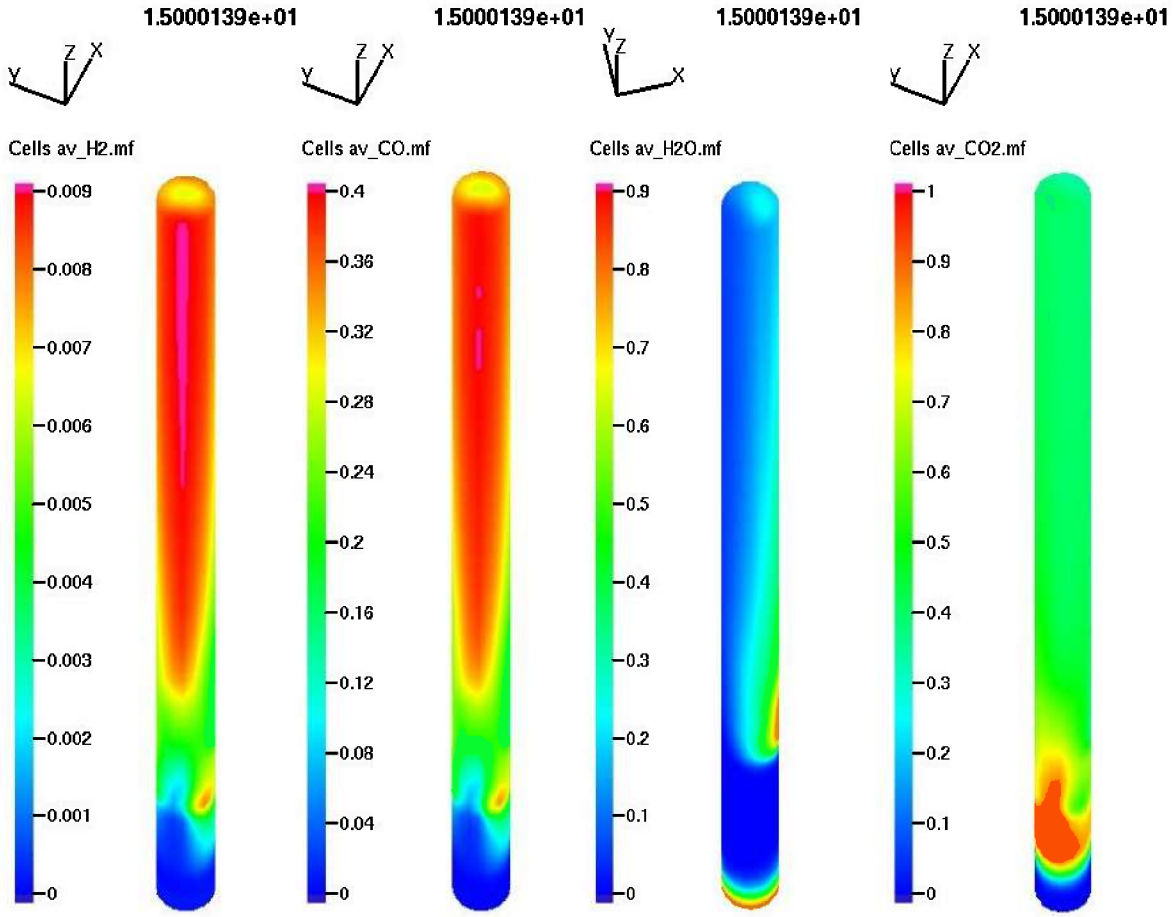

Figure 6-38: Average mass fraction of (a)H2 (b)CO (c)H2O (d)CO2 at 15s

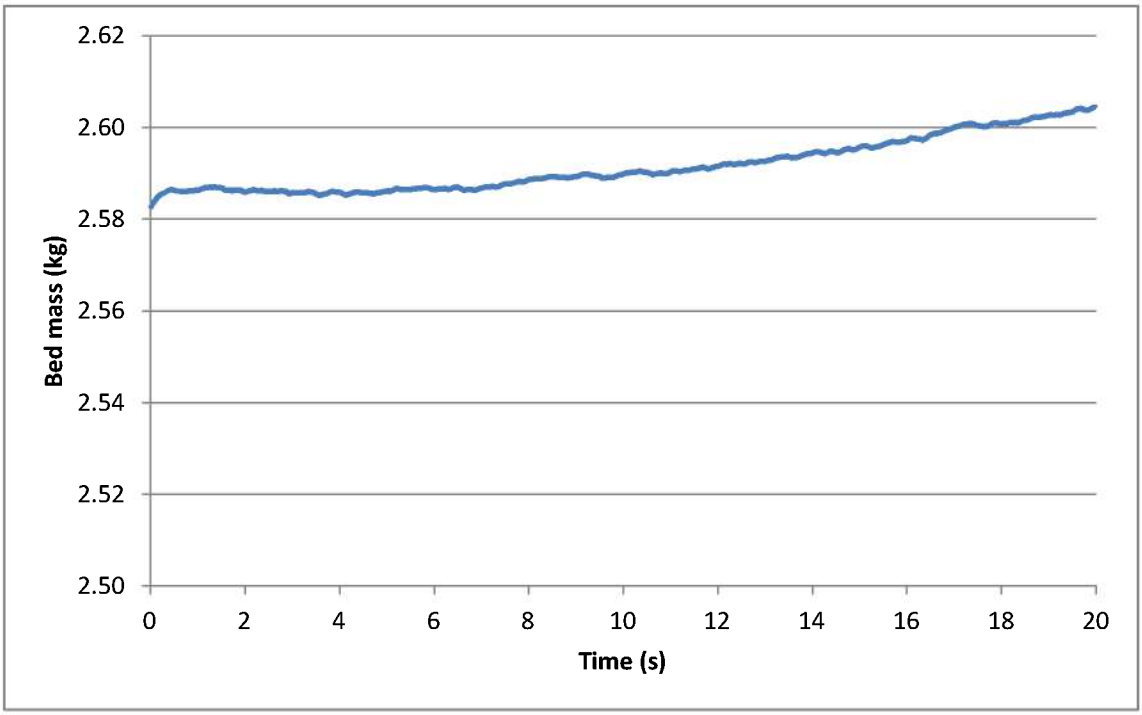

Figure 6-39: Reactor bed mass vs time

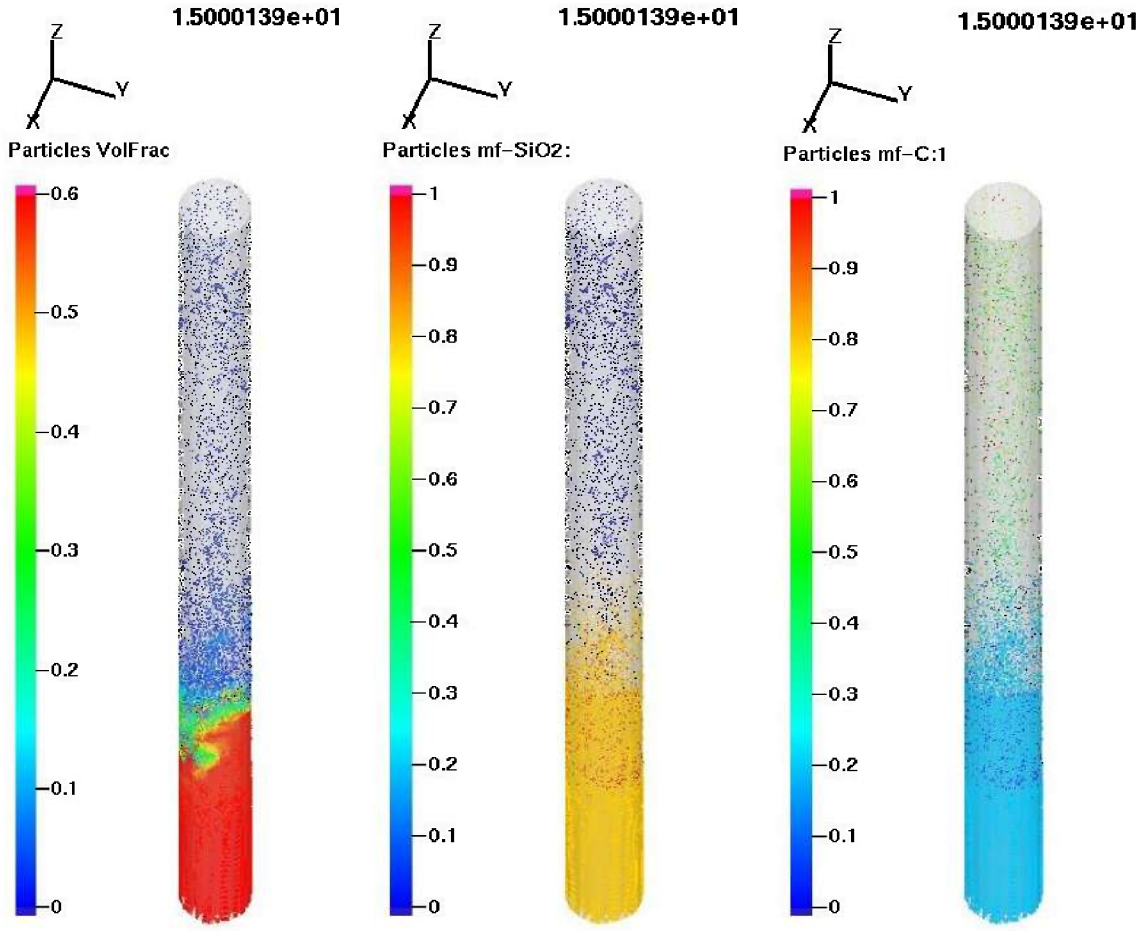

Figure 6-40:(a)Particle volume fraction (b)Mass fraction of SiO2 (c)Mass fraction of C

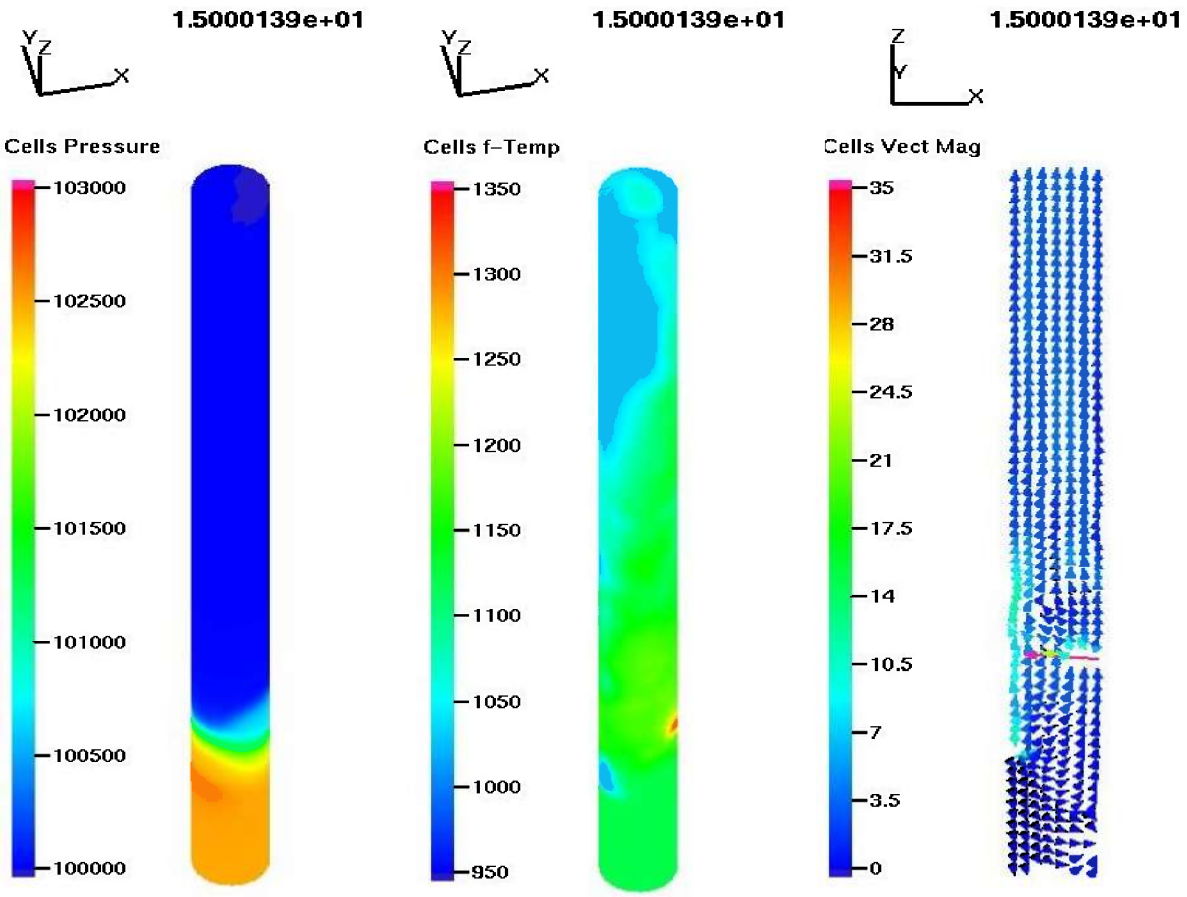

Figure 6-41:(a)Pressure (b)Temperature (c)Fluid velocity vectors across cross section

6.7 Case-G

The size of biomass was increased up to 5mm, in Case-G. This is five times bigger than in the previous cases. The rest of the variables were kept as in Case-C. The simulation results are compared with Case-C, as a reference case. According to Figure 6-42, the molar composition is steady and quite the same as in Case C. But the rate of gas production and the cumulative gas production curves have significant improvements as shown in Figure 6-43 and Figure 6-44. The cumulative gas production of combustible gasses, during the 20s of simulation period is 92×10^{-3} Sm^3 and this can be predicted as nearly 400 Sm^3/day.

Figure 6-45 shows the mass fractions of H_2, CO and H_2O at 15s. According to calculations the mass fraction of the H_2O is reduced significantly down to 25% at the reactor outlet. This is proved by Figure 6-45(c). The bed mass is nearly constant around 2.6kg as presented in Figure 6-46. According to Figure 6-47, a proper fluidization is visible and the particles released out at the reactor outlet are very little in comparison to the previous cases. The calculated amount of particles in product gas is 19.5% of the input mass.

Pressure, temperature and vector magnitude within the reactor at 15s of simulation are shown in Figure 6-48. Accordingly, the pressure drop across the bed is approximately 1900 Pa and

the temperature profile high lights cold spots within the reactor. The instantaneous fluid vectors seem to be much higher across the reactor in comparison to the previous cases.

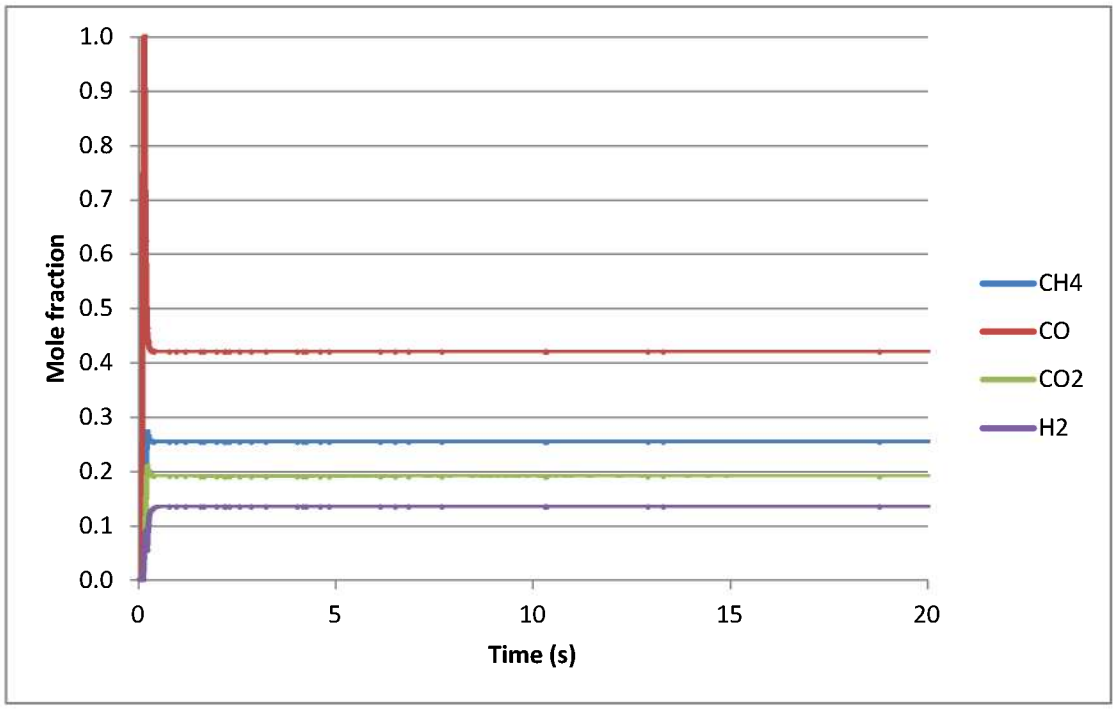

Figure 6-42: Molar composition of product gas vs time

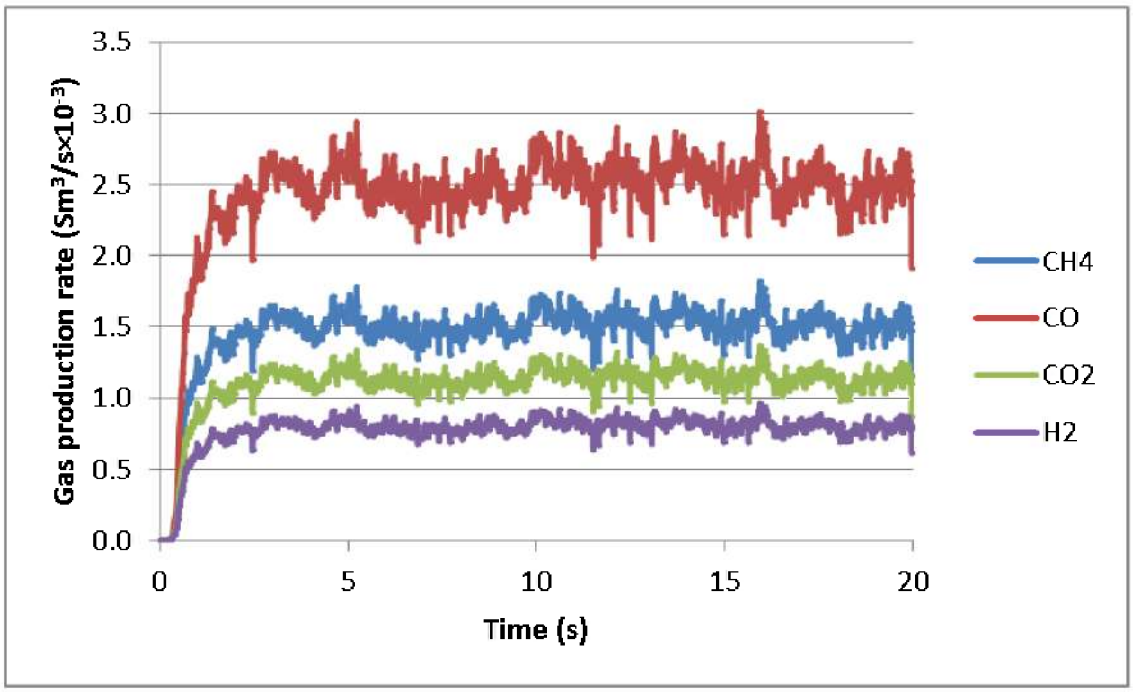

Figure 6-43: Rate of gas production vs time

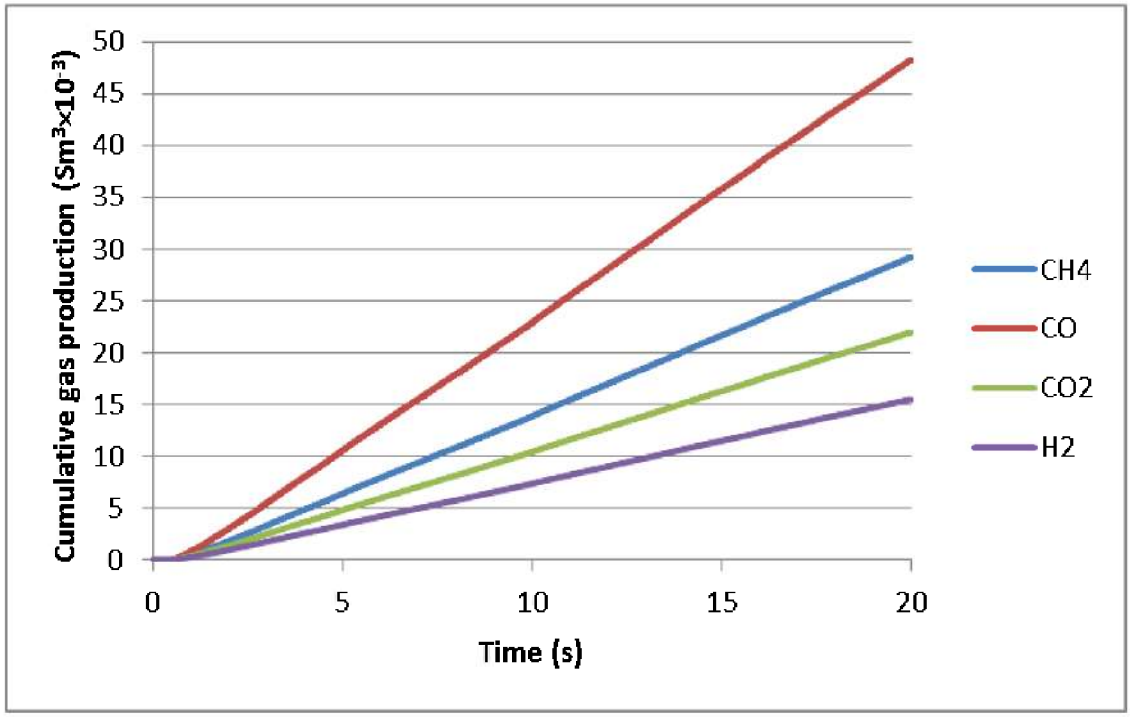

Figure 6-44: Cumulative gas production vs time

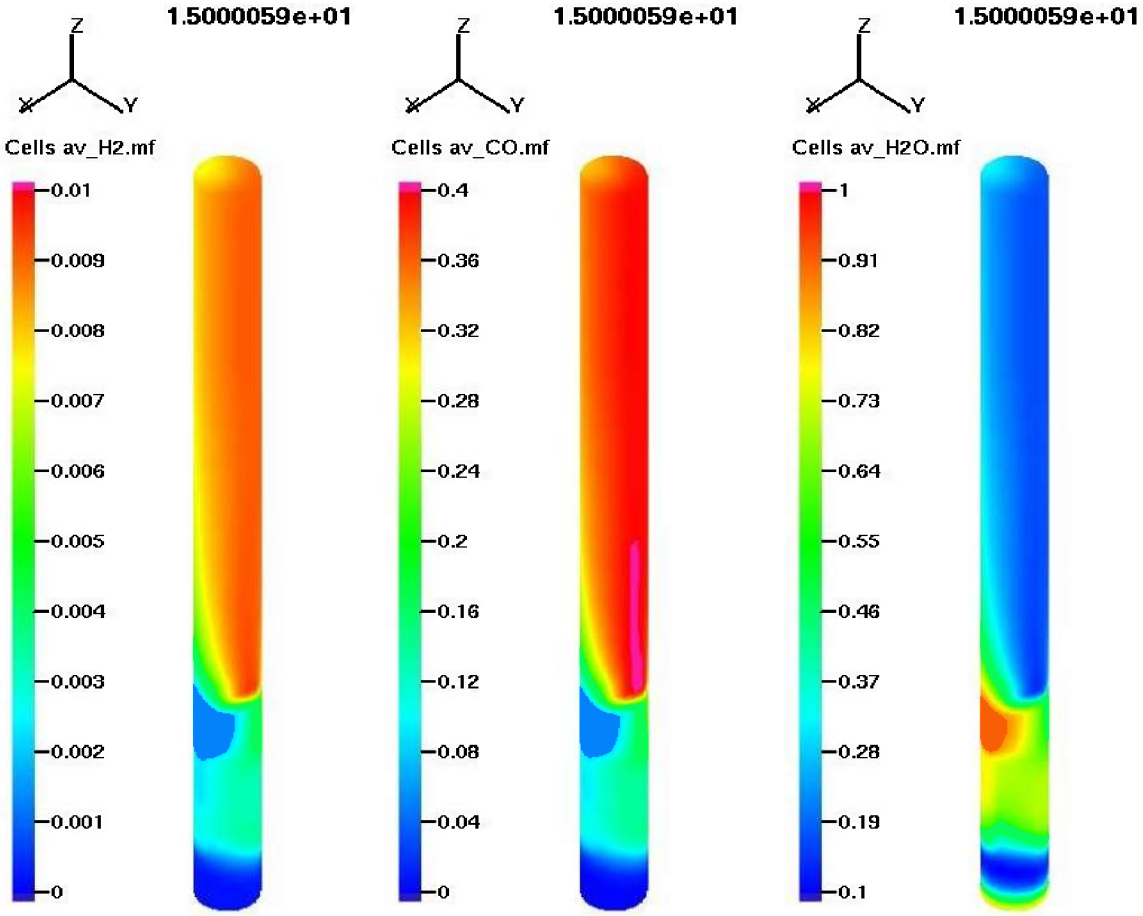

Figure 6-45: Average mass frction of (a)H2 (b)CO (c)H2O at 15 s

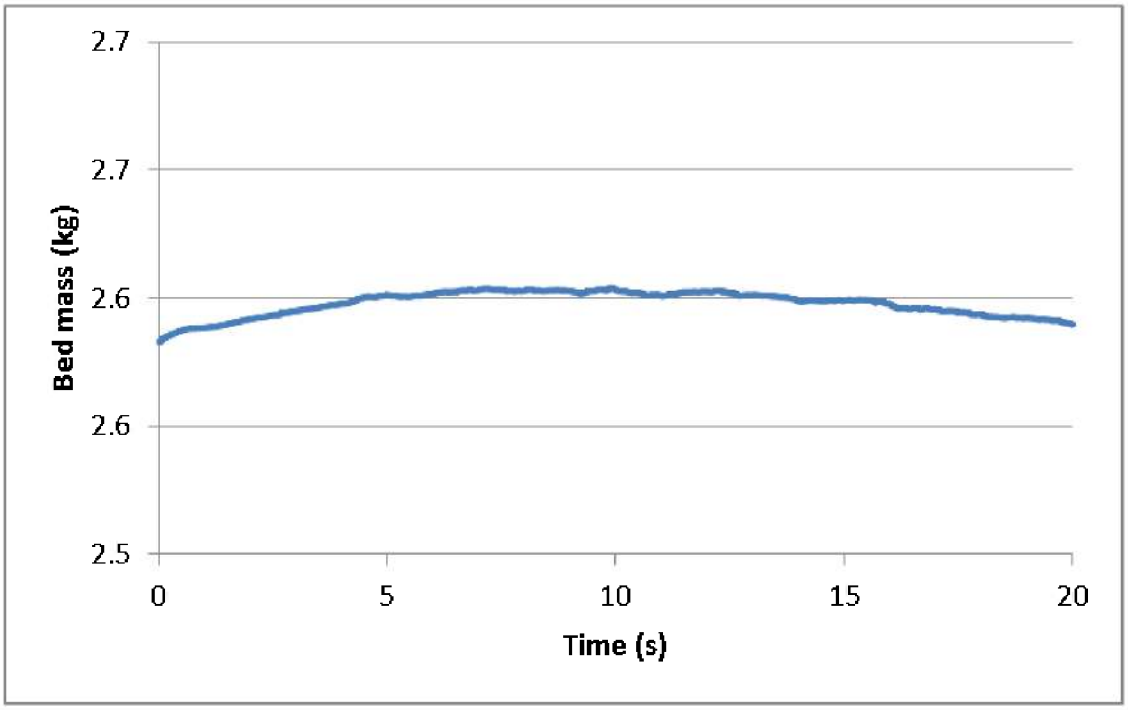

Figure 6-46: Reactor bed mass vs time

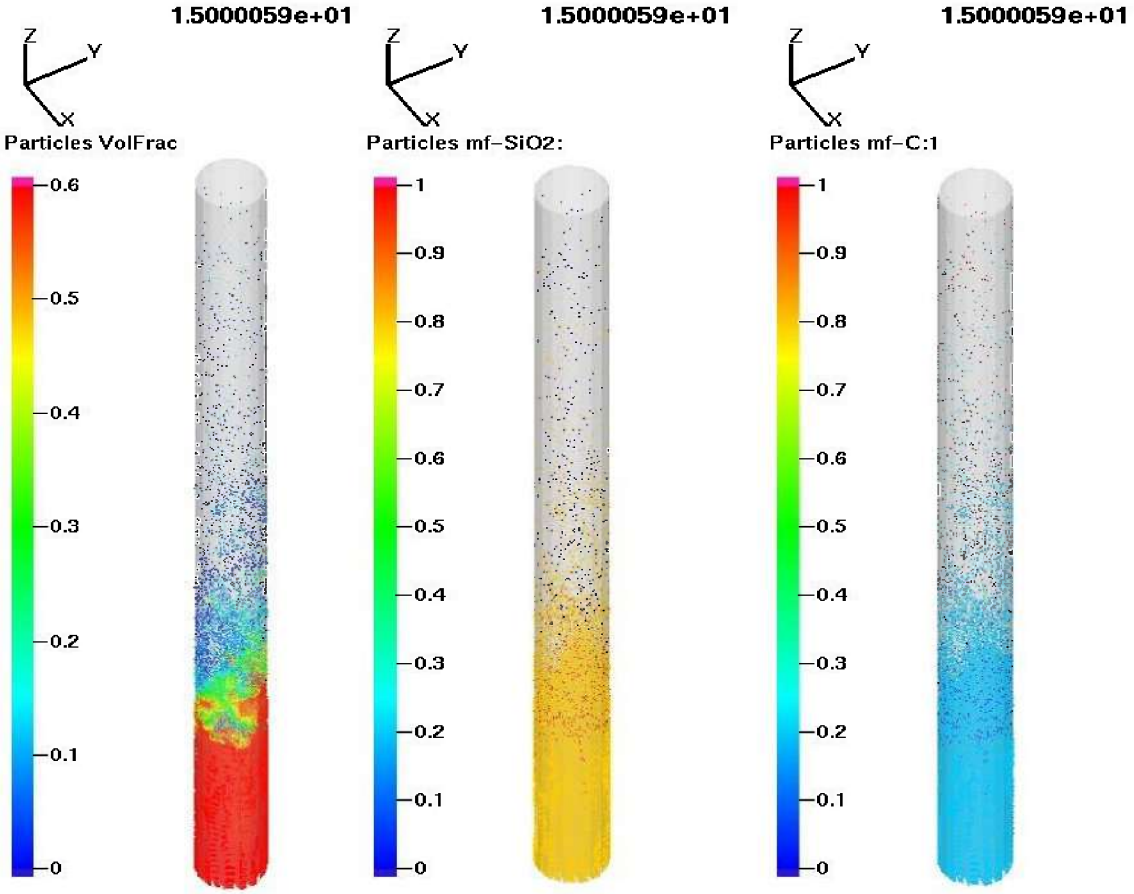

Figure 6-47:(a) Particle volume fraction (b)Mass fraction of SiO2 (c)Mass fraction of C

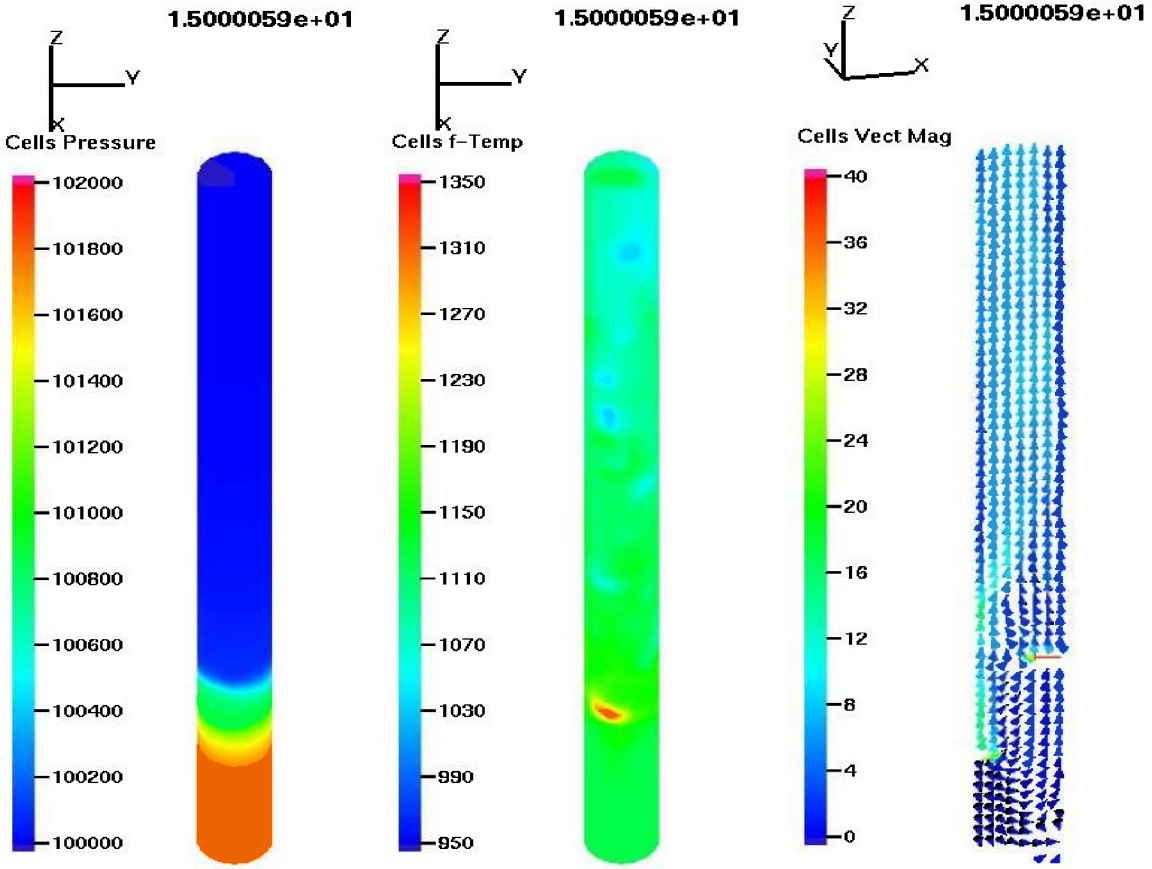

Figure 6-48:(a)Pressure (b)Temperature (c)Fluid velocity vectors across cross section

7 Discussion

The results obtained in the seven cases are discussed in this chapter. The trends of plotted variables and a comparison between the cases are discussed, in order to derive the conclusions of the overall study.

7.1 Consistency of gas production

The main parameter that can be used to check the success of each case is to look at the product gas generated under particular conditions of each case. The consistency of the gas production has a higher importance as same as the volume of production. All the cases except Case-B were able to produce the product gas in a steady manner. This is visible in the figures that show the rate of production and the production curve fluctuates around a constant mean value. In case-B, the gas production is intermittent as shown in Figure 6-9 and it can be noticed a good correlation between the rate of production and pattern of bed mass variation which is shown in Figure 6-11.This depicts that a constant supply of bio mass and consistency of bed mass is a key factor that leads to a constant production. In addition, nearly constant curves of bed-mass shown in Figure 6-5, Figure 6-18, Figure 6-25, Figure 6-32, Figure 6-39 and Figure 6-46 could be the reason for the steady production of combustible gasses which are shown in Figure 6-2, Figure 6-13, Figure 6-22, Figure 6-29, Figure 6-36 and Figure 6-42.

7.2 Volume of production

There are seven cases simulated in this study and Case-B was performed to inspect the controller action in the bio mass feed flow. Therefore Case-B is excluded in the comparison between cases. Figure 7-1 summarizes the percentage of product gas and steam content in the outlet gas stream. There is a clear reduction of the water content between Case-A and all the other cases. More moisture in the product gas may create problems such as extra efforts for moisture removal, prior to use and this raises the equipment cost as well as the maintenance cost too. The water content in ‘Case-A’ is more than 80%, while in all the other cases it is less than 40%. This result depicts that the size of bed material can make a big difference in product gas yield. Because in ‘Case-A’, the bed material size was four times bigger than the other cases. The other main advantage is that it reduction of the bed material size significantly reduced the demand of steam input for fluidization. In fact the steam input velocity in Case A was 0.12m/s and it was enough to supply steam in 0.001 m/s to fluidize the bed in the other cases which is a 120 times lower velocity. The results are confirmed by a study done by Kern et al [3], that the reduction of bed material particle size offers the possibility to operate the gasification reactor with a lower amount of steam for fluidization.

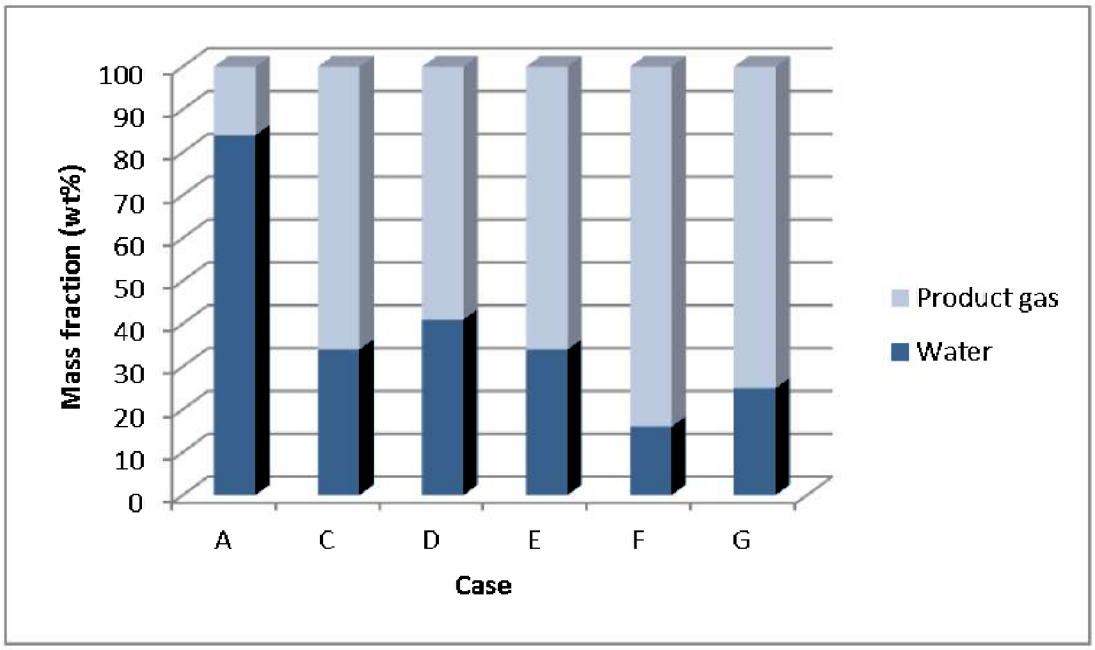

Figure 7-1: Comparison in Mass fraction of water and product gas

Figure 7-2 illustrates a bar graph that shows the daily production of combustible gasses in each case. Case-A shows the least possible daily production. This describes the fact that larger bed material size can hinder the gas formation. The reason could be that the small particles are easy to fluidize and can lead to a proper mixing of biomass. This can be resulted with good heat transfer capabilities, proper contact between reactants, higher reaction rates and more product gas in turn. Case-G shows the highest daily production among all the cases. The main difference is the size of the biomass particles sent in to the reactor. Here, the particle size was five times bigger than other cases. Logically it was expected that the lesser the size of bio mass, the higher the yield of gasses, due to the fact that small sized particles provide a larger surface area for the thermochemical reactions. On the other hand it facilitates the heat transfer too. Therefore it was examined the particle content released out with the product gas to see any relationship between the released amount of particles and the rate of gas formation. The bar graph illustrated in Figure 7-3 shows the amount of particles released out with the product gas as a percentage out of input mass (biomass and bed material recycle).

In fact a proper answer was found when comparing Figure 7-2 and Figure 7-3. Case-G has the highest production of combustible gasses and lowest release of particles out with the product gas stream. Case-A and Case-D (two cases are entirely different) have the lower gas production and the release of particles too is higher. This depicts that the size of biomass particles is very important in two ways.

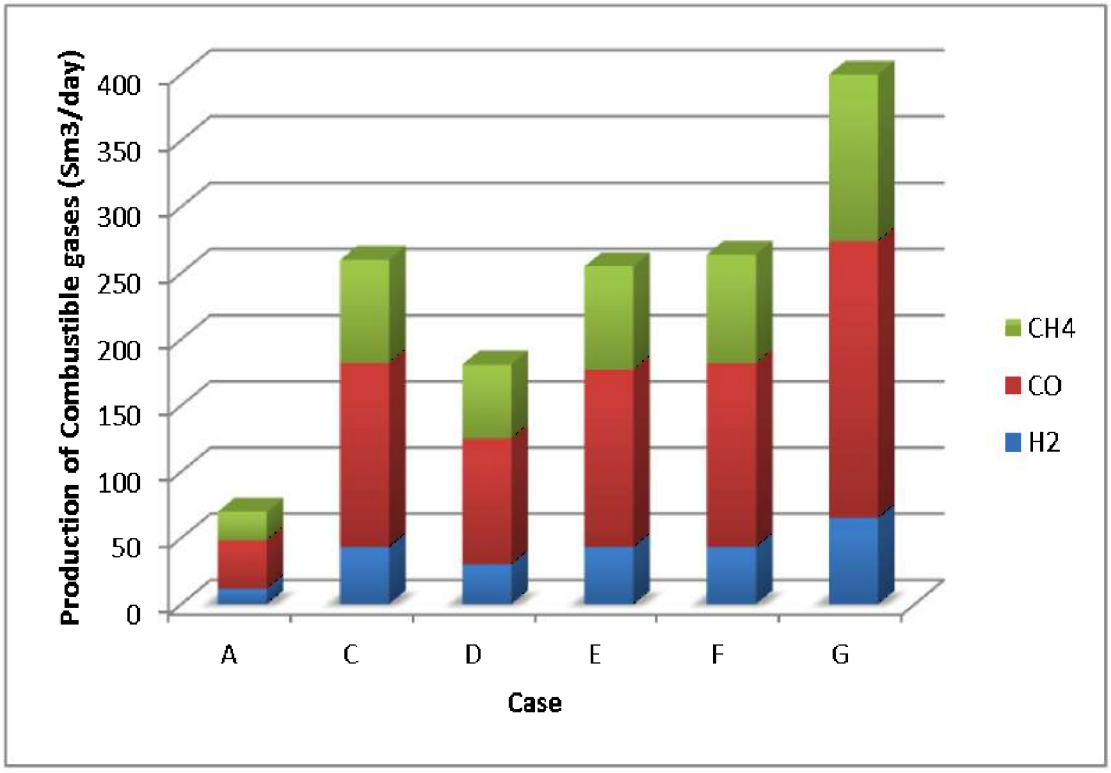

Figure 7-2: Combustible gas production vs Case

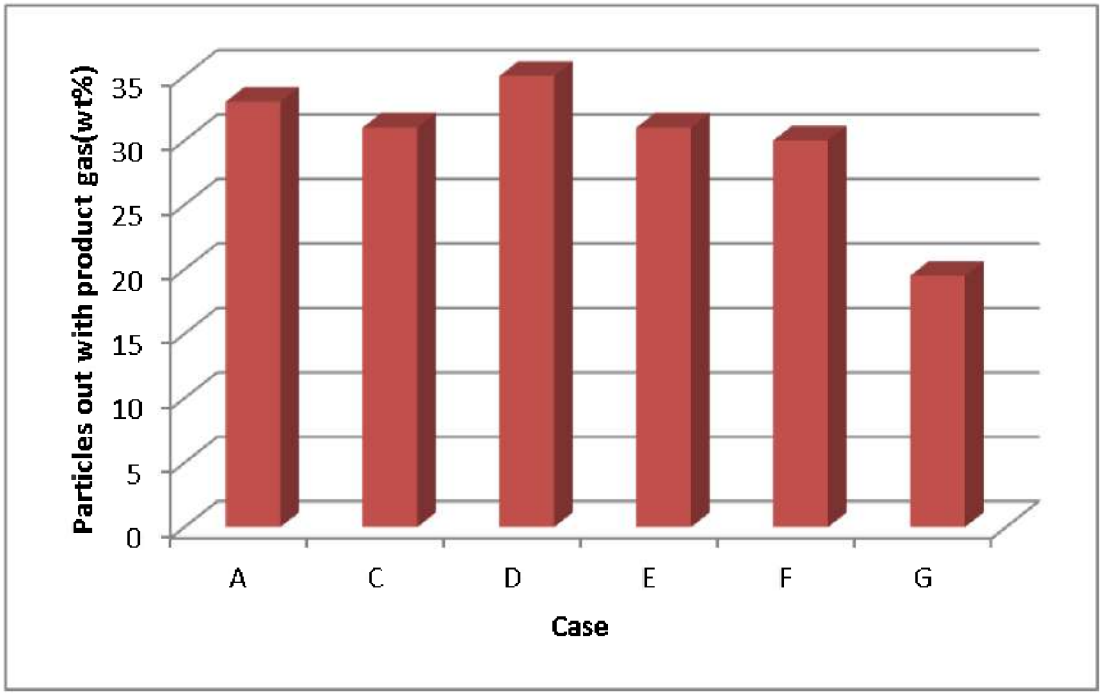

Figure 7-3: Particles release out with product gas vs Case

That means the particles should be small enough to facilitate the fast reaction and they should be large enough to retain them in the reactor. Therefore it is wise to find the optimum biomass particle size for optimize the production of combustible gasses. Efforts were made to run the simulation for much larger biomass particle size which is 10mm. But it was restricted by the program as that particle size was not compatible with the defined mesh size.

Focusing back on Figure 7-2, Case-C, E and F have nearly equal amount of daily gas production around 250 Sm^3/day. This depicts that increasing the steam velocity or replacing steam with CO_2 in the biomass inlet stream, does not make any significant change in product gas formation. Instead unnecessary amount of steam will lead to higher operating costs for steam as in 'Case-A'. Case- F shows a lower production in comparison to the Case-C, E and F. This is obvious, as it had a lower steam temperature which is 500K instead of 900K in the other cases. In fact lower steam temperature fails to maintain the required reactor temperature due to reason that most of the reactions occurred in the steam gasification process are endothermic. Therefore lower reactor temperature does not facilitate the required heat energy for the gasification reactions and produces fewer amounts of product gas. This fact has been experimentally proved by the study done by Lv et al [22].

7.3 Composition of product gas

Approximately similar molar compositions are resulted in all the cases except in Case-F, which uses CO_2 with the biomass feed. In those cases, the highest fraction of gas is CO (~ 40%vol). The mole fraction of H_2 (~15%vol) is quite less than expected and the CH_4 (~25%vol) is significant. This could be due to the contribution of pyrolysis gasses to generate more CH_4. On the other hand the available H_2 could have been favorably spent for hydrogenating gasification. The bed material used in the simulations is non-catalytic SiO_2 and according to some previous studies, the yield of combustible gasses and especially the yield of H_2 could have been enhanced by using other types of catalytic bed materials [45]. Koppatz et al [46], conclude their study, with the remarks that, the Olivine (catalytic bed material) favors the CO-shift reaction (R4) towards equilibrium composition and the H_2 content is increased in the presence of Olivine in comparison to SiO_2. The simulation stage would require, including the specific kinetic data regarding to the specific catalytic material to examine these effects through a computational study.

According to Figure 6-35, Case-F shows more CO_2, more CH_4, less CO and H_2 than the other cases, when it is referred to the molar composition of the product gas. This raises a question whether the extra CO_2 supplied, has not contributed for CO_2 gasification reaction as expected. Perhaps the reaction has been favored in backward direction or the resulted CO in CO_2 gasification has been consumed for water gas shift reaction. Because the H_2 amount is quite the same as in Case-C but CH_4 and CO_2 content is higher. Then it can be assumed that the

water gas shift reaction could have been occurred among CO_2 and H_2O and the resulted H_2 has been consumed for methanation to form more CH_4 while increasing the CO_2 content.

7.4 Reactor temperature, Pressure and Vectors

Temperature is a key factor of successful production of the product gas in bio mass steam gasification process, due the involvement of endothermic gasification reactions. As it is described by Kern et al [3], in a fluidized bed gasification reactor, the temperature reduction across the bed is limited due to the good intermixing of steam, bed material and fuel particles, and the high heat capacity of the bed material. This can be clearly seen in the Figure 6-7(b), Figure 6-20(b), Figure 6-27(b), Figure 6-34(b), Figure 6-41(b) andFigure 6-47(b). There, the bed region has a uniform temperature kept around 1123K (850 ^{0}C) which is ideal for the gasification process. The hot spot in the bed region is the hot bed material recycle point and the cold spot is the bio mass inlet point. But it can be seen that there exist blue areas which indicates the cold region in the upper part of the reactor above the bed except in Case-A. These cold spots and regions are signs that evident the endothermic gasification reactions occur within the reactor. The absence of the cold spots in Figure 6-7(b) describes the lowest gas production in Case-A.

The reactor pressure was always kept close to atmospheric pressure. The pressure is higher at the bottom of the reactor and it is dropped across the bed. The pressure drop across the bed varies from approximately 1000 Pa to 3000Pa and it is slightly under the ambient pressure at the reactor gas outlet. Operating at the ambient pressure or at slightly under pressure helps to prevent gas leakages from the reactor [47].

The instantaneous fluid velocity vectors in different cases have a common trend, though there are increments or decrements of magnitude in one case to the other. The vectors are higher at the bed mass recycle point and biomass inlet point. The entrance of steam at these points is one reason. On the other hand, the biomass is subjected to pyrolysis as soon as it enters into the high temperature region of the reactor at the biomass inlet. In addition, the reactions will accelerate to produce more gasses due to the too high temperature of the recycled bed materials at the bed mass recycled point. When it comes to the upper part of the reactor, more and more gasses are generated and they flow towards the outlet of the reactor, where the vectors take higher magnitude.

8 Conclusion

Biomass steam gasification is a thermochemical process that is used to produce a high quality product gas to overcome the problems of conventional air gasification. Gasification process in a dual fluidized bed was studied and simulations were performed for a simplified cylindrical gasification reactor, using the commercial software 'Barracuda VR^{TM}'. The effect of bed material size, consistency of biomass supply, steam temperature, steam input velocity, effect of CO_2 supply and size of inlet biomass particles were studied.

Product gas quantity and composition indicate the success of the gasification process. A steady production of gasses was achieved in all the cases except in Case-B. The molar composition of the product gas was approximately similar in all the cases except in Case-F, so that the volume of CO is~40%, CH_4 is ~25%, CO_2 is ~20%, and H_2 is ~15%. The amount of CH_4 is more than expected and the H_2 is below the desired level.

Reduction of the particle size of the bed material (SiO_2), lead to yield a higher gas production. The highest production of 400 Sm^3/day of combustible gasses was achieved in case-G where the bed materials were small and biomass particle size was five times bigger than the other cases. The increased size of the biomass particles helps to retaining the biomass without releasing it with the product gas. The size should be small enough to facilitate the higher reaction rates and heat transfer. The combustible gas production was adversely affected by the reduction of steam temperature. Increase of steam inlet velocity or addition of extra CO_2 did not contribute to increase the production.

The temperature in the bed region was uniform and close to the gasification temperature due to the proper mixing and higher heat capacity of the bed materials. The cold spots in the reactor are signs for the presence of endothermic gasification reactions.

The pressure was close to atmospheric pressure and the pressure drop across the bed was 1000 Pa to 3000Pa and it was slightly negative at the top of the reactor. This is useful in a way that a slight under pressure can help to prevent gas leakages.

8.1 Suggestions for future work

According to the experiences gained throughout this study, there is room for expanding this project to optimize the biomass steam gasification process using the software. They are listed here.

- Run pre-simulations to find the minimum fluidization velocity for the isothermal system without including chemistry, before starting with the exact simulations. This would help to find the required minimum inlet velocity of steam and avoid the release of particles with product gas outlet.

- Study, each variable examined in this project for a wide range of values. For example, the effect of bed material size on the gas production can be investigated for a range of particle sizes and the trends can be examined.
- Consider the biomass in the real compositions, including moisture and ash content too instead of treating it as cellulosic biomass.
- Account for the tar, char and combustible gasses as the pyrolysis products and include the kinetics [48] for tar cracking too.
- Gather and experiment the kinetic data for catalytic bed materials and run the simulations to find the effect of different catalytic materials on the gasification process.
- Run the simulations for longer time to see the long term effects of each parameter.
- Use different particle size distributions for feed biomass
- Have trials with coarser and finer meshes for the reactor in order to see the effect of mesh size on the results
- If possible, arrange a series of experiments to check the pyrolysis gas composition, pyrolysis kinetics, and gasification gas composition as well as gasification kinetics, with respect to a particular biomass. Then compare the results with simulation results. So the results will be more trusted.

References

[1] A. Demirbaş, "Biomass resource facilities and biomass conversion processing for fuels and chemicals," *Energy Conversion and Management*, vol. 42, pp. 1357-1378, 7// 2001.

[2] E. Ranzi, A. Cuoci, T. Faravelli, A. Frassoldati, G. Migliavacca, S. Pierucci, *et al.*, "Chemical kinetics of biomass pyrolysis," *Energy & Fuels*, vol. 22, pp. 4292-4300, 2008.

[3] S. Kern, C. Pfeifer, and H. Hofbauer, "Gasification of lignite in a dual fluidized bed gasifier—Influence of bed material particle size and the amount of steam," *Fuel Processing Technology*, vol. 111, pp. 1-13, 2013.

[4] R. R. Proll T., Aichernig C., Hofbauer H., , "Performance characteristics of an 8 MW dual fluidized bed steam gasification of solid biomass," presented at the The 12th International Conference on Fluidization, 2007.

[5] G. Schuster, G. Löffler, K. Weigl, and H. Hofbauer, "Biomass steam gasification–an extensive parametric modeling study," *Bioresource technology*, vol. 77, pp. 71-79, 2001.

[6] K. Matsuoka, K. Kuramoto, T. Murakami, and Y. Suzuki, "Steam gasification of woody biomass in a circulating dual bubbling fluidized bed system," *Energy & Fuels*, vol. 22, pp. 1980-1985, 2008.

[7] C. Di Blasi, G. Signorelli, C. Di Russo, and G. Rea, "Product distribution from pyrolysis of wood and agricultural residues," *Industrial & engineering chemistry research*, vol. 38, pp. 2216-2224, 1999.

[8] M. C. Blanco López, C. G. Blanco, A. Martínez-Alonso, and J. M. D. Tascón, "Composition of gases released during olive stones pyrolysis," *Journal of Analytical and Applied Pyrolysis*, vol. 65, pp. 313-322, 12// 2002.

[9] O. Oyj. (2013, 24.05.2013). *Fluidized bed*. Available: http://www.outotec.com/en/About-us/Our-technologies/Fluidized-bed/

[10] D. Bai, A. Issangya, and J. Grace, "Characteristics of gas-fluidized beds in different flow regimes," *Industrial & engineering chemistry research*, vol. 38, pp. 803-811, 1999.

[11] M. Barletta, "Progress in abrasive fluidized bed machining," *Journal of Materials Processing Technology*, vol. 209, pp. 6087-6102, 11/19/ 2009.

[12] G. S. Lee and S. D. Kim, "Pressure fluctuations in turbulent fluidized beds," *J. Chem. Eng. Japan*, vol. 21, p. 515, 1988.

[13] J. Mele, *Scale-up of a Cold Flow Model of FICFB Biomass Gasification Process to an Industrial Pilot Plant – Example of Dynamic Similarity*, 2011.

[14] S. S. Chauk and L.-S. Fan, "Heat transfer in packed and fluidized beds," *Rohsenow, WN et al., Handbook of Heat Transfer*, vol. 3, pp. 13.1-13.45, 1998.

[15] A. Oasmaa and S. Czernik, "Fuel oil quality of biomass pyrolysis oils state of the art for the end users," *Energy & Fuels*, vol. 13, pp. 914-921, 1999.

[16] C. Couhert, J.-M. Commandre, and S. Salvador, "Is it possible to predict gas yields of any biomass after rapid pyrolysis at high temperature from its composition in cellulose, hemicellulose and lignin?," *Fuel*, vol. 88, pp. 408-417, 3// 2009.

[17] L. Devi, M. Craje, P. Thüne, K. J. Ptasinski, and F. J. J. G. Janssen, "Olivine as tar removal catalyst for biomass gasifiers: Catalyst characterization," *Applied Catalysis A: General*, vol. 294, pp. 68-79, 10/4/ 2005.

[18] J. Corella, A. Orio, and J.-M. Toledo, "Biomass gasification with air in a fluidized bed: Exhaustive tar elimination with commercial steam reforming catalysts," *Energy & Fuels*, vol. 13, pp. 702-709, 1999.

[19] Q. Xu, S. Pang, and T. Levi, "Reaction kinetics and producer gas compositions of steam gasification of coal and biomass blend chars, part 2: Mathematical modelling and model validation," *Chemical Engineering Science*, vol. 66, pp. 2232-2240, 2011.

[20] T. R. Rao and J. V. Ram. Bheemarasetti, "Minimum fluidization velocities of mixtures of biomass and sands," *Energy*, vol. 26, pp. 633-644, 6// 2001.

[21] S. Koppatz, C. Pfeifer, R. Rauch, H. Hofbauer, T. Marquard-Moellenstedt, and M. Specht, "H2 rich product gas by steam gasification of biomass with in situ CO2 absorption in a dual fluidized bed system of 8 MW fuel input," *Fuel Processing Technology*, vol. 90, pp. 914-921, 7// 2009.

[22] P. M. Lv, Z. H. Xiong, J. Chang, C. Z. Wu, Y. Chen, and J. X. Zhu, "An experimental study on biomass air–steam gasification in a fluidized bed," *Bioresource Technology*, vol. 95, pp. 95-101, 10// 2004.

[23] C. Franco, F. Pinto, I. Gulyurtlu, and I. Cabrita, "The study of reactions influencing the biomass steam gasification process☆," *Fuel*, vol. 82, pp. 835-842, 2003.

[24] C. Pfeifer, B. Puchner, and H. Hofbauer, "Comparison of dual fluidized bed steam gasification of biomass with and without selective transport of CO2," *Chemical Engineering Science*, vol. 64, pp. 5073-5083, 12/1/ 2009.

[25] P. A. Cundall and O. D. Strack, "A discrete numerical model for granular assemblies," *Geotechnique*, vol. 29, pp. 47-65, 1979.

[26] A. A. Amsden, P. J. Orourke, and T. D. Butler, "KIVA-2: A computer program for chemically reactive flows with sprays," *NASA STI/recon technical report N*, vol. 89, p. 27975, 1989.

[27] M. Andrews and P. O'rourke, "The multiphase particle-in-cell (MP-PIC) method for dense particulate flows," *International Journal of Multiphase Flow*, vol. 22, pp. 379-402, 1996.

[28] D. M. Snider, "An Incompressible Three-Dimensional Multiphase Particle-in-Cell Model for Dense Particle Flows," *Journal of Computational Physics*, vol. 170, pp. 523-549, 7/1/ 2001.

[29] W. Godlieb, N. G. Deen, and J. Kuipers, "A discrete particle simulation study of solids mixing in a pressurized fluidized bed," 2007.

[30] G. Batchelor, "A new theory of the instability of a uniform fluidized bed," *Journal of Fluid Mechanics*, vol. 193, pp. 75-110, 1988.

[31] R. Jackson, *The dynamics of fluidized particles*: Cambridge University Press, 2000.

[32] D. Gidaspow, *Multiphase flow and fluidization: continuum and kinetic theory descriptions*: Academic press, 1994.

[33] D. M. Snider, S. M. Clark, and P. J. O'Rourke, "Eulerian–Lagrangian method for three-dimensional thermal reacting flow with application to coal gasifiers," *Chemical Engineering Science*, vol. 66, pp. 1285-1295, 3/15/ 2011.

[34] P. J. O'Rourke, "Collective drop effects on vaporizing liquid sprays," Los Alamos National Lab., NM (USA)1981.

[35] D. Snider, "An incompressible three-dimensional multiphase particle-in-cell model for dense particle flows," *Journal of Computational Physics*, vol. 170, pp. 523-549, 2001.

[36] D. M. Snider, "Three fundamental granular flow experiments and CPFD predictions," *Powder Technology*, vol. 176, pp. 36-46, 7/10/ 2007.

[37] A. G. Bradbury, Y. Sakai, and F. Shafizadeh, "A kinetic model for pyrolysis of cellulose," *Journal of Applied Polymer Science*, vol. 23, pp. 3271-3280, 1979.

[38] A. K. James, R. W. Thring, S. Helle, and H. S. Ghuman, "Ash Management Review—Applications of Biomass Bottom Ash," *Energies*, vol. 5, pp. 3856-3873, 2012.

[39] C. Dupont, G. Boissonnet, J.-M. Seiler, P. Gauthier, and D. Schweich, "Study about the kinetic processes of biomass steam gasification," *Fuel*, vol. 86, pp. 32-40, 1// 2007.

[40] R. Radmanesh, Y. Courbariaux, J. Chaouki, and C. Guy, "A unified lumped approach in kinetic modeling of biomass pyrolysis," *Fuel*, vol. 85, pp. 1211-1220, 2006.

[41] P. Basu, *Biomass gasification and pyrolysis: practical design and theory*: Academic press, 2010.

[42] M. Syamlal and L. Bissett, "METC gasifier advanced simulation (MGAS) model," USDOE Morgantown Energy Technology Center, WV (United States)1992.

[43] F. Bustamante, R. Enick, A. Cugini, R. Killmeyer, B. Howard, K. Rothenberger, *et al.*, "High-temperature kinetics of the homogeneous reverse water–gas shift reaction," *AIChE journal*, vol. 50, pp. 1028-1041, 2004.

[44] F. Bustamante, R. Enick, R. Killmeyer, B. Howard, K. Rothenberger, A. Cugini, *et al.*, "Uncatalyzed and wall-catalyzed forward water–gas shift reaction kinetics," *AIChE journal*, vol. 51, pp. 1440-1454, 2005.

[45] S. Hurley, C. C. Xu, F. Preto, Y. Shao, H. Li, J. Wang, *et al.*, "Catalytic gasification of woody biomass in an air-blown fluidized-bed reactor using Canadian limonite iron ore as the bed material," *Fuel*, vol. 91, pp. 170-176, 2012.

[46] S. Koppatz, C. Pfeifer, and H. Hofbauer, "Comparison of the performance behaviour of silica sand and olivine in a dual fluidised bed reactor system for steam gasification of biomass at pilot plant scale," *Chemical Engineering Journal*, vol. 175, pp. 468-483, 2011.

[47] J. Vos, "Guideline for safe and eco-friendly biomass gasification," 2009.

[48] J. Corella, J. M. Toledo, and M.-P. Aznar, "Improving the modeling of the kinetics of the catalytic tar elimination in biomass gasification," *Industrial & engineering chemistry research*, vol. 41, pp. 3351-3356, 2002.

Appendices

Appendix 1: Project Description

Appendix 2: Abstract of the research paper for the conference ‘‘Multiphase Flows 2013’’

Appendix 3: Extra information about fuels

Appendix 4: More simulation results

Appendix 1: Project Description

Telemark University College

Faculty of Technology

FMH606 Master's Thesis

Title: Optimisation of a biomass gasification reactor

Student: Kshanthi Perera

TUC supervisor: Prof. Britt Halvorsen, Rajan Thapa (co-supervisor)

External partner: Vienna University of Technology

Task background:

Biomass is an alternative to fossil fuels in production of heat and power. Gasification of biomass is a technology that is used for combined heat and power production (CHP). Timber and waste from timber production can be used as raw material in a CHP-plant. Vienna University of Technology (TUV) has the leading researchers in the world within biomass gasification and has more than 15 years of experience within this field. TUC and TUV are cooperating on research on gasification of biomass. The efficiency of the gasification reactor is crucial for the overall efficiency of a CHP-plant. Optimization of the gasification reactor is therefore very important.

Task description:

1. Literature survey
2. Experimental study of fluidization properties by using pressure measurements.
3. Simulation of gasification reactor using the particle simulation software Barracuda

Student category:
PT, EET

Practical arrangements:

The work will mainly be carried out at TUC.

The study will include:

- Barracuda training course arranged at one of the Barracuda distributors in Europe

Address: Kjølnes ring 56, NO-3918 Porsgrunn, Norway. **Phone:** 35 57 50 00. **Fax:** 35 55 75 47.

Signatures:

Student (date and signature): 

Supervisor (date and signature): 26.02.2013 Britt Tabersen

Appendix 2: Abstract of the research paper for the conference ‘‘Multiphase Flows 2013’’

Simulation and optimization of steam gasification process using CPFD

Kshanthi K. Perera, Rajan K. Thapa, Britt M. Halvorsen
Department of Technology, Telemark University College, Porsgrunn, Norway

Abstract
Steam Gasification is a well-known technology which is used to produce a high quality product gas, especially for power generation applications. The gas composition, gas quality and the purity has a great role to play depending on the end application. Hence the bio mass steam gasification was studied using the Computational Particle Fluid Dynamics (CPFD) simulation tool, ‘Barracuda VR^{TM}’. The software is well suited for simulating the dense particle laden fluids due to its numerical solving methods for both the particles and the fluid.
Both the experiments and simulations were carried out for a cylindrical isothermal fluidized bed reactor without chemistry, to compare the deviations of simulation results from the experimental results. The simulation results were agreed with experimental results and confirmed the same minimum fluidization velocity.
Three dimensional simulations were carried out for a cylindrical geometry to study about the energy, and momentum transport within a simplified dual fluidized bed steam gasification reactor and the important chemistry was included. According to the simulation results, the product gas was mainly consisted of CO and the amount of H_2 was quite less in comparison to the higher amounts of CH_4.The cumulative production of combustible gasses (CO, CH_4 and H_2) was estimated as 280 Sm^3/day based on the simulation results.

Keywords: Bio mass steam gasification, Barracuda, CPFD, Product gas

Appendix 3: Extra information about fuels

Classification of solid fuels by their H/C and O/C ratios

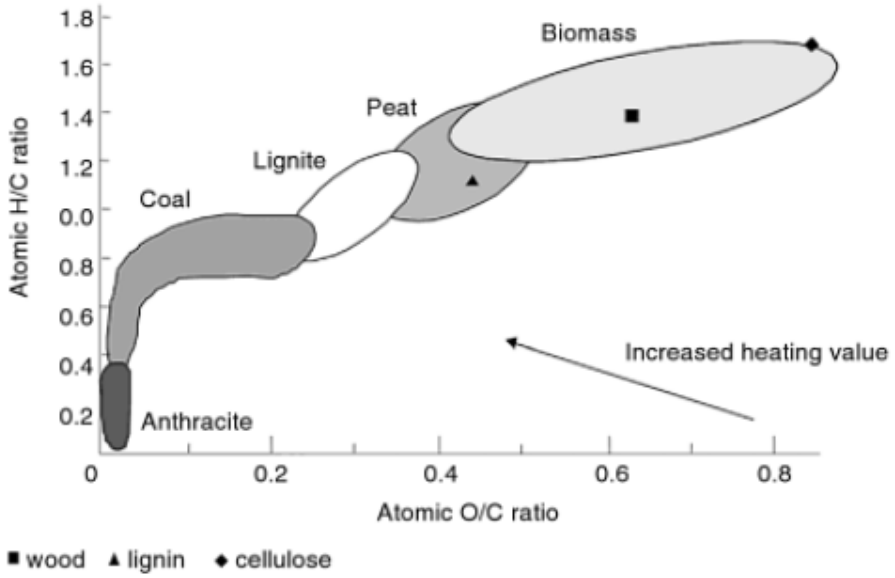

Classification of biomass by their constituent ratios

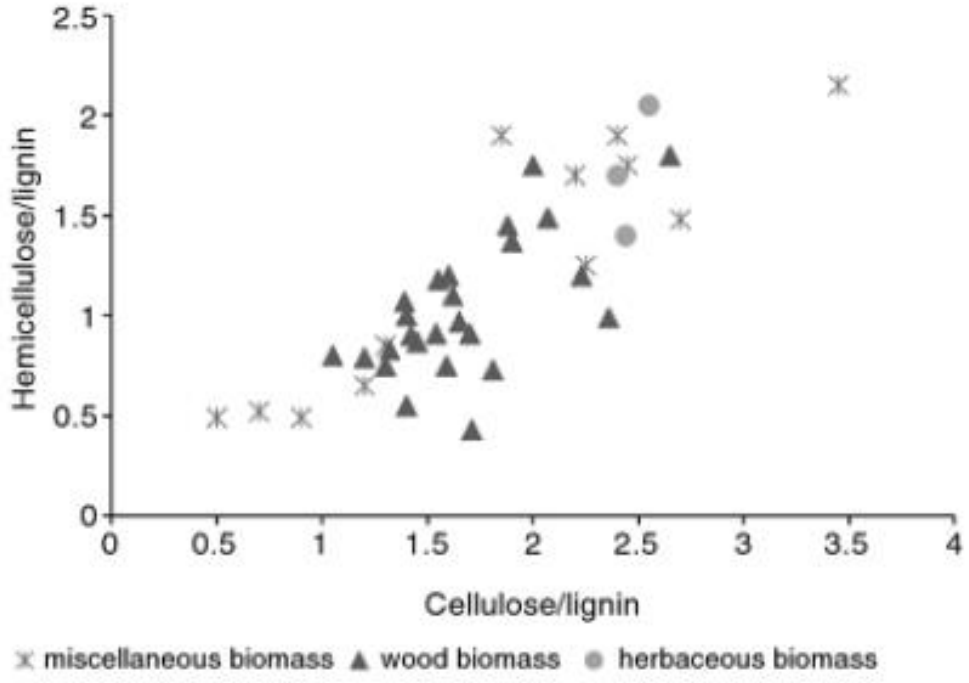

Data source: Biomass Gasification and Pyrolysis Practical Design, Prabir Basu

Appendix 4: More simulation results

Case-A

Location; at (x=4.2cm, y=4.9cm, z) Time; 15s

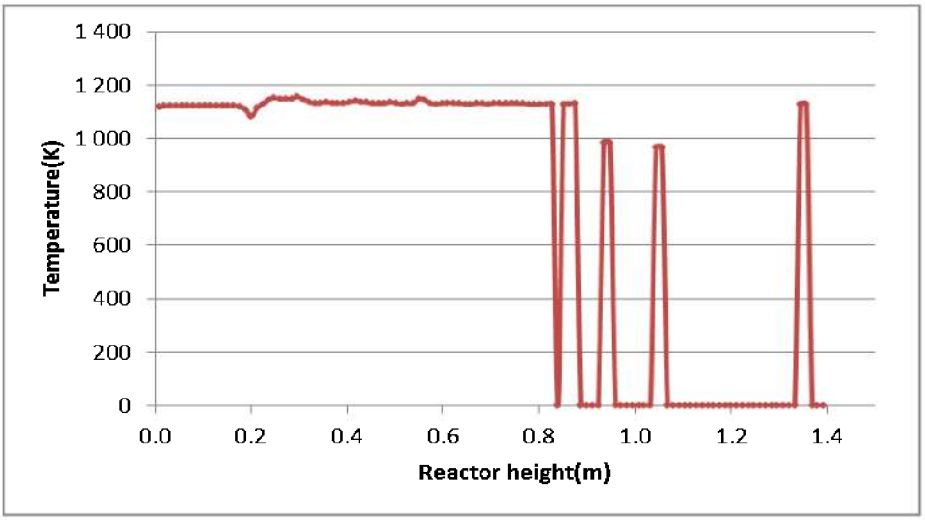

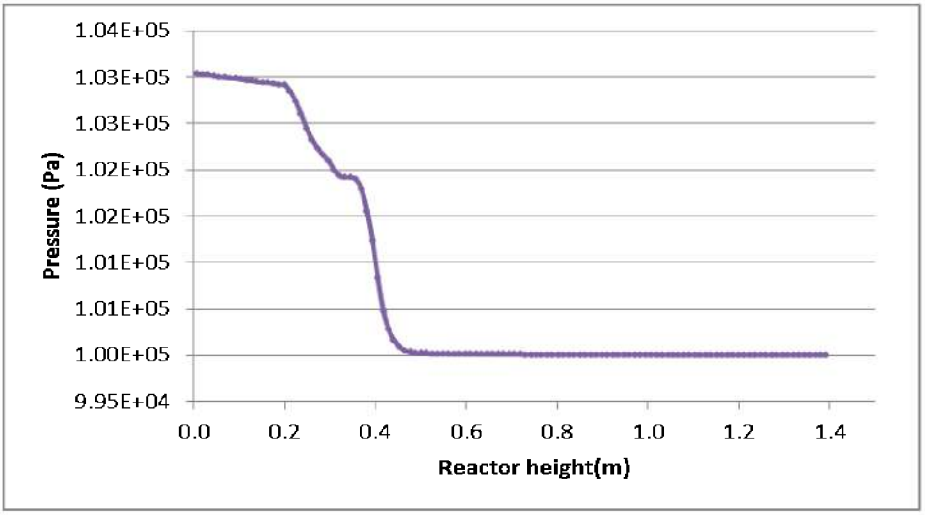

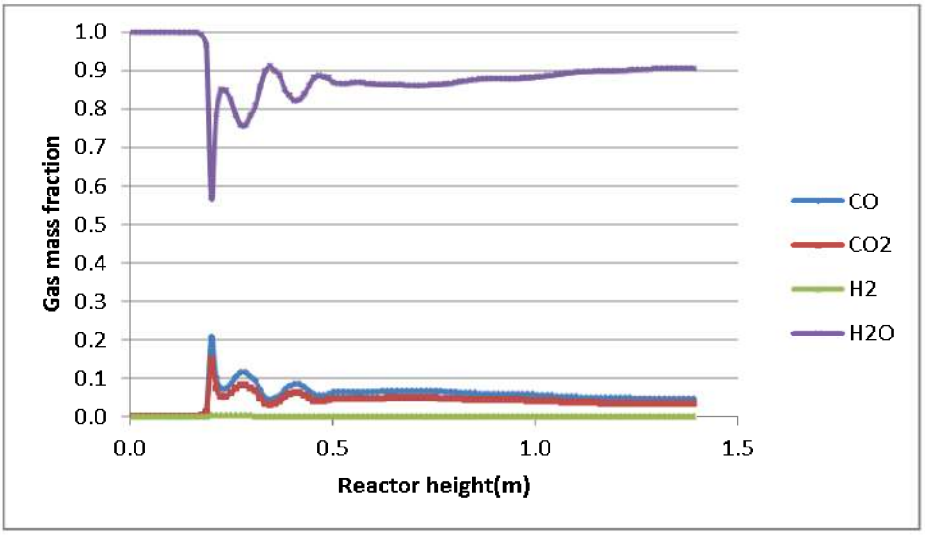

Case-C

Location; at (x=4.2cm, y=4.9cm, z) Time; 15s

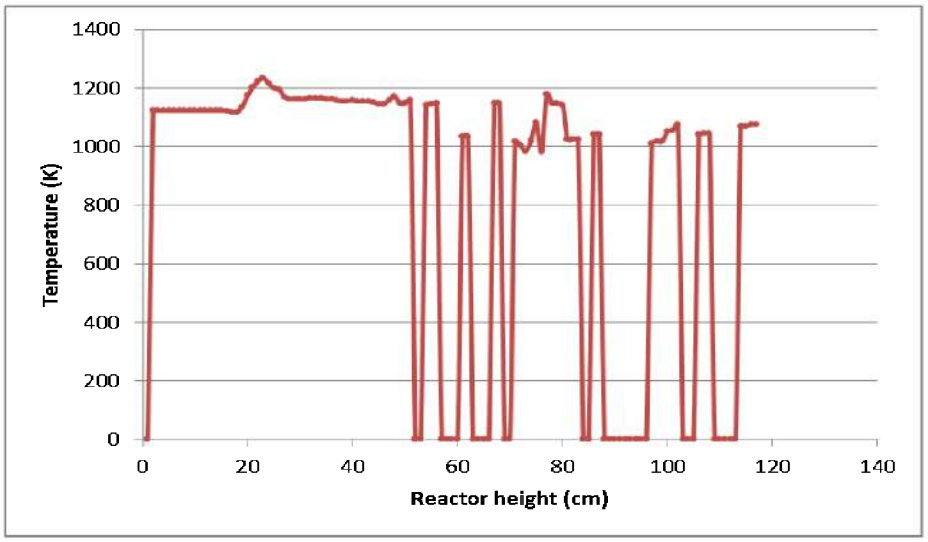

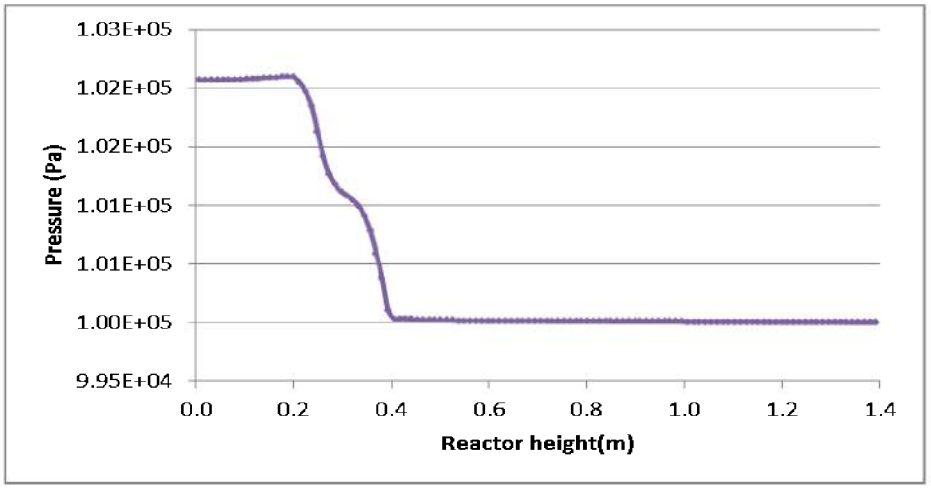

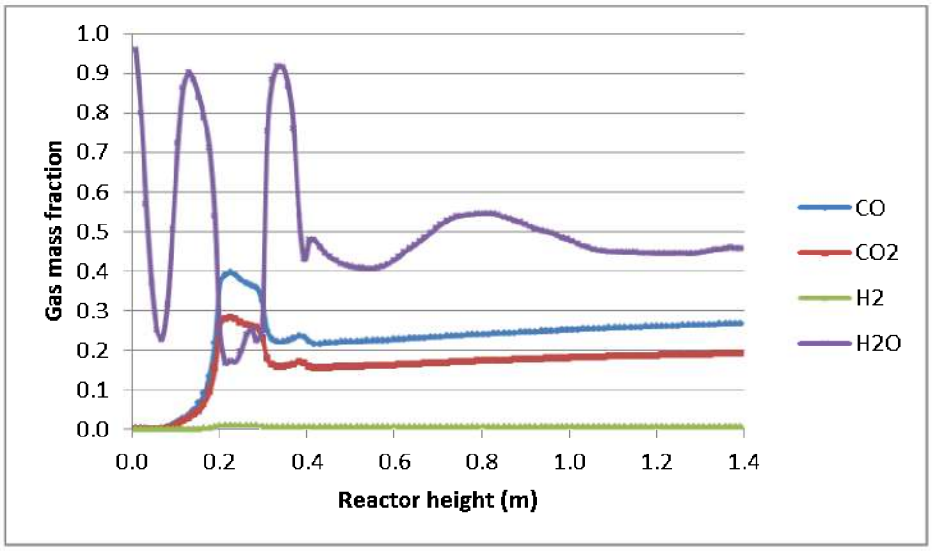

Case-D

Location; at (x=4.2cm, y=4.9cm, z) Time; 15s

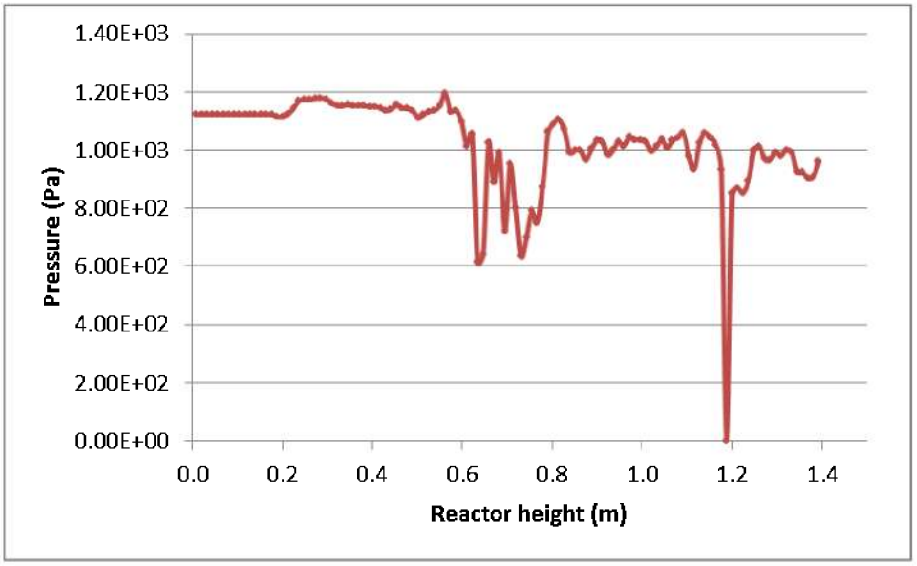

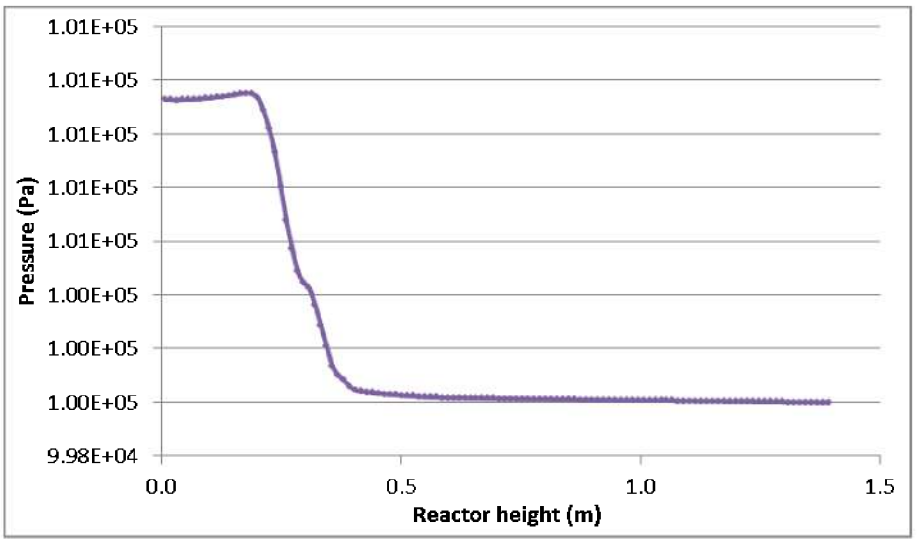

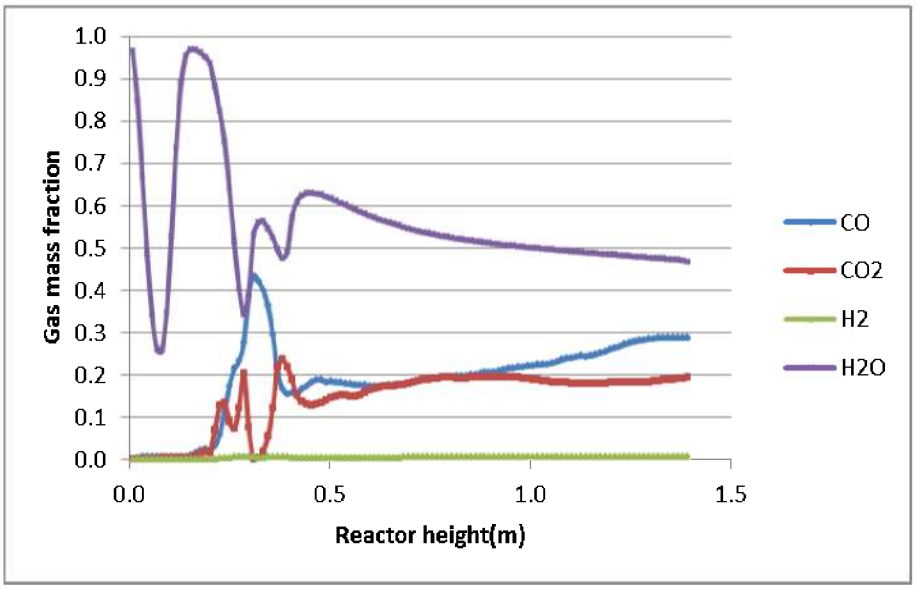

Case-E

Location; at (x=4.2cm, y=4.9cm, z) Time; 15s

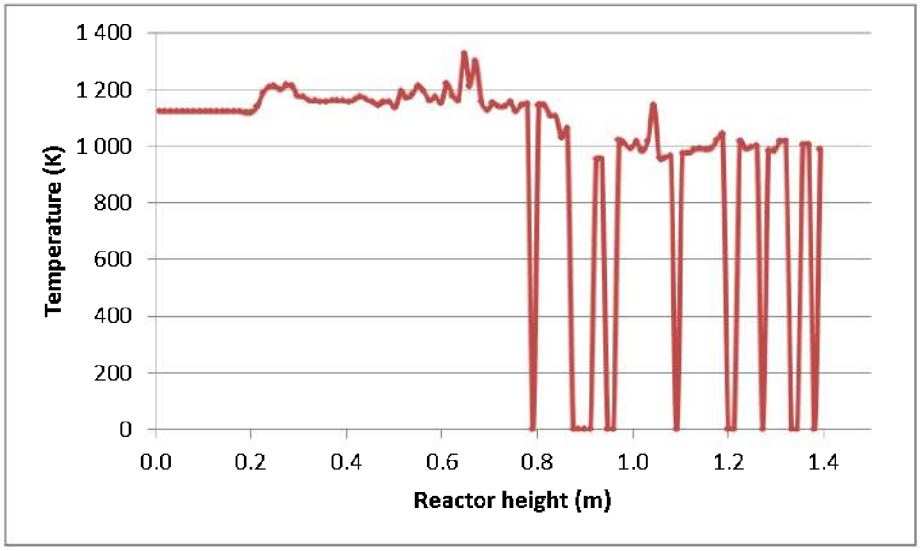

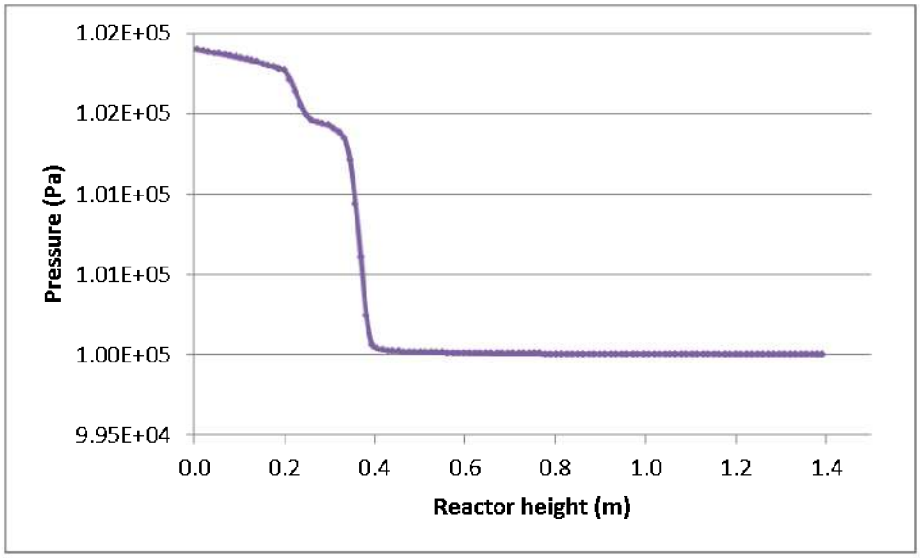

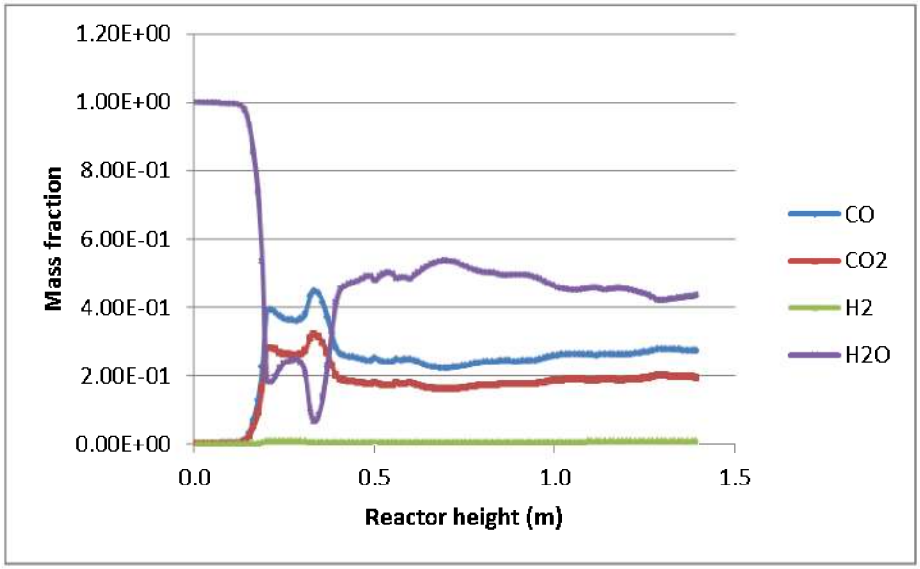

Case-F

Location; at (x=4.2cm, y=4.9cm, z) Time; 15s

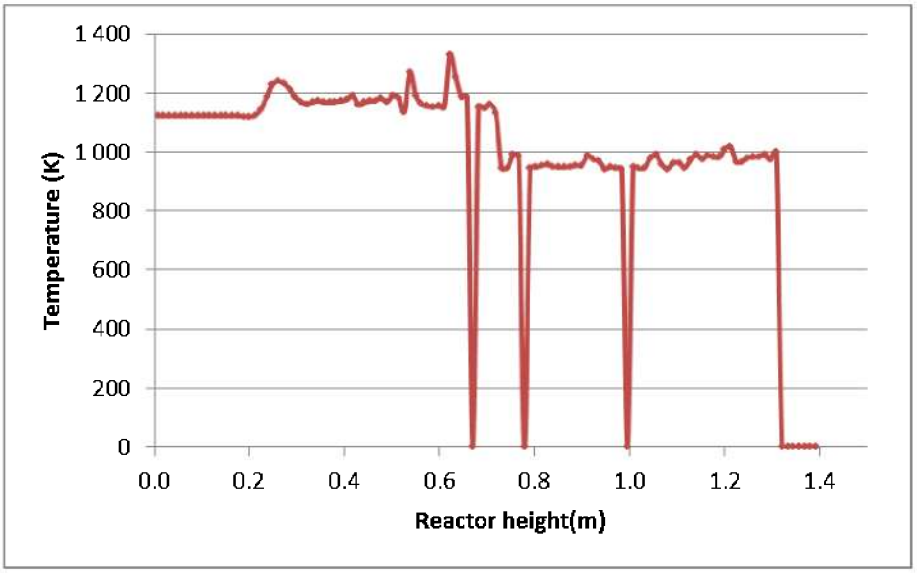

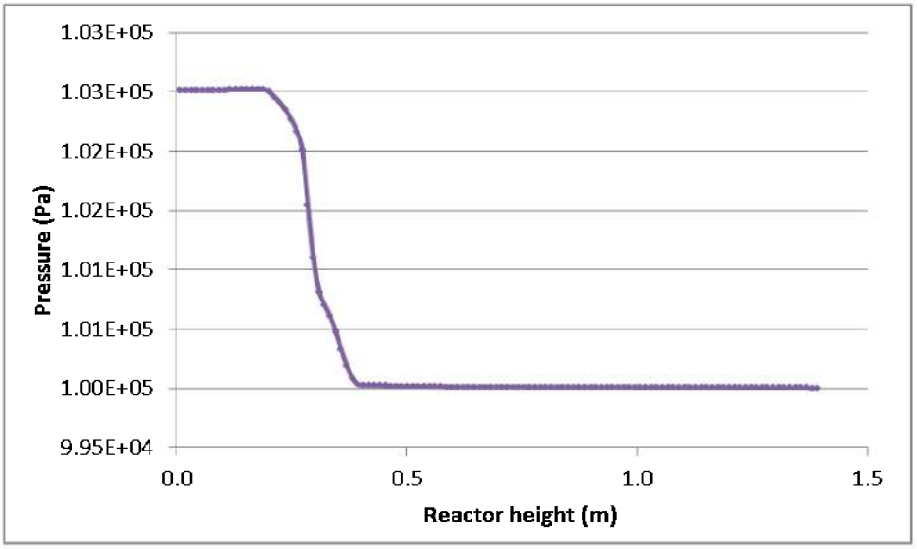

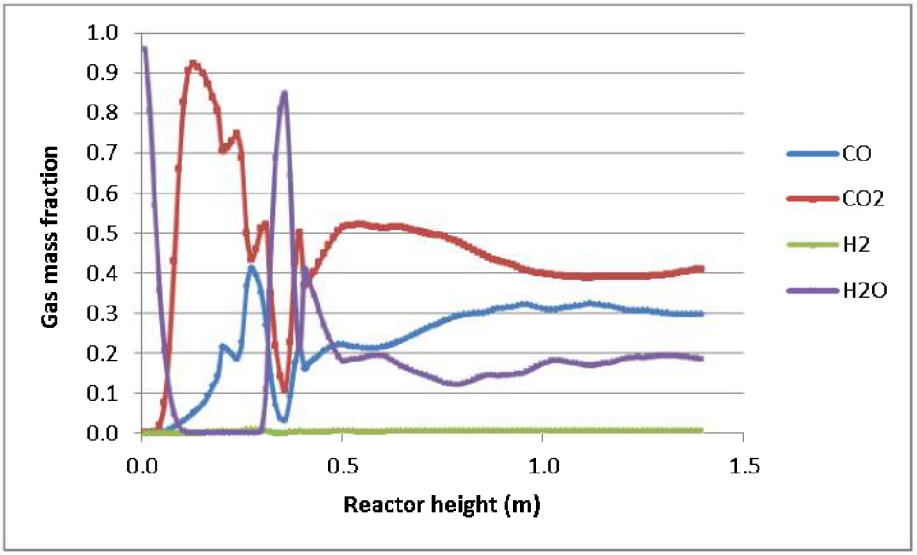

Case-G

Location; at (x=4.2cm, y=4.9cm, z) Time; 15s